Application of the random storm method to global structural loading on fixed offshore structures

by M.R. Kraneveld

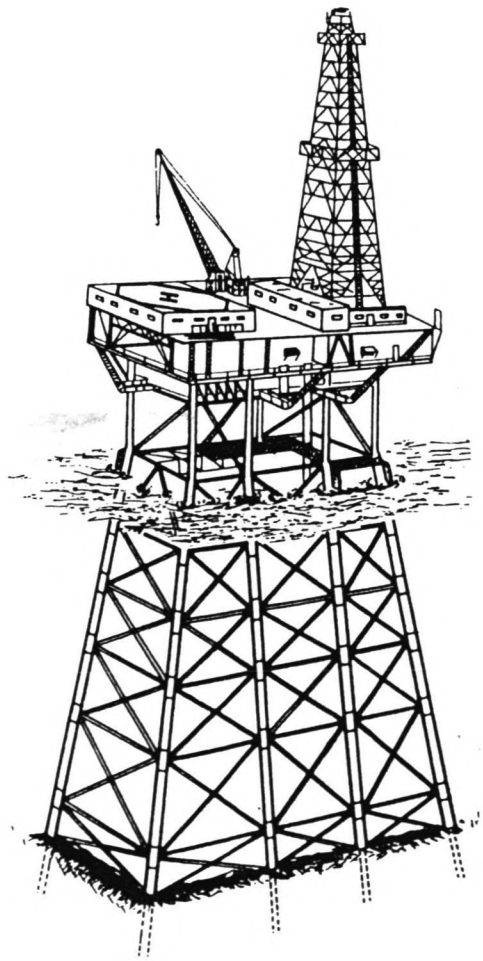

TU Delft
Technische Universiteit Delft

Faculteit der Civiele Techniek

Application of the random storm method to global structural loading on fixed offshore structures

by M.R. Kraneveld

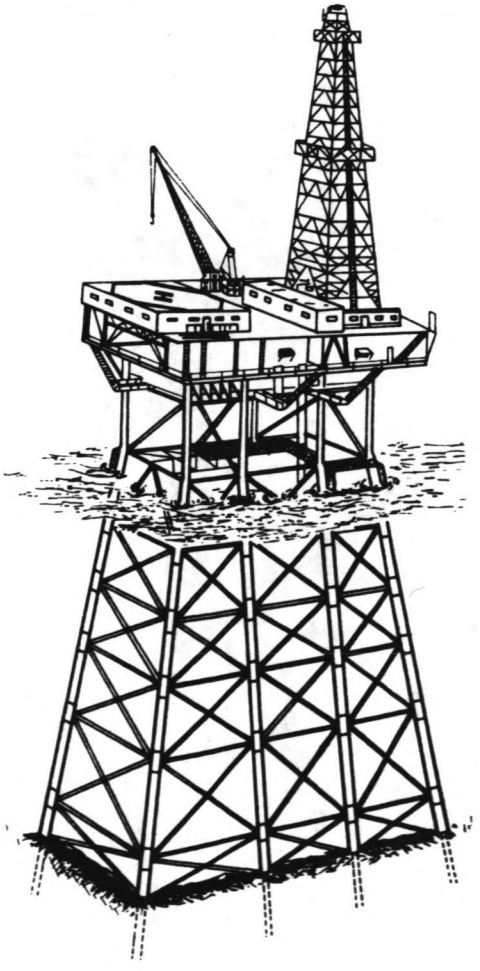

ACKNOWLEDGEMENT

Working on a project at the Koninklijke/Shell Exploration and Production Laboratory was a very challenging and interesting experience. Therefore I was very pleased to be given the opportunity to work on a project here. I like to thank especially dr P.S. Tromans, my supervisor in the K.S.E.P.L., for all his stimulating and encouraging support. Furthermore I like to thank my professor, prof. dr. ir. J.A. Battjes, who arranged the first contact with the K.S.E.P.L., and the other members of my steering commitee, dr. ir. L.H. Holthuijsen and W.W. Massie Msc. P.E. for their support. The final thanks go to P.P. de Wolf, a mathematics student who was also working on the random storm method. The discussions we had, have been very helpful for me to obtain a proper understanding of the statistics.

Maarten Kraneveld
July 1991

ABSTRACT

In conventional practice extreme design conditions for offshore structures are obtained very conservatively by extrapolating 3-hourly statistics of wind, wave and current data to a (say) 100 year return level, assuming that the 100-year extremes occur simultaneously and act in the same direction. This study involves an alternative approach accounting for the joint probability and directionality of wind, waves and currents. Design conditions are generated from the statistics of extreme global loads in individual storms, resulting in a 100-year base shear and overturning moment. Treatment in terms of storms avoids the dificulties arising from correlation between successive 3-hour intervals. The base shear forces are determined by a loading model, an analytical relationship between base shear and crest height, and most of the important environmental parameters.

The inverse of the crest height-base shear relation is used to derive from the crest elevation statistics a cumulative distribution of the extreme base shear for individual storms. This is done for every storm from the north-west quadrant in the 25 years of hindcast data base in the North European Storm Study (NESS) for one location in the northern North Sea. Each storm is characterized by its most probable extreme base shear value, F_{mp}. These representative storm parameters are used to describe the short term and the long term statistics of extreme base shear.

It has been found that the short term variability of all storms can be well represented by one model distribution, $P(f|F_{mp})$. With this probability distribution for the model storm, in combination with the results of a new asymptotic method estimating the probability distribution of F_{mp}, $P(F_{mp})$, the probability distribution of the largest base shear for any random storm, $P(f|\text{any storm})$, is determined. The same analysis is followed for overturning moment.

Since the average arrival rate of the storms is known the probability distribution of the largest base shear (and overturning moment) with a return period of 100 years, f_{100} (and m_{100}), can be deduced. From a back calculation it appears that the resulting design loads are caused by combinations of extreme wind, waves and currents, which are significantly less severe than the values conventionally used for design.

LIST OF CONTENTS

1. PROJECT INTRODUCTION

1.1 Introduction

This report gives an overview on the work done for the project "Application of the random storm method to global structural loading on fixed offshore structures". This project is a continuation of previous research, a.o. done by B.H. Heijermans, my predecessor at the KSEPL. A random storm method was developed by Heijermans, where the statistics of individual severe storms were used for the generation of a 100-year design wave. Also surge and tide were included in the model. Since the results of the new method were quite satisfactory, it was suggested to extend the theory to environmental loading on offshore structures, so that besides wave height all the other environmental parameters are considered as well. This project deals with the generation of a 100-year design condition for an offshore structure in terms of base shear and overturning moment with the random storm method.

1.2 Problem Analysis

One of the first steps in the design procedure for offshore structures is the careful characterization of the environmental forces and effects that a proposed structure may experience during its operational lifetime. In some cases, the intensity of storms and their effects may be limited by geographic and hydrographic factors in such a way that a most severe design storm exists. More commonly, however, there will be a small but finite probability that the structure will experience another storm that has some aspects more severe than the selected storm. This dilemma is due to the fact that storm intensity cannot really be expressed as a single deterministic number; instead it is a collection of extreme environmental data such as significant wave height and period, wind speed, current, various directions and so on. Moreover there is a lack of a true upper bound in most natural

phenomena, thus statistical considerations and risk or reliability concepts must be introduced into the offshore design procedure.

It has been traditional design practice to estimate the probabilities of extreme winds, waves, currents and levels independently and combine these extreme values, assuming they occur simultaneously and act in the same direction, to obtain the extreme environmental design conditions. However, this assumption is invalid and it is therefore inevitable that this results in some over-design.

According to the traditional method the estimate of a design wave is based on the extrapolation of data from a series of measurement results collected over a few years or data determined with a hindcasting technique. Design levels for current and wind are defined in a similar way. The data is usually obtained from records of surface elevation $\eta(t)$, or respectively current velocity v(t) and windspeed W(t), taken every 3 hours for a period of 15 or 20 minutes. In the statistical analysis the environmental variables in successive 3 hour intervals are assumed to be independent, which they are not: they are correlated.

Since individual storms are much more likely to be uncorrelated than the environmental parameters in successive 3 hour intervals, it was suggested in KSEPL to consider particular severe storms and look for a similarity, so that it might be possible to create a model storm and describe its statistics with only one parameter, for example the most probable extreme, $H_{37\%}$ or H_{mp}, the wave height with a probability of non-exceedence of 37 %. In addition to this, if an analytical relationship between the base shear force F (or the overturning moment M) and wave crest elevation can be established, probabilities for load can be deduced from probabilities for crest elevation, conditioned on the other enviromental parameters. Thus a model can be created for the load statistics of a storm, that is rather similar to the model for the wave statistics.

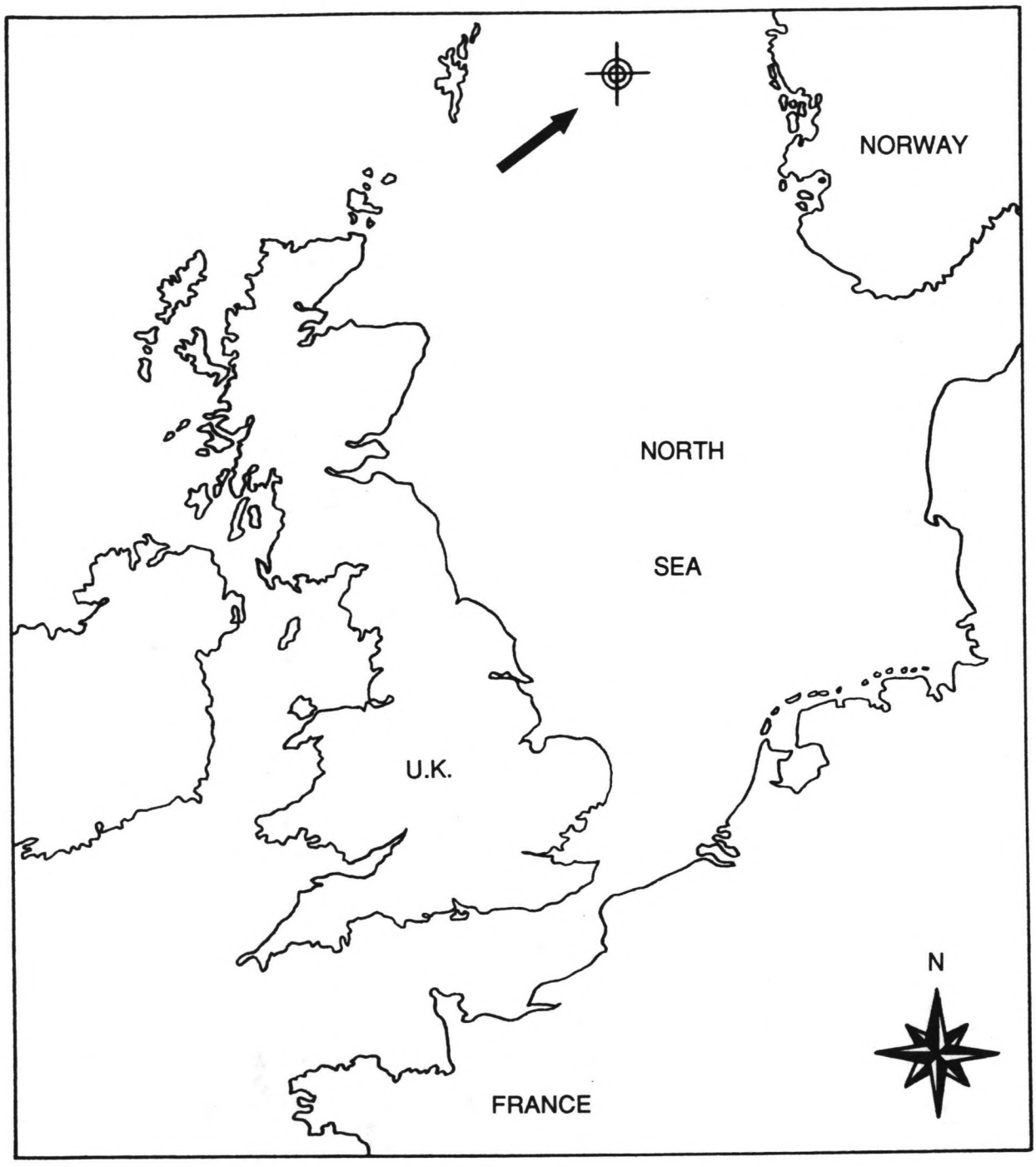

Figure 1.1: Location considered in this study.

Besides the objections to the traditional methods this study has some other motivations. It may be of economic interest to extend the operational lifetime of an existing structure. If an alternative method is developed for determining a design load (base shear or overturning moment) the reliability of the existing structure can be checked. A new attempt at describing the statistics of the forces on an offshore structure has been made possible by the developement of a new technique assuming that certain asymptotic properties of extreme values are applicable to storms, and by the availability of information of 25 years of hindcasting for the North Sea. The North European Storm Study (NESS) model contains all relevant environmental data, such as significant wave height, current, wind speed, directions, surge and so on, simulated according to all meteorological and environmental information available.

With the new technique and the information available from the NESS data base a model will be created which describes the load statistics and includes both short term and long term statistics. The new method is applied for a location in the Northern North Sea in the UK sector (figure 1.1).

1.3 Problem Definition

Traditional design methods for offshore structures assume that the most unfavourable extreme values of wind, waves and current occur simultaneously and act in the same direction, and that their values in successive 3 hour intervals are uncorrelated, and they neglect the short term variability. Overall these shortcomings result in a conservative design condition.

1.4 General Objectives

The overall objective of the study is to develop a new method for the calculation of a design condition, with all environmental data included, as

well as short term statistics and long term influences on the statistics. Extreme values of wind, waves and current do not necessarily occur simultaneously and their values in successive 3 hour intervals are not treated as independent in the way they are treated in the traditional methods. To succeed in the intention three major objectives are pursued:

1) Creating a model for base shear and overturning moment as a function of crest height, with all the other environmental data included.

2) Deriving the probability distribution of the largest base shear and overturning moment for any random storm, based upon 25 years of storm histories from the NESS data base.

3) Calculating a 100-year value for base shear and overturning moment as a design condition by extrapolating the random storm distribution to 100 year conditions.

1.5 Strategy

In this study a real, spaceframe structure is represented by a group of closely spaced vertical columns. By introducing the assumptions that the wave motion is narrow-banded and that large peaks are drag dominated, an analytical relationship can be established between the wave motion and a wave load. This relationship can be derived from the Morison equation and contains all the environmental variables and some constants which are related to the structure itself and its location. These constants are calibrated against a numerical loading model using some representative extreme hindcast data as an input. The structure considered here is a single column in deep water with a constant diameter of 1.2 m. Extension of the theory to a group of closely spaced piles may be achieved easily by adjusting the constants in the analytical load relationship.

Structural responses, i.e. base shear forces and overturning moments, are considered in this study. For the determination of these loads the structure is assumed to response quasi-statically. The structural dynamics are excluded. In this approximation the base shear is the total horizontal force on the structure and is used as a representative structural response. Nevertheless any other quasi-static response may be treated in a similar way. In this report the derivation of the load equations and statistics is explained for base shear only. For overturning moment merely the results will be given, but in fact the same procedure is followed.

The inverse of the crest height-load relation can be used for deriving a cumulative distribution of the extreme base shear for every single storm of the data base, $P(f|S_j)$, where a storm is defined as a period of a number of successive 3 hour intervals with a continuous severe sea state. Each storm is characterized by its most probable extreme base shear value, F_{mp}. These representative storm parameters will be used to describe the short term and the long term statistics of extreme base shear. Based upon the results of previous research it is expected that the short term variability of all storms can be well represented by one model storm distribution curve, i.e. $P(f|F_{mp})$. With this probability distribution for the model storm, in combination with the results of a new asymptotic method estimating the robability distribution of F_{mp}, $P(F_{mp})$, the probability distribution of the largest base shear for any random storm, $P(f|\text{any storm})$, can be determined.

For design purposes conditions with a return period of (say) 100 years are of interest. Since the average arrival rate of the storms is known, the 100-year return values may be deduced from the distribution curve for any random storm. In fact this can be done for any desired return period.

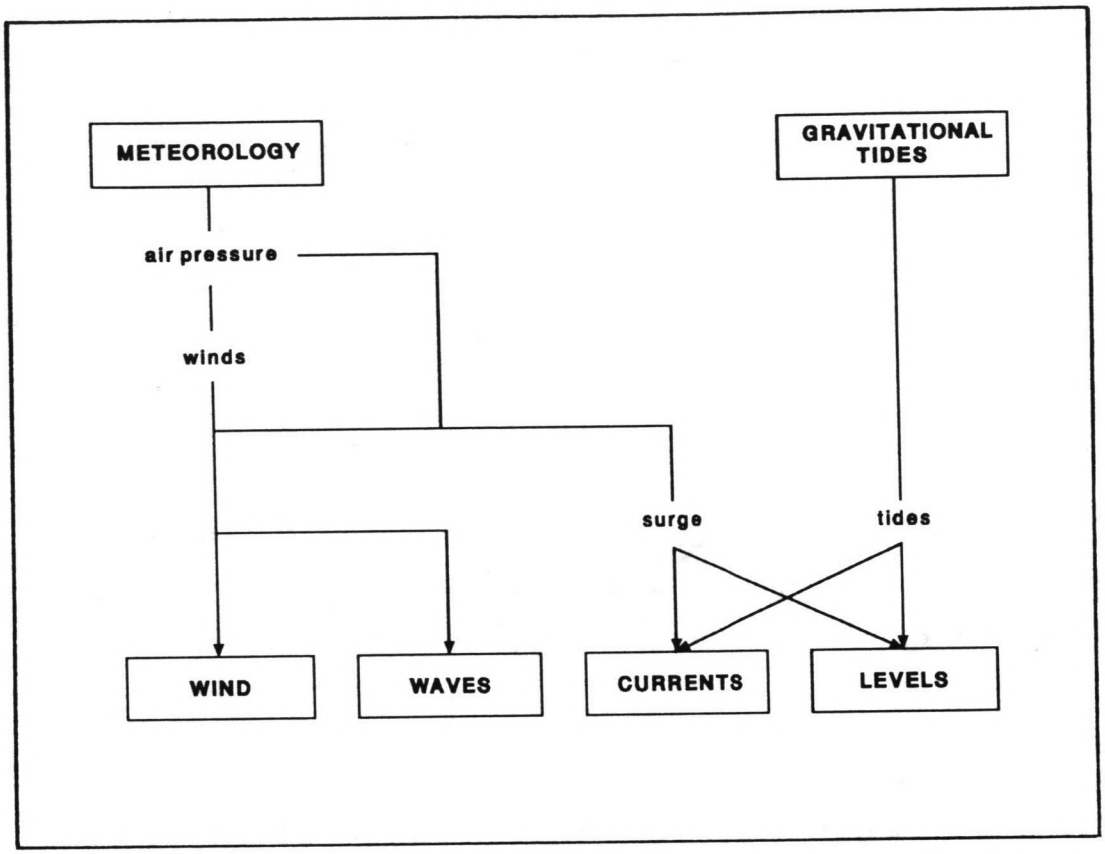

Figure 2.1: The interaction between wind, waves and currents.

2. OFFSHORE STRUCTURES AND ENVIRONMENTAL CONDITIONS

2.1 Introduction

Offshore structures suffer from huge forces due to the ocean environment and the atmosphere above it, especially under extreme circumstances. The design and operation of offshore platforms require a proper understanding of the physical character and behaviour of these natural phenomena and of their interaction. The two basic independent factors which govern changes in the marine environment are the weather and gravitational tides. Extreme winds, waves, currents and levels generated by these factors are not independent, as shown in figure 2.1. The wind stresses on the sea surface produce waves, currents and changes of sea level. The total observed currents and levels are produced by a combination of surge and tidal movements. Winds, waves and levels are related, but statistical correlations will be different for each specific site, particularly when the directions of winds, waves and currents are considered. The only way to determine the correlations is through long series of simultaneous measurements. The problem is further complicated by the strong seasonal variations which occur especially for winds, waves and surges (refs. 8,10).

2.2 The interaction between wind, waves and currents

Wind waves are usually the dominant contribution to the environmental forces on offshore structures. Wave heights, periods and directions are important and these may all be related to the winds by a combination of theoretical and empirical rules. The higher waves are associated with longer wave lengths and longer periods. They are also associated with higher wind speeds, longer durations of wind action, and longer fetches - the distances of sea over which the wind has blown before reaching the design site.

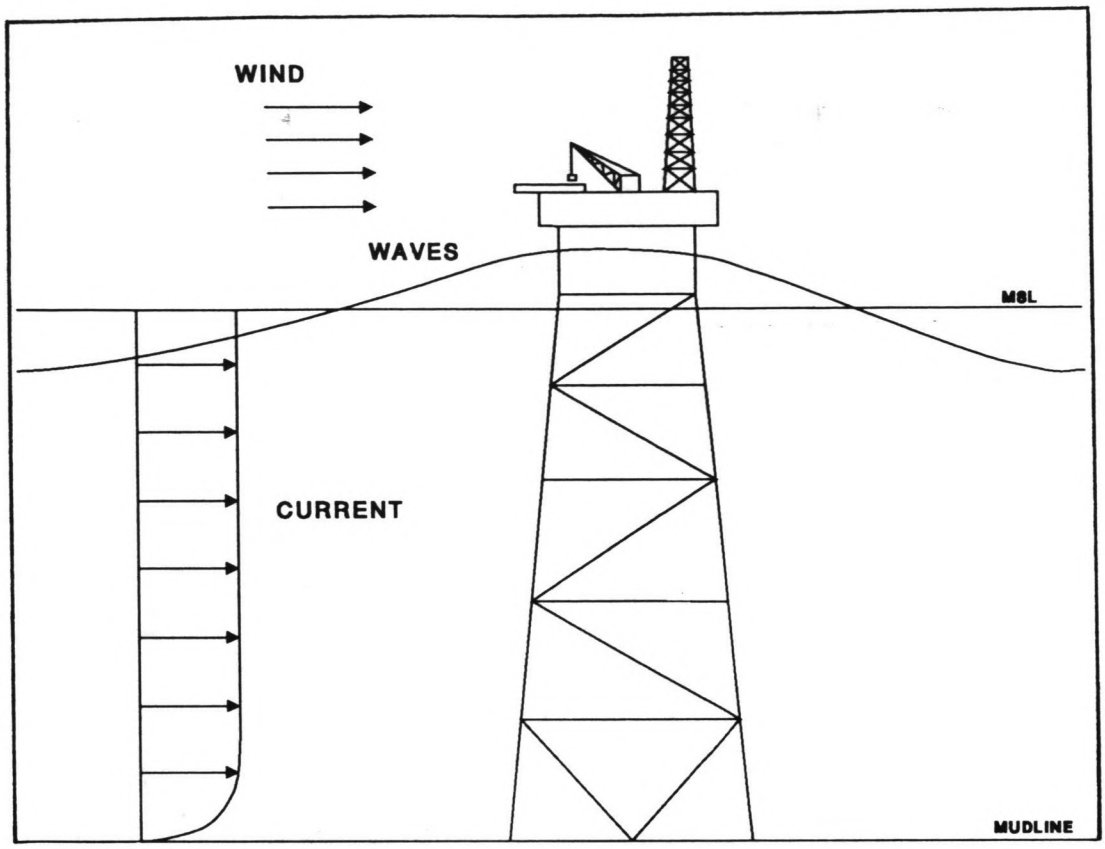

Figure 2.2a: Environmental loading on an offshore structure.

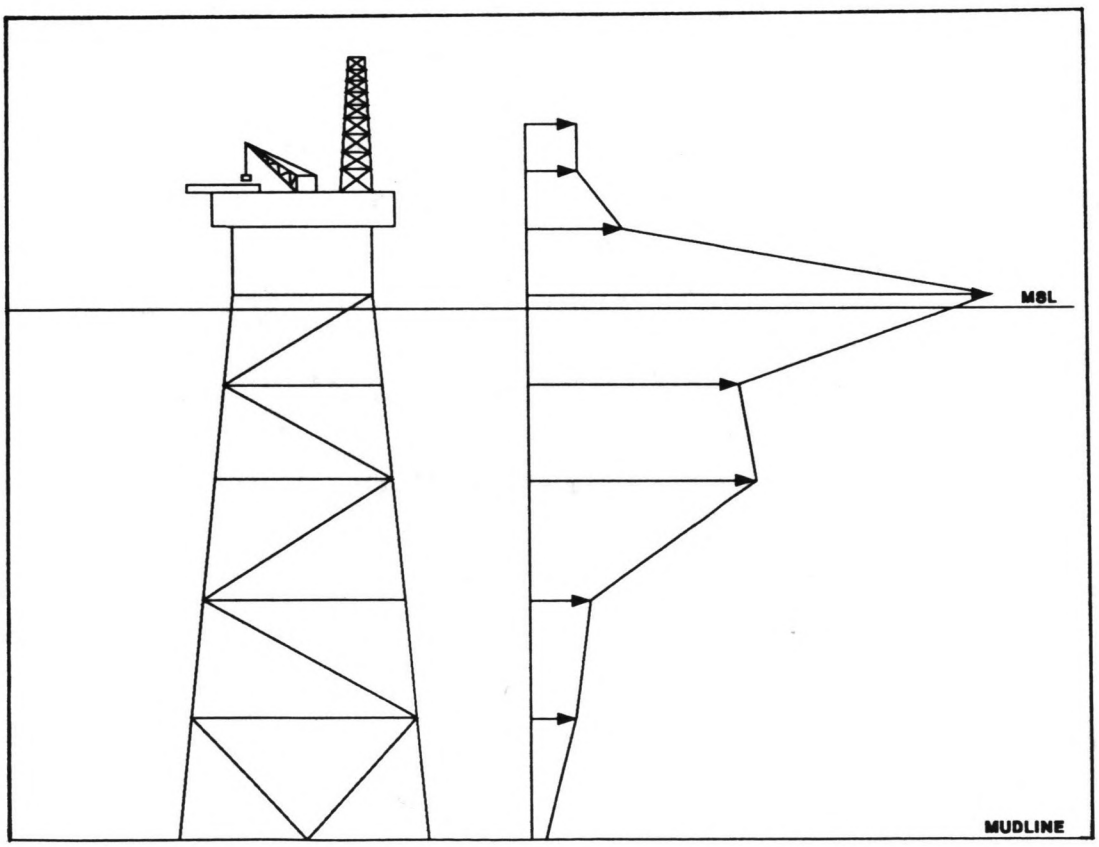

Figure 2.2b: Global environmental load distribution.

The winds which produce extreme waves will also produce extreme surge currents and levels, but the time scales and directions may be different. Wave directions in the open sea may be similar to wind directions, but near the coast and in other areas where the water depths become comparable with half the wave lengths, the waves will be refracted towards the region of shallower water.

Currents can also affect the direction of propagation of a wave train, but the most significant interaction between waves and currents occurs when they are opposed to each other. In this case the wave propagation speed is reduced, but the amplitudes are increased. The physical reason for this is the need to conserve the net energy flux, in the same way as tidal amplitudes increase when travelling over the shallow waters of the continental shelf. Even more significant for calculating forces on structures, the wave steepness and the associated accelerations are increased (ref. 10).

2.3 Forces on offshore structures

Offshore structures are subjected to both steady and time varying forces due to the action of winds, currents and waves (figure 2.2). In general, an air or water flow incident on an offshore structure will exert forces that arise from two primary mechanisms. A steady or unsteady flow will directly exert a corresponding steady or unsteady force with a line of action that is parallel to the incident flow direction ("in-line" forces). However, the localized interaction of steady or unsteady flow with a structural member will also cause vortices to be shed in the flow and will induce unsteady "transverse" forces with lines of action that are perpendicular to the incident flow direction.

Wind forces on offshore structures account for approximately 10 to 15 % of the total forces from wind, current and waves acting on the structure. In deep water, wind induced forces can have a larger relative effect on the

base overturning moment of bottom emplaced structures because of the large moment arms involved. Winds exert predominantly steady forces on the exposed parts of offshore structures, although there are significant gust or turbulence components in winds which induce high, unsteady, local forces on structural components as well as a low frequency total force on the whole structure.

The general equation for the wind force on a slender member of an open space framed offshore structure exposed to a wind is:

$$F_W = \frac{1}{2} \rho_a W^2 S C_D \qquad (2.1)$$

where: W = wind velocity
ρ_a = air density
S = frontal area facing the wind
C_D = drag coefficient

Ocean currents also exert largely steady forces on submerged structures, although the localized effects of vortex shedding induce unsteady force components on structural members. Current forces on offshore structures are calculated using the same methods as for wind forces alone except that currents do not exhibit fluctuations similar to those of wind gusts. The current velocities used are much smaller than those for wind force calculations, although, of course, the water density is higher.

Gravity waves produce by far the largest force on most offshore structures. The applied force is oscillatory in nature, although non-linear wave properties gives rise to mean and low-frequency drift forces. For relatively small structural members where the ratio between diameter of the member, D, and wave length, λ, is less than 0.2, Morison's equation is used to estimate forces due to wave action. This equation is based on the assumption that wave forces can be expressed as the sum of a drag force due to wave fluid velocity (i.e. wave induced and current velocity) and an inertia force due

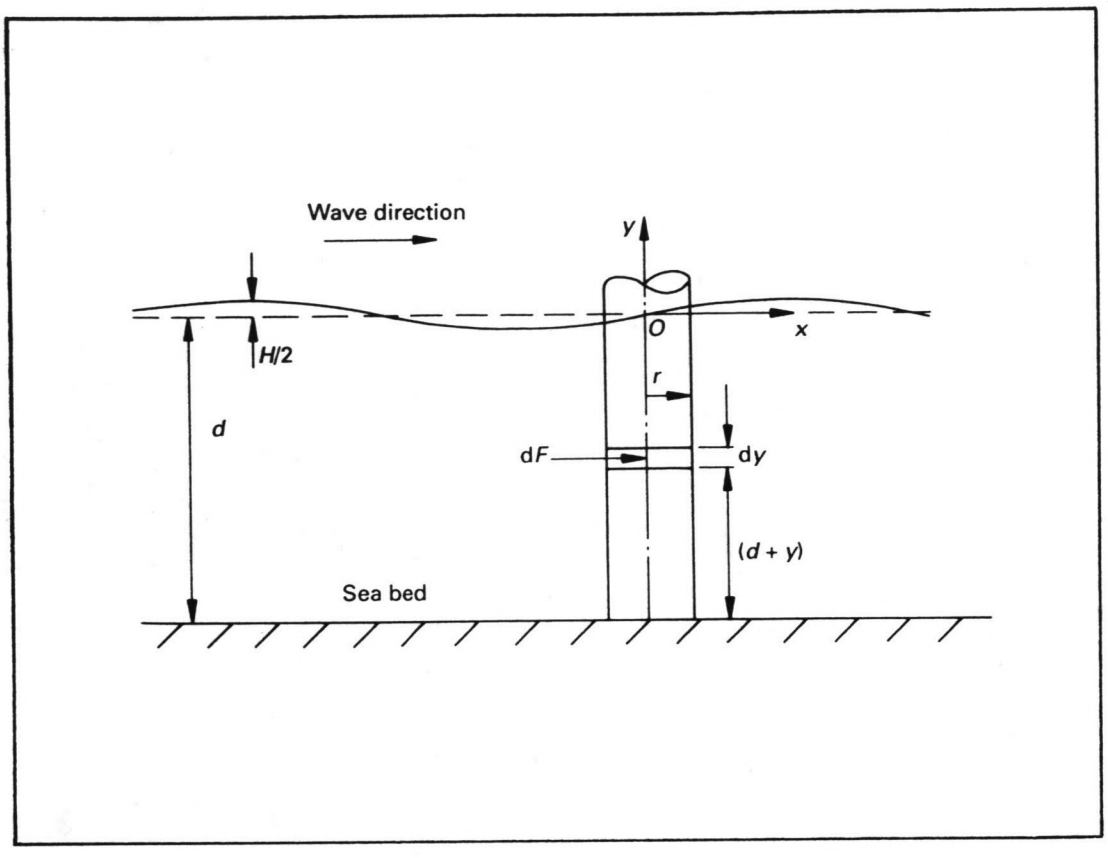

Figure 2.3: Wave force on a vertical cylinder.

to wave acceleration. Moreover it is assumed that wave properties are not affected by the presence of the structure. An equation to represent this loading can be written as:

$$dF = C_M \rho dV \dot{u}_n + C_D \frac{1}{2} \rho dS (v+u_n) |v+u_n| \tag{2.2}$$

where: dF = the total wave force on a cylinder of volume, dV and frontal area, dS

$\dot{u}_n$ = instantaneous wave fluid acceleration normal to the cylinder

u_n = instantaneous wave fluid velocity normal to the cylinder

v = current velocity

ρ = fluid density

C_M = inertia coefficient

C_D = drag coefficient

The drag force includes a modulus to ensure that the drag force acts in the same direction as the resultant fluid velocity. Consider an element of a vertical circular cylinder of radius r and length dy, then the total force dF acting on this element in the direction of wave propagation can be integrated over depth to yield the total force F and moment M about the sea bed as (figure 2.3):

$$F = C_M \rho \pi r^2 \int_{-d}^{0} \dot{u}\, dy + C_D \rho r \int_{-d}^{0} (v+u_n) |v+u_n| dy \tag{2.3}$$

and

$$M = C_M \rho \pi r^2 \int_{-d}^{0} (d + y)\dot{u}\, dy + C_D \rho r \int_{-d}^{0} (d + y)(v+u_n) |v+u_n| dy \tag{2.4}$$

Marine growth causes the surfaces of offshore structures, below the water line, to become highly roughened. This has the effect of increasing the effective diameter of individual members and to modify the inertia and drag coefficients due to the changed interaction between the cylinder boundary layer and the roughness elements (refs. 8,12).

3. EXTREME ENVIRONMENTAL CONDITIONS

3.1 Introduction

For the design of offshore structures one is especially interested in the extreme environmental conditions, since the structure has to be able to withstand forces and moments from waves, current and wind under such extreme circumstances. In general, the extreme conditions may be parameterized as the probability that a stated extreme will be exceeded at least once during the specified design life of a structure. An alternative is to calculate the level which has a stated probability of being exceeded during the design life. If the probability of a level η being exceeded once in a single year is $Q_Y(\eta)$, the level has a return period $R(\eta)$ of $[Q_Y(\eta)]^{-1}$ years. This is based on the implicit assumption that the same statistics are valid for the whole period. The level which has a probability of being exceeded once in 100 years, is called the 100-year return level.

The return period may also be related to the encounter probability or design risk, which is the probability that the level will be exceeded at least once during the lifetime of a structure:

$$\text{Risk} = 1 - [1 - Q_Y(\eta)]^{T_L} \tag{3.1}$$

where T_L is the design lifetime expressed in years. The appropriate value of $Q_Y(\eta)$ will depend on the value of the property at risk. It should be remembered that a structure has a probability of near 0.635 of encountering a level which has a return period equal to its design life; for acceptable risk factors the design level must have a return period which considerably exceeds the expected lifetime of the structure (ref. 10).

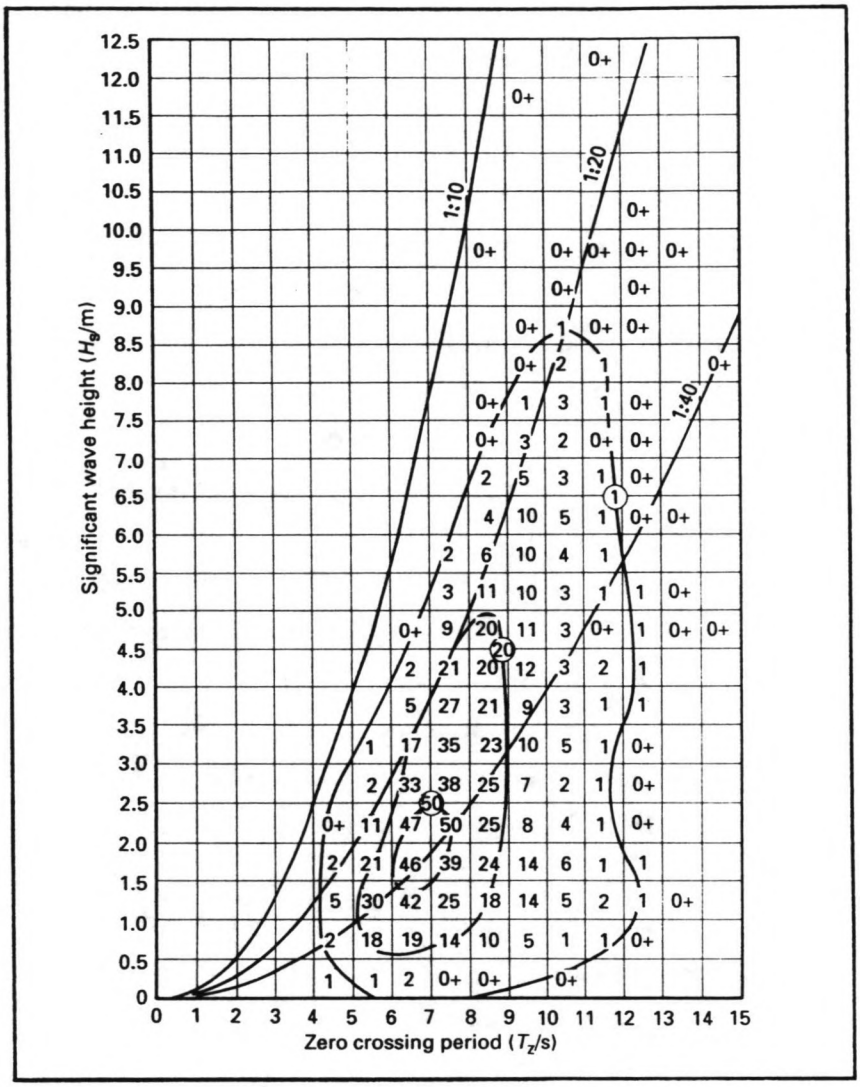

Figure 3.1: Example of a scatter diagram for wave heights and periods (units indicated in parts per thousand).

3.2 Extreme waves

The design wave approach is applied by defining a wave of large height H and a corresponding wave period range whose probability of occurrence is such that it represents the maximum wave that the structure on average will encounter once in a finite but long time interval known as the return period R. The low probability of occurrence is achieved by statistically defining the highest wave that is likely to be encountered once in a large number (50 or 100) of years. Thus the structure can be designed to withstand this rare occurrence which is likely to be the worst encountered condition over its lifetime. Since additional safety factors are involved with the design, the actual failure rate will be much less than once in 100 years.

According to the traditional method the estimate of a design wave is based on the extrapolation of instrumentally measured waves over a period of a few years. The data is obtained from records of wave elevation $\eta(t)$, taken every 3 hours for a period of 15 or 20 minutes. Each sample is reduced to two representative parameters: the significant wave height H_s and the average zero crossing period T_z. For a long time period data can be represented by a bivariate histogram or scatter diagram of H_s and T_z, in which each box denotes the number of wave conditions in parts per thousands (figure 3.1). From the scatter diagram the probability of occurrence of H_s can be derived for the various significant wave heights. These probabilities then can be plotted against H_s according to a chosen probability distribution function (Weibull, Gumbel etc.), as shown in figure 3.2.

The fitting of a convenient probability distribution plays a fundamental role in the extrapolation process. The probability distribution function is selected in such a way that the plotted data lies on a straight line as nearly as possible. In the most simple approach one can draw a straight line through the data plotted on probability paper by eye. The line can be extrapolated and a design wave height can be selected on the basis of a return period, which is the average time interval between successive 3-hourly

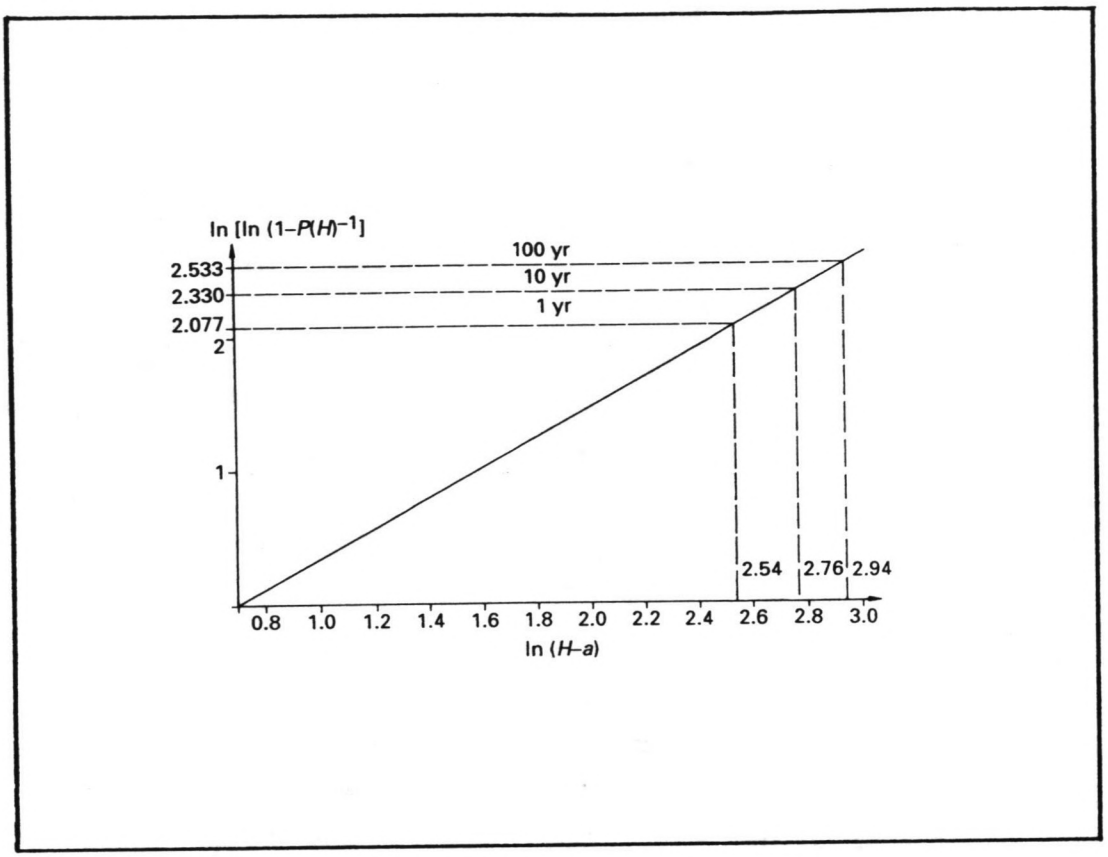

Figure 3.2: Extrapolation plot with Weibull distribution.

events of the design wave height being exceeded. A prescribed return period of a 3-hour interval in which the design wave height is exceeded has an associated value of P(H) and the corresponding wave height may be derived from the extrapolated best-fit line (ref. 8).

Several studies have been done in order to diminish the shortcomings of the traditional extrapolation method. Battjes proposed a method, where the probability distribution of individual waves was used, because the traditional approach did not take into account the possibility that the highest wave in a 50 or 100 year period may occur during the second severest storm or even less severe storms. Tann and Fortnum used the fitted curve of cumulative probability instead of the measured H_s-values. Tucker added a kind of treshold level to the 'Battjes'-method, to exclude all the waves below this level. A more detailed description of these methods is given by Tucker (ref. 17). In spite of the improvements all these methods still suffer from the shortcomings mentioned in paragraph 1.2.

3.3 Extreme currents

Extreme currents are difficult to estimate. The first difficulty is to obtain a sufficiently long series of observations; few series extending over more than a year exist because of the expense and the technical difficulties of making good measurements. Further complications arise because currents are variable with depth at each location, and because they change over short distances, particularly near the shore and around shallow sandbanks. Finally, although most of the techniques for estimating extreme levels are theoretically available for currents, their applications to the speed and direction components of the current is much more complicated.

The simplest method of analysing current observations at a particular depth is to produce cumulative frequency distributions of the recorded speeds, averaged over each sampling interval, and to extrapolate according to some

		West					East				
		−0.4	−0.3	−0.2	−0.1	0.0	0.1	0.2	0.3	0.4	0.5
	1.4										
	1.3										
	1.2										
	1.1										
	1.0			1	2	1	2	2			
North	0.9			7	20	25	20	13	10	1	
	0.8			28	46	74	96	59	29	5	
	0.7		2	44	122	148	142	89	43	3	
	0.6		4	96	143	146	115	88	50	5	
	0.5		2	84	150	125	120	110	41	1	
	0.4		2	100	158	77	112	113	38		
	0.3		1	99	122	38	81	134	40		
	0.2		1	107	113	1	71	158	20		
	0.1			74	110	0	47	185	11		
	0.0			103	87	1	32	182	11		
	−0.1			78	96	4	75	180	3		
	−0.2			79	105	6	92	150	1		
	−0.3			92	101	20	162	130			
	−0.4			64	116	81	216	35			
	−0.5		2	88	121	127	166	13			
	−0.6		3	96	115	146	89	2			
	−0.7		10	85	104	113	41				
	−0.8		20	112	111	77	5				
South	−0.9		25	106	91	31					
	−1.0	1	41	72	34	2					
	−1.1	1	34	39	5						
	−1.2	4	16	7							
	−1.3										
	−1.4										

Table 3.1: Example of a joint frequency distribution of predicted tidal current components. Totally hourly values = 8784.

		West					East				
		−0.5	−0.4	−0.3	−0.2	−0.1	0.0	0.1	0.2	0.3	0.4	0.5
	0.6											
	0.5											
	0.4						3					
North	0.3		1		1	8	28	9		1		
	0.2		1	3	9	38	258	79	4			
	0.1		3	10	38	280	1289	358	36	13	4	
	0.0	2	6	26	95	562	1995	599	104	28	3	1
	−0.1		2	13	47	379	1139	289	28	17	1	
	−0.2	1		3	11	96	248	61	4	2		
South	−0.3				1	12	36	9				
	−0.4							1				
	−0.5											

Table 3.2: Example of a joint frequency distribution of surge current components. Totally hourly values = 8301.

fitted distribution. This method may also be applied to produce directional estimated extremes by treating the speeds observed in each directional sector as separate distributions. This method is fairly easy to apply, but the reliability is invariably limited by the short periods of data available, the strong seasonal effects, and the correlation between successive measurements.

Extreme currents may also be estimated by separation of the observed current vectors into tidal and surge components. Two-dimensional frequency distributions are obtained for each component, but in the simplest case of the currents being rectilinear or if only speeds are considered, the problem may be treated in exactly the same way as for estimating extreme waves. Where the flow is not rectilinear, the flow in two orthogonal directions may be treated separately. North-south and east-west components are usually chosen, but the directions of the major and minor axes of the current ellipses are also suitable. The maximum components in each of the four directions may then be estimated from probability plots produced by combining the probability distributions of the separate tidal and surge components. Tables 3.1 and 3.2 show examples of these distributions, in increments of 0.1 m/s.

The probability of joint events is computed by multiplying the separate probabilities from tables 3.1 and 3.2, and the total probability of a particular observed current is obtained by summing along the appropriate diagonals of the joint probability matrices. This combination may be expressed mathematically as a two dimensional convolution process:

$$D_O(u,v) = \int_{-\infty}^{\infty} \int_{-\infty}^{\infty} D_T(u-x,v-y) D_S(x,y) dxdy \qquad (3.2)$$

where $D_T(u,v)$ is the two-dimensional density function for the tidal currents, where $D_S(x,y)$ is the two-dimensional probability density function

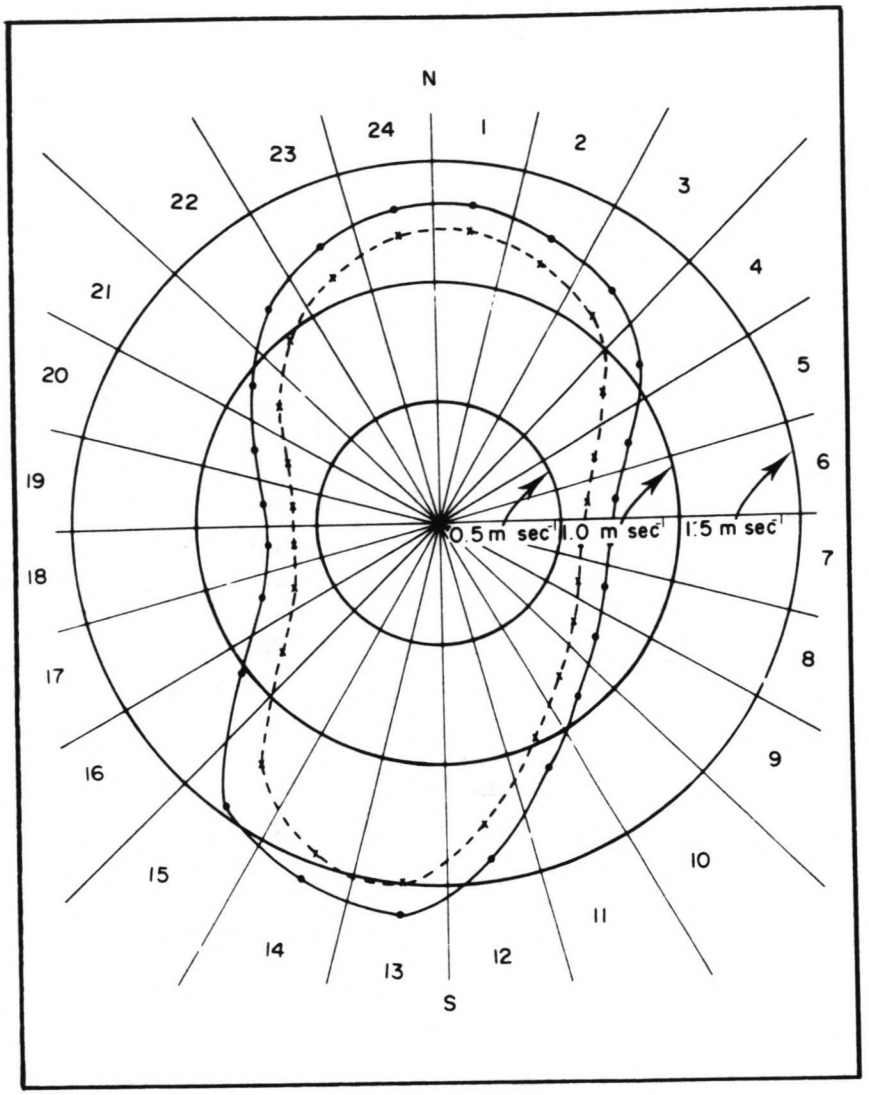

Figure 3.4: Joint-probability estimates drawn for all segments, with the continuous line representing the 100-year return current and the broken line the 50-year return current.

for the surge residual currents, and $D_o(u,v)$ is the two-dimensional probability density function for total observed currents. The parameters u and v are the two orthogonal components of the total current. The frequency distributions are first normalized by the total number of hourly values. The probability of each total current element is then computed as the sum:

$$D_o(u,v) = \sum_i \sum_j D_T(u-ih,v-jh)D_s(ih,jh) \qquad (3.3)$$

where i and j are integers and h is the class interval of 0.1 m/s. Figure 3.3 shows a way of presenting joint probability estimates of extreme total currents flowing to directions within segments 10,11 and 12 (numbering clockwise from north: 135-150°, 150-165°, and 165-180°). An alternative presentation, shown in figure 3.4, involves drawing the speeds which have a particular return period, within the several segments. For calculation of extreme levels and extreme currents, it is wise to make conservative estimates and to apply these with caution; however, for currents, because the uncertainties are greater, extra caution is necessary (ref. 10).

3.4 Extreme winds

The lack of suitable measurements makes the estimation of wind speeds at sea difficult. Estimates are possible by extrapolating the many years of continuous recording at land stations in conjunction with the irregular observations from ships at sea. These ship measurements are usually not very accurate and are biased to low wind speeds because ships seek shelter in extreme weather conditions.

For calculating wind forces on structures the three-second gust speed is usually used. Hourly mean wind speeds are more appropriate for calculations of wave generation. If no directional analysis is available it must be assumed that the extreme winds may blow from any direction. The wind

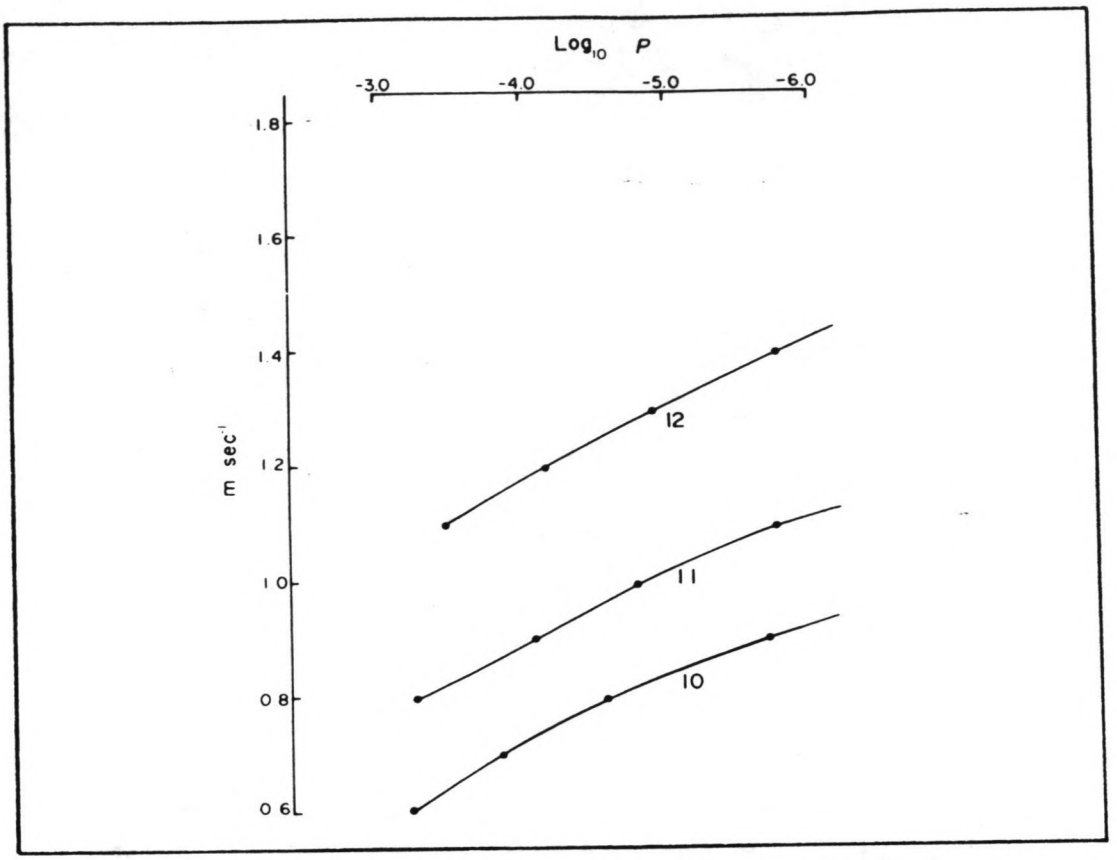

Figure 3.3: Example of presenting joint-probability estimates of extreme total current, in segments 10, 11 and 12.

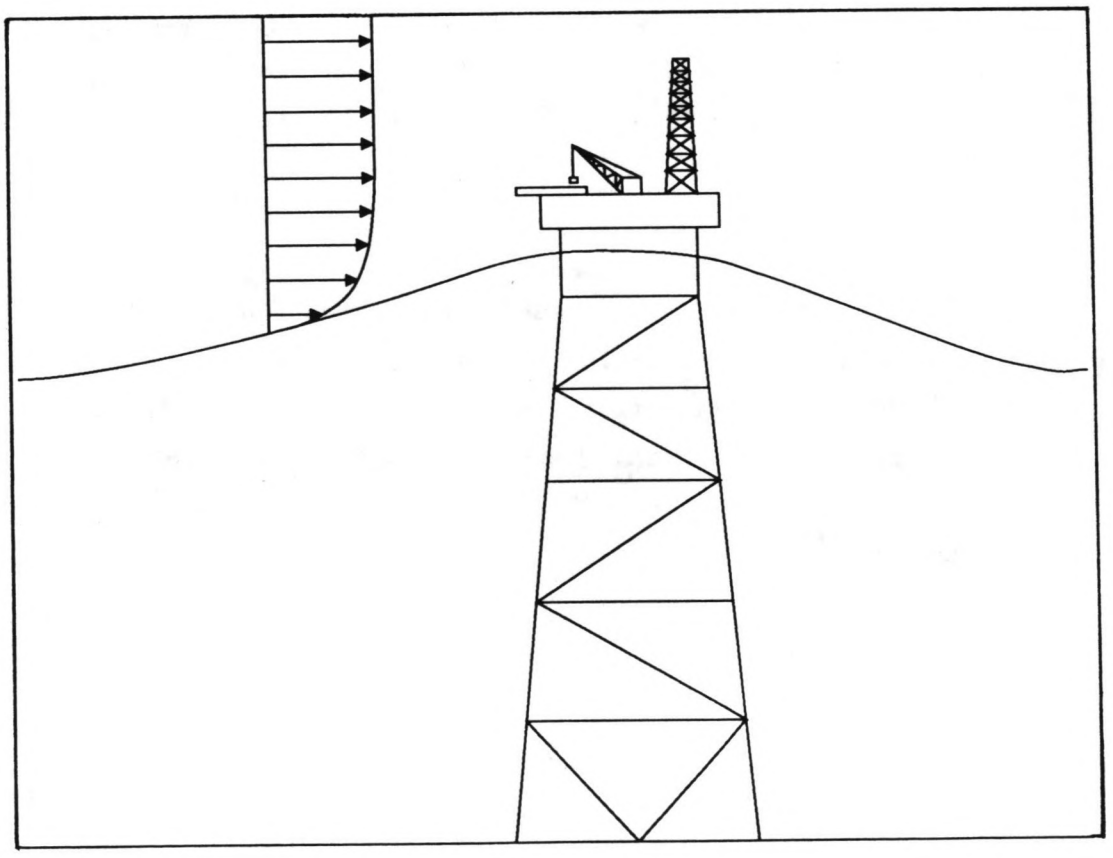

Figure 3.5: Wind average velocity profile.

velocity above mean sea level varies significantly with height due to the boundary layer induced by viscosity (figure 3.5). The speed at a height z above mean sea level can be related to the speed at 10 meters height, W_{10}, according to the relationship:

$$W_z = W_{10}(\frac{z}{10})^{0.100} \quad [m/s] \tag{3.4}$$

For design purposes, it is usual to define a gust wind speed value with a 50 or 100-year return period. In general, design will be most accurate if the wind speed values used for the extrapolation are based on local meteorological data sources (refs. 6,10).

3.5 Extreme loads due to wind, waves and currents

Steel framed jackets in not too deep water can be analysed for extreme structural stresses with acceptable accuracy by assuming a quasi-static structural behaviour of the structure. In this approach, wind and current are assumed to apply static loads with wave action applying a dynamic loading which is translated into dynamic structural stresses through a quasi-static stress analysis. The technique assumes that resonant frequencies of structural vibrations are sufficiently separated from wave frequencies, so that dynamic magnification has a very small effect on calculated stresses.

Theoretically, the problem of finding extreme values for a specific type of load is not more complicated than for any other parameter, such as wave height or a current velocity. Once input data from a sufficiently long period are available, standard statistical procedures can be applied for the assessment of extreme values corresponding to any required return period. Unfortunately, however, input data in terms of many years of recordings of base shear forces or overturning moments are in general not available. Since the joint probability distribution of wind, wave and current action over

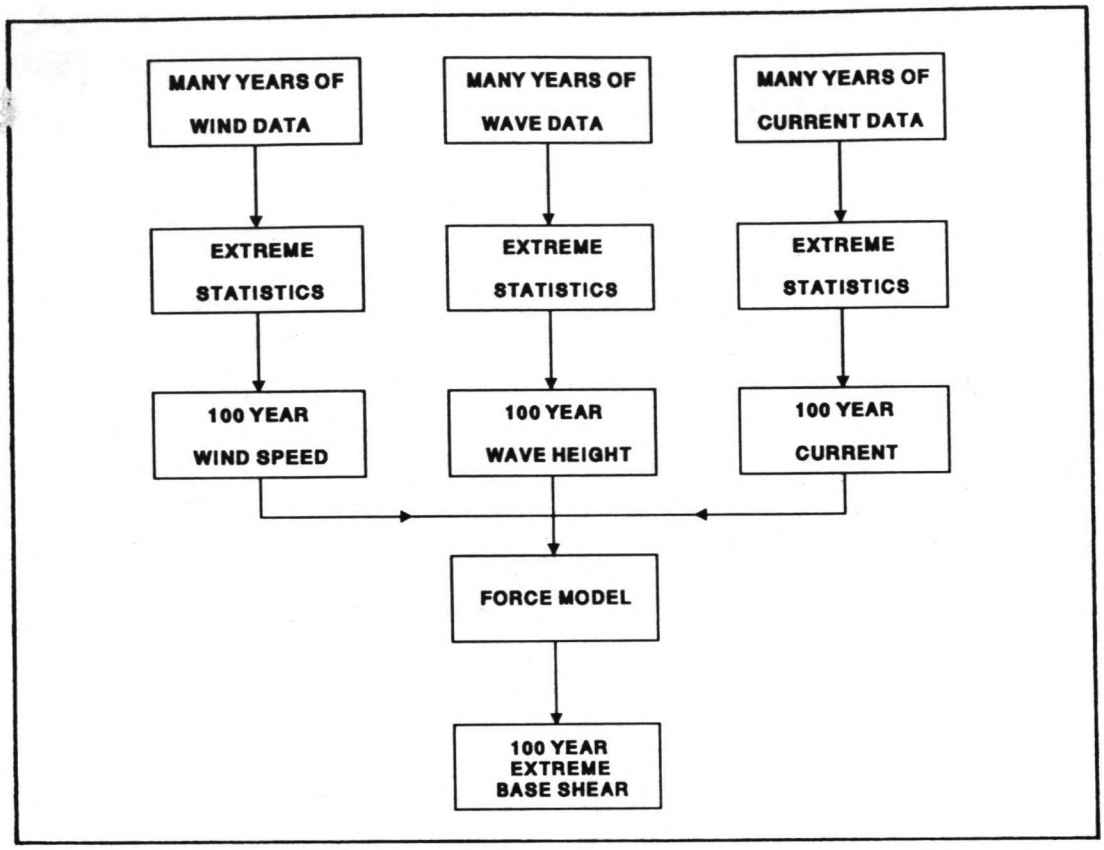

Figure 3.6: Traditional procedure for assessment of extreme values of base shear.

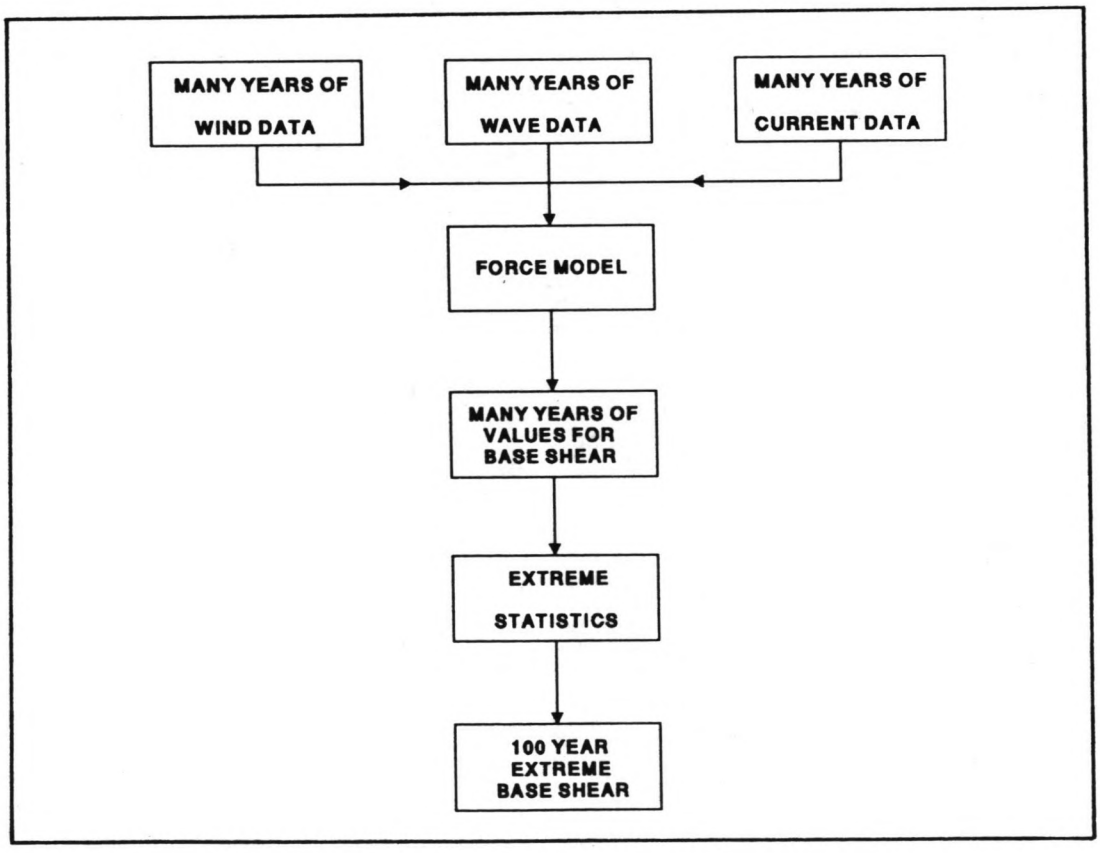

Figure 3.7: Alternative approach accounting for the joint probability and directionality of environmental data.

such long time scales is unknown, the design engineer has to choose a different route to reach his goal.

The route which is traditionally chosen involves the assessment of extreme 50 or 100-year return values of the individual environmental parameters followed by the computation of the base shear and overturning moment induced by these extreme conditions in combination, assuming that they occur simultaneously and act in the same direction (figure 3.6). As stated in paragraph 1.2 this is of course a rather conservative approach.

The importance of joint probability and directionality of wind, wave and current data applied in the design of offshore structures was already investigated by Nielsen a.o. (ref. 7). Their approach involved the computation of the maximum base shear and overturning moment for the worst storms during a three year period of site specific measurements and a subsequent extrapolation to a 50 and 100-year return period (figure 3.7). This resulted in significant reductions of the 100-year values of base shear and overturning moment.

4. THE ANALYTICAL LOAD RELATIONSHIP

4.1 Introduction

Forces on a structural member of an offshore structure due to waves and currents, are commonly determined with the Morison equation (i.e. equation 2.2). By integrating this equation over depth and simplifying it according to some linearisations and assumptions to be mentioned later, an analytical relationship can be established between the global loads on a vertical column (base shear, F, or overturning moment, M) on the one hand, and crest height, a, current velocity, v, and period, T, on the other. In addition to this a term representing the wind force may be added, so that all environmental elements are included.

The result of the analysis is a rather simple equation with wind, wave, and current parameters, multiplied by some constants. These constants can be refined numerically with a computer program, LOAD, that uses more sophisticated kinematics models. Representative hindcast data cab be used as input conditions. Here a case will be considered of single column with constant diameter. Extending the analysis to a real structure may be possible by representing the structure by a group of closely spaced vertical columns, and by simply adjusting the constants in the equation.

4.2 Morison's equation integrated over a single column

The starting point for obtaining an approximate analytical relationship between crest height, a, and base shear, F, is Morison's equation. This equation describes the resultant force per unit length on a single column with constant diameter, submerged to a mean water depth, d, see definition sketch in figure 4.1:

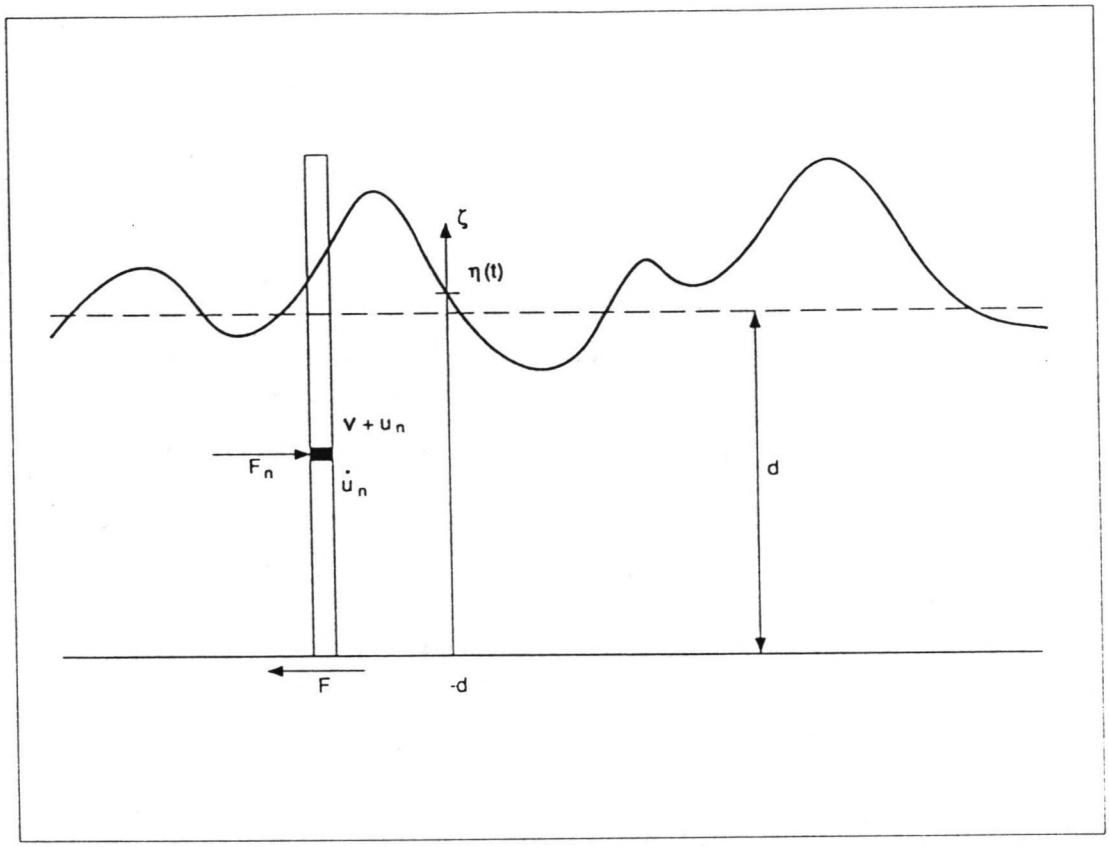

Figure 4.1: Single pile under fluid loading, definition sketch.

$$F_n = A_n \dot{u}_n + B_n (v + u_n)|v + u_n| \tag{4.1}$$

where: $A_n = (C_M \rho \frac{\pi}{4} D^2)_n$

and $B_n = (C_D \rho \frac{1}{2} D)_n$

The horizontal component of water particle velocity is composed of a mean depth current, v, and a wave-induced velocity, u_n, at a point below the surface. Initially only cases are considered where current and wave induced velocity are both in the direction of wave propagation, so that $(v + u_n)$ will always be positive. Equation (4.1) can then be expressed as:

$$F_n = A_n \dot{u}_n + B_n (v + u_n)^2 \tag{4.2}$$

The influence of the wave and current directions will be taken into account in a later stage.

The total base shear, F, can be obtained by integrating F_n over the entire submerged length of the column. A vertical coordinate, ζ, is defined with its origin at mean sea level. The instantaneous water level at the column is $\eta(t)$. Thus:

$$F = \int_{-d}^{\eta} F_n \, d\zeta \tag{4.3}$$

The velocity u_n equals u_o at mean sea level when corrections for non-linearity under large crests are neglected, and can be expressed as a function of the vertical coordinate, ζ. If the waves are assumed to be of small-amplitude and narrow banded, then:

$$u_n = u_o \frac{\cosh k(d+\zeta)}{\sinh kd} \tag{4.4a}$$

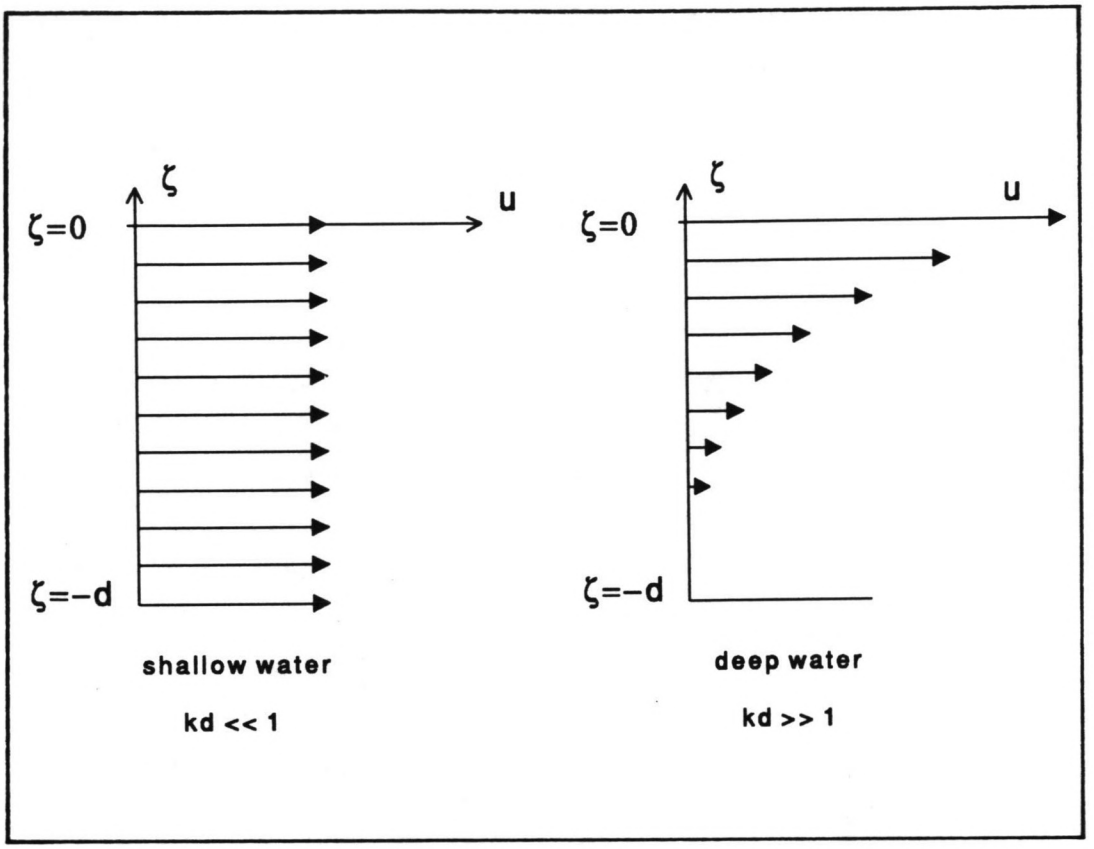

Figure 4.2: Wave induced fluid partical velocity profile for shallow and deep water conditions.

where k is the wave number (ref. 1). The corresponding accelerations, $\dot{u}_n$, can be obtained according to a similar relation:

$$\dot{u}_n = \dot{u}_o \frac{\cosh k(d+\zeta)}{\sinh kd} \tag{4.4b}$$

Assuming that kd is very large, i.e. only deep water cases are considered, these expressions can be simplified into (see figure 4.2):

$$u_n = u_o e^{k\zeta} \tag{4.5a}$$

and

$$\dot{u}_n = \dot{u}_o e^{k\zeta} \tag{4.5b}$$

However, waves that are likely to generate an extreme response are large-amplitude waves, for which equations (4.5a) and (4.5b) overpredict the velocities and accelerations in the wave crests. Therefore a technique called delta-stretching has been developed. It is a simple empirical correction involving a linear transformation of the ζ axis in the linear theory (ref. 11). It is characterized by two parameters: the stretching depth, D_s, and the stretching parameter, ∇. If $\zeta > -D_s$ it is replaced in equation (4.3) by ζ_s, where:

$$\zeta_s = (\zeta + D_s) \frac{\eta\nabla + D_s}{\eta + D_s} - D_s \tag{4.6}$$

where D_s is typically set to one half of the significant wave height, H_s, and ∇ typically equals 0.3.

Integrating equation (4.2) over depth involves the integration of the inertia term, $A_n\dot{u}_n$, and the drag term, $B_n(v + u_n)^2$. A_n and B_n are depth dependent parameters. For this study A_n and B_n are taken as constants A and B for $\zeta \leq 0$, and A_s and B_s for $\zeta > 0$, taking into account the change in inertia and drag coefficients due to fouling by marine life below mean sea level.

Working out equation (4.3) results in:

$$F = \int_{-d}^{\eta} A_n \dot{u}_n d\zeta + \int_{-d}^{\eta} B_n v^2 d\zeta + \int_{-d}^{\eta} 2B_n v u_n d\zeta + \int_{-d}^{\eta} B_n u_n^2 d\zeta \qquad (4.7)$$

For example integration of the inertia term gives as a result:

$$\int_{-d}^{\eta} A_n \dot{u}_n d\zeta = \frac{A}{k}\dot{u}_o e^{-kD_s} + \frac{\eta+D_s}{\eta\nabla+D_s}\cdot\frac{A}{k}\dot{u}_o\left[e^{kD_s\frac{\nabla\eta(\nabla-1)}{\eta+D_s}} - e^{-kD_s} + \frac{A_s}{A}\left\{e^{k\nabla\eta} - e^{kD_s\frac{\nabla\eta(\nabla-1)}{\eta+D_s}}\right\}\right] \qquad (4.8)$$

Since only deep water conditions are considered here, a term with e^{-kd} has been neglected. For $x << 1$ an exponential term $e^{\pm x}$ can be approximated by its first order Taylor series into $(1 \pm x)$. So expressions like equation (4.8) can be simplified by linearisations of the exponential terms.

$$e^{-kD_s} \simeq 1 - kD_s \qquad (4.9a)$$

$$e^{k\eta\nabla} \simeq 1 + k\eta\nabla \qquad (4.9b)$$

$$e^{kD_s\frac{\nabla\eta(\nabla-1)}{\eta+D_s}} \simeq 1 + kD_s\frac{\nabla\eta(\nabla-1)}{\eta+D_s} \qquad (4.9c)$$

So for each term a simplified expression can be obtained:

$$\int_{-d}^{\eta} A_n \dot{u}_n d\zeta = \frac{A}{k}(1 + \frac{A_s}{A}k\eta)\dot{u}_o \qquad (4.10)$$

$$\int_{-d}^{\eta} B_n v^2 d\zeta = Bd(1 + \frac{B_s}{B}\frac{\eta}{d})v^2 \qquad (4.11)$$

$$\int_{-d}^{\eta} 2B_n v u_n d\zeta = \frac{2B}{k}(1 + \frac{B_s}{B}k\eta)vu_o \qquad (4.12)$$

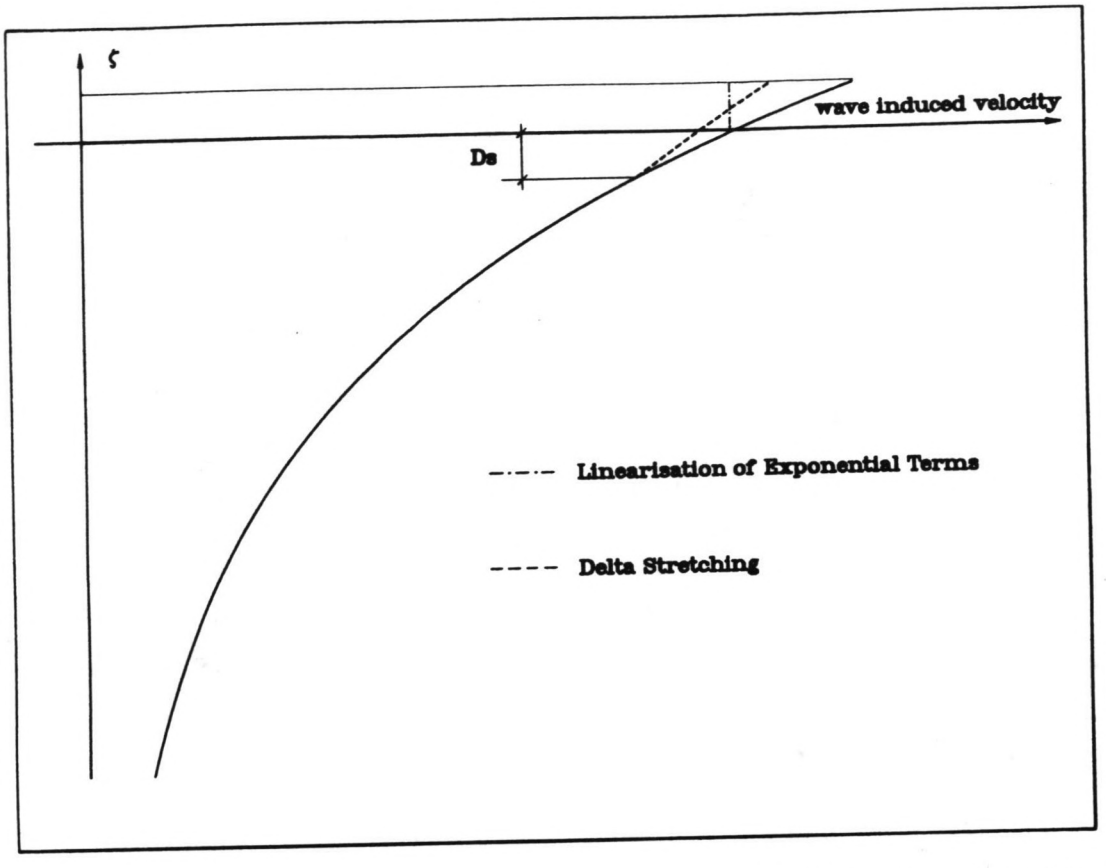

Figure 4.3: The effect of delta stretching compared to linearisation of exponential terms.

$$\int_{-d}^{\eta} B_n u_n^2 d\zeta = \frac{B}{2k}(1 + 2\frac{B_s}{B}k\eta)u_o^2 \qquad (4.13)$$

Linearisation of the exponential terms near mean sea level eliminates the delta-stretching parameters so that they do not appear in the approximations above, but for global loading calculations it is almost exactly equivalent to delta-stretching as shown in figure 4.3 (ref. 16). As a result of the integration of equation (4.2), using the approximations mentioned above, the base shear force, which is the total integrated force due to waves and currents under a wave crest, is given by:

$$F = \frac{A}{k}\dot{u}_o(1 + \frac{A_s}{A}k\eta) + Bv^2 d(1 + \frac{B_s}{B}\frac{\eta}{d}) + \frac{2vB}{k}u_o(1 + \frac{B_s}{B}k\eta) + \frac{Bu_o^2}{2k}(1 + 2\frac{B_s}{B}k\eta)$$

(4.14)

This expression includes non-linear free surface effects and changes in the force coefficients due to marine roughness. The $k\eta$-term in the equation is of the same order as the wave slope, which is generally small in deep water. So $\eta << k^{-1}$ and also, again based upon the deep water assumption, $k^{-1} << d$, thus the η/d correction to the current-induced drag term can be neglected safely.

Equation (4.14) would be more practical if $\dot{u}_o$ could be substituted with some function of u_o. This may be an approximate function, since extreme base shear forces on steel structures tend to be drag dominated, so the inertial contribution is expected to be small, that is:

$$\frac{A}{k}\dot{u}_o(1 + \frac{A_s}{A}k\eta) << \text{Extreme } (F) \qquad (4.15)$$

In this sense it may be useful to consider the peak force, $\hat{F}$, which occurs during the passage of a wave, rather than the instantaneous force, F(t). Since the horizontal wave-induced particle velocities are in phase with the

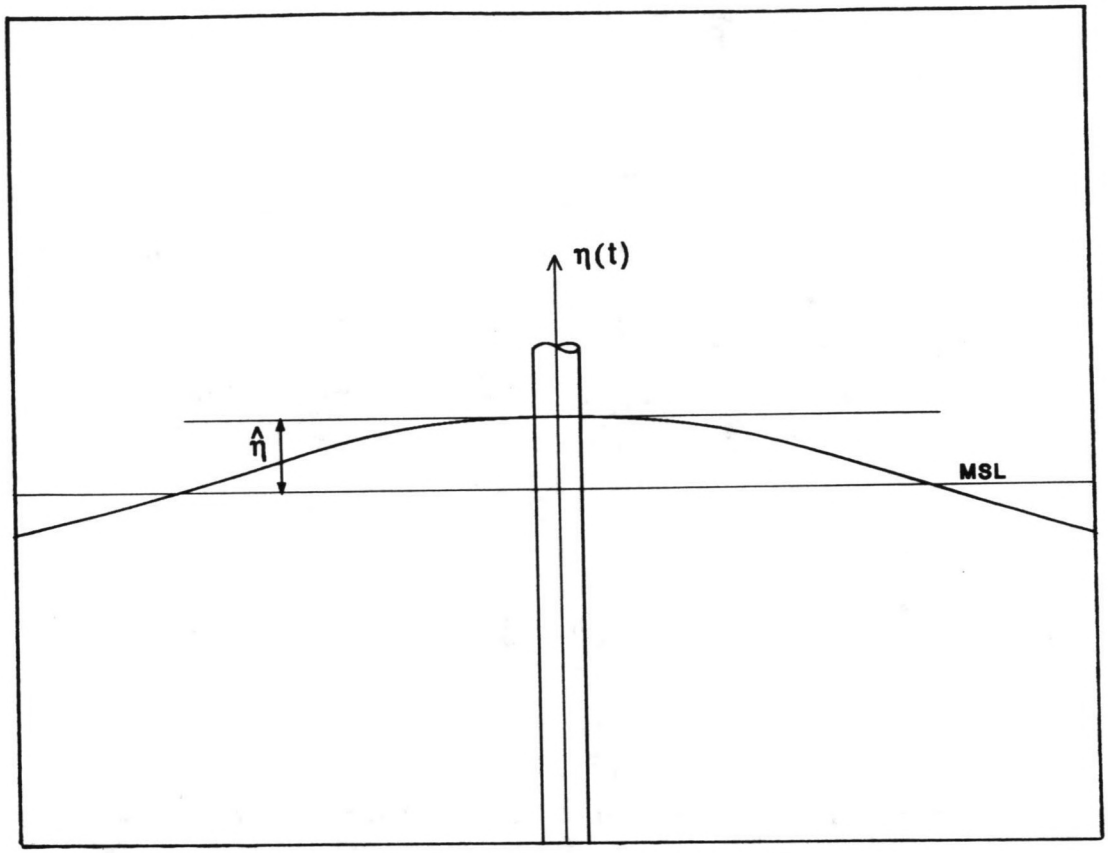

Figure 4.4: Surface elevation profile during the passage of a large wave.

surface elevation, a maximum drag force comes simultaneously with a peak value of surface elevation, $\hat{\eta}$. Considering peak values only and assuming that the waves are nearly narrow-banded, the wave-induced velocity can be approximated by:

$$u_o \simeq \hat{u} \cos \psi \tag{4.16a}$$

$$\dot{u}_o \simeq -\hat{u}\omega \sin \psi \tag{4.16b}$$

$$\eta \simeq \hat{\eta} \cos \psi \tag{4.16c}$$

where $\hat{u}$ is a slowly varying amplitude that defines the peaks in u_o and $\psi=\omega t$, a smoothly varying phase defined such that $\psi=0$ at a wave crest. The instantaneous surface elevation, $\eta(t)$, relatively hardly varies near the peak of a passing wave (figure 4.4).

Approximations (4.16a) and (4.16b) can be further reduced by taking the first order Taylor series of the cos-term, since ψ will be small for small inertial contributions, so:

$$\hat{u} \cos \psi \simeq \hat{u}(1 - \psi^2/2) \tag{4.17a}$$

$$-\hat{u}\omega \sin \psi \simeq -\hat{u}\omega\psi \tag{4.17b}$$

Substitution of these approximations in equation (4.14) yields:

$$F = -\frac{A}{k}\hat{u}\omega\psi(1+\frac{A_s}{A}k\hat{\eta}) + Bdv^2 + \frac{2B}{k}\hat{v}u(1+\frac{B_s}{B}k\hat{\eta}) + \frac{B}{2k}\hat{u}^2(1+2\frac{B_s}{B}k\hat{\eta}) - \ldots$$

$$\ldots[v(1+\frac{B_s}{B}k\hat{\eta})\frac{B}{k} + \hat{u}(1+2\frac{B_s}{B}k\hat{\eta})\frac{B}{2k}]u\psi^2 \tag{4.18}$$

where terms with ψ^4 have been neglected, since ψ is small in the vicinity of the crest. The instantaneous force is at its maximum value when the

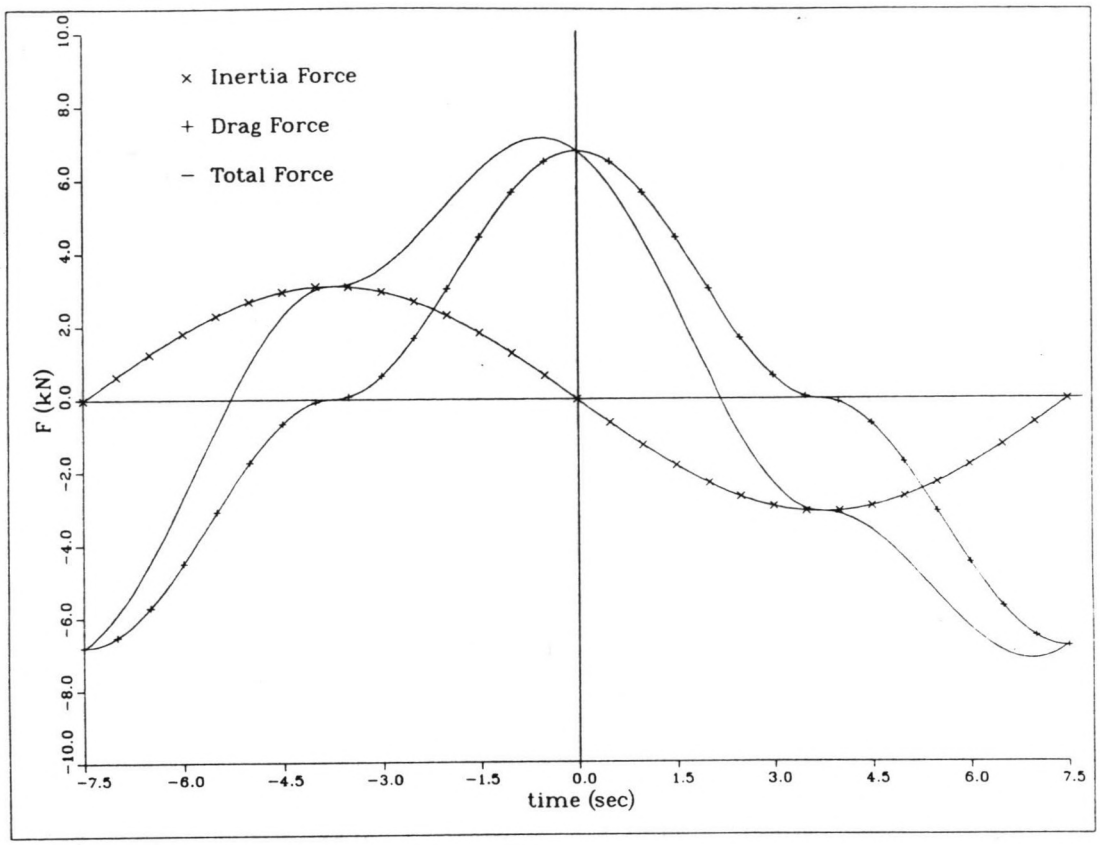

Figure 4.5: Typical wave force time history profile during the passage of a large wave.

derivative of the force with respect to the phase angle, ψ, equals zero. Physically this implies for drag dominant fluid forces, that the peak force, $\hat{F}$, occurs shortly before the wave crest passes the column (figure 4.5). Thus at peaks in F, $dF/d\psi = 0$ or:

$$\psi = -\frac{A\omega}{2k}\frac{(1+A_s k\hat{\eta}/A)}{v(1+B_s k\hat{\eta}/B)B/k + \hat{u}(1+2B_s k\hat{\eta}/B)B/2k} \tag{4.19}$$

and

$$-\frac{A\omega}{k}\hat{u}\psi(1+A_s k\hat{\eta}/A) - [v(1+B_s k\hat{\eta}/B)+\hat{u}(1+2B_s k\hat{\eta}/B)B/2k]\hat{u}\psi^2 = \ldots$$

$$\ldots = \frac{A^2\omega^2}{2Bk}\frac{(1+A_s k\hat{\eta}/A)^2}{2v/\hat{u}(1+B_s k\hat{\eta}/B) + 1 + 2B_s k\hat{\eta}/B} \simeq \frac{A^2\omega^2}{2Bk}\frac{1}{2v/\hat{u} + 1}$$

Since $A_s/A < 1$, $B_s/B < 1$ and $\hat{\eta} \ll k^{-1}$, the correction terms $A_s k\hat{\eta}/A$ and $B_s k\hat{\eta}/B$ in this expression have been omitted, because they represent small corrections on an already small quantity. Thus finally the following equation for maximum base shear force in a single wave is obtained:

$$F = \frac{A^2\omega^2}{2Bk}\frac{1}{2v/u + 1} + Bdv^2 + \frac{2B}{k}vu(1+\frac{B_s}{B}k\eta) + \frac{B}{2k}u^2(1+2\frac{B_s}{B}k\eta) \tag{4.20}$$

Though the caps (^) over F, u and η have been omitted for convenience, it has to be emphasized that this equation strictly refers to peak values only. Nevertheless, especially when F is large, the base shear force will be drag dominated, so that the inaccuracies, which will develop only in the inertial term, will be small.

To facilitate the calibration of the constants in the loading equation and the generation of base shear statistics some of the parameters will be substituted, so that data derived from the NESS database can be used as an input. Since $\eta = u_o/\omega$, where ω is the peak frequency of ocean surface

elevation, and $u_o = \omega^* a$ in view of the assumption of deep water, η in the equation can be replaced by crest height, a. According to the dispersion relation for deep water ω^2 equals gk, so wave number k can be written down as ω^2/g. Substitution of these changed parameters in equation (4.20) yields:

$$F = \frac{A^2 g}{2B} \frac{\pi a}{vT + \pi a} + Bdv^2 + \frac{Bg}{\pi} vaT + 4\pi B_s \frac{va^2}{T} + \frac{Bg}{2} a^2 + 4\pi^2 B_s \frac{a^3}{T^2} \quad (4.21)$$

where $T = \frac{2\pi}{\omega}$, the peak period of ocean surface elevation. With this equation a relationship between crest height, a, and base shear, F, has been established. For a particular structure, here a single column, A, B and B_s are considered to be constant. Now equation (4.21) gives base shear, F, as a function of three parameters: crest height, a, current velocity, v, and wave period, T. Thus:

$$F(a,v,T) = A^* \frac{\pi a}{vT + \pi a} + B^* v^2 + C^* vaT + D^* \frac{va^2}{T} + E^* a^2 + F^* \frac{a^3}{T^2} \quad (4.22)$$

where A^*, B^*, C^*, D^*, E^*, and F^* are constants related to the structure.

The analytical relationship according to equation (4.22) still does not contain all environmental conditions. Current and waves are considered, but wind and directional spreading of the waves have to be taken into account as well. Moreover waves and current are assumed to act in the same direction, so a reduction of current, v, related to the angle between the direction of wave propagation and current direction, is required.

4.3 Wave and current directions

The loading equation (4.22) generated in the previous paragraph assumes that waves and currents act in the same direction. This leads to an overestimate

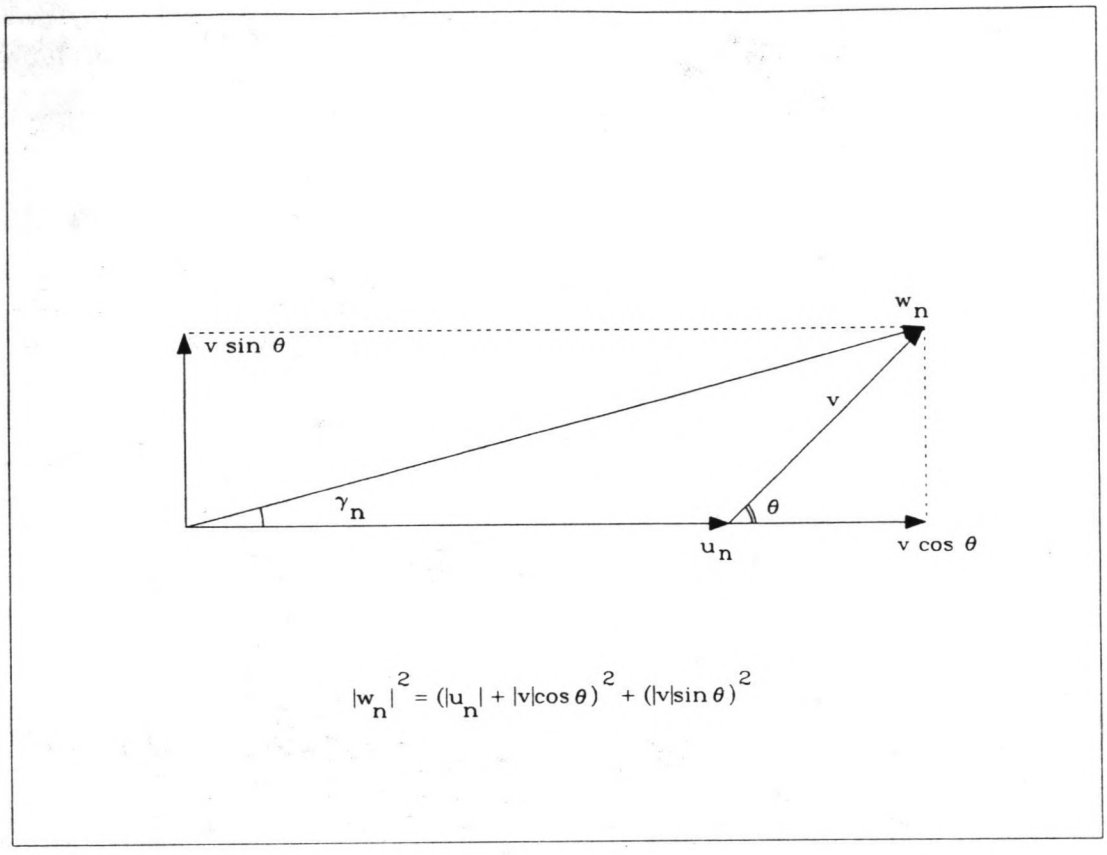

Figure 4.6: Resultant horizontal fluid particle velocity due to waves and currents, acting under a mutual angle θ.

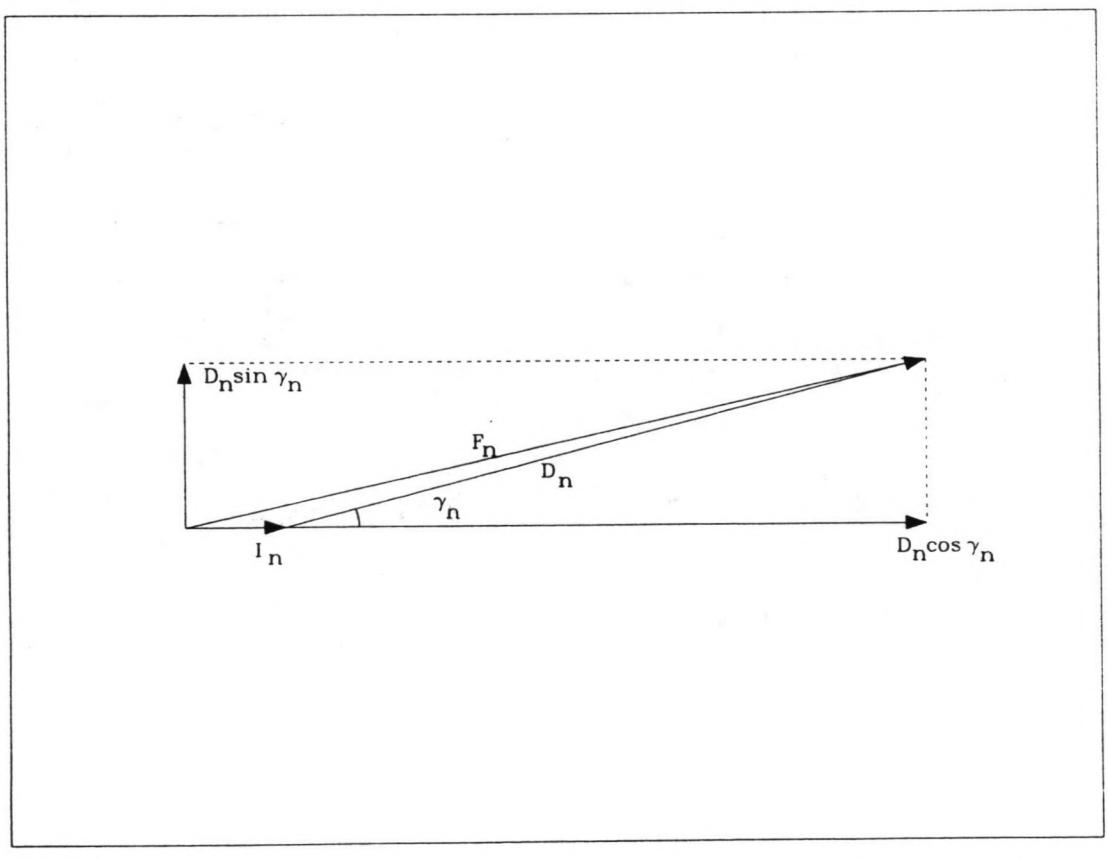

Figure 4.7: Resultant horizontal loading, F_n, due to drag and inertia components, acting under a mutual angle γ_n.

of the structural loading, since waves and currents with the same direction are the exception, rather than the rule. To account for the influence of the directions on the loading an extra parameter is introduced: θ, the angle between the wave direction and the current direction.

If w_n is the resultant horizontal fluid particle velocity due to waves and currents, then equation (4.2) can be rewritten as:

$$F_n = I_n + D_n = A_n \dot{u}_n + B_n w_n^2 \tag{4.23}$$

Figure (4.6) shows that the drag term in this equation can be expressed as:

$$D_n = B_n[(u_n + v*\cos\theta)^2 + (v*\sin\theta)^2]$$

$$D_n = B_n(u_n^2 + 2u_n v*\cos\theta + v^2) \tag{4.24}$$

Since directions are involved, the inertia and drag force in equation (4.23) do not necessarily act in the same direction, and they have to be added as vectors (figure 4.7).

$$\underline{F}_n = \underline{I}_n + \underline{D}_n \tag{4.25}$$

$$|\underline{F}_n|^2 = (|\underline{I}_n| + |\underline{D}_n|*\cos\gamma_n)^2 + (|\underline{D}_n|*\sin\gamma_n)^2 \tag{4.26}$$

where γ_n is the depth dependent angle between the direction of the waves and the drag force. This angle equals θ near the sea bottom (figure 4.8).

If the influence of γ_n is ignored then an equation like (4.23) remains, which is easy to integrate.

$$F = \int_{-d}^{\eta} A_n \dot{u}_n d\zeta + \int_{-d}^{\eta} B_n(u_n^2 + 2u_n v*\cos\theta + v^2)d\zeta \tag{4.27}$$

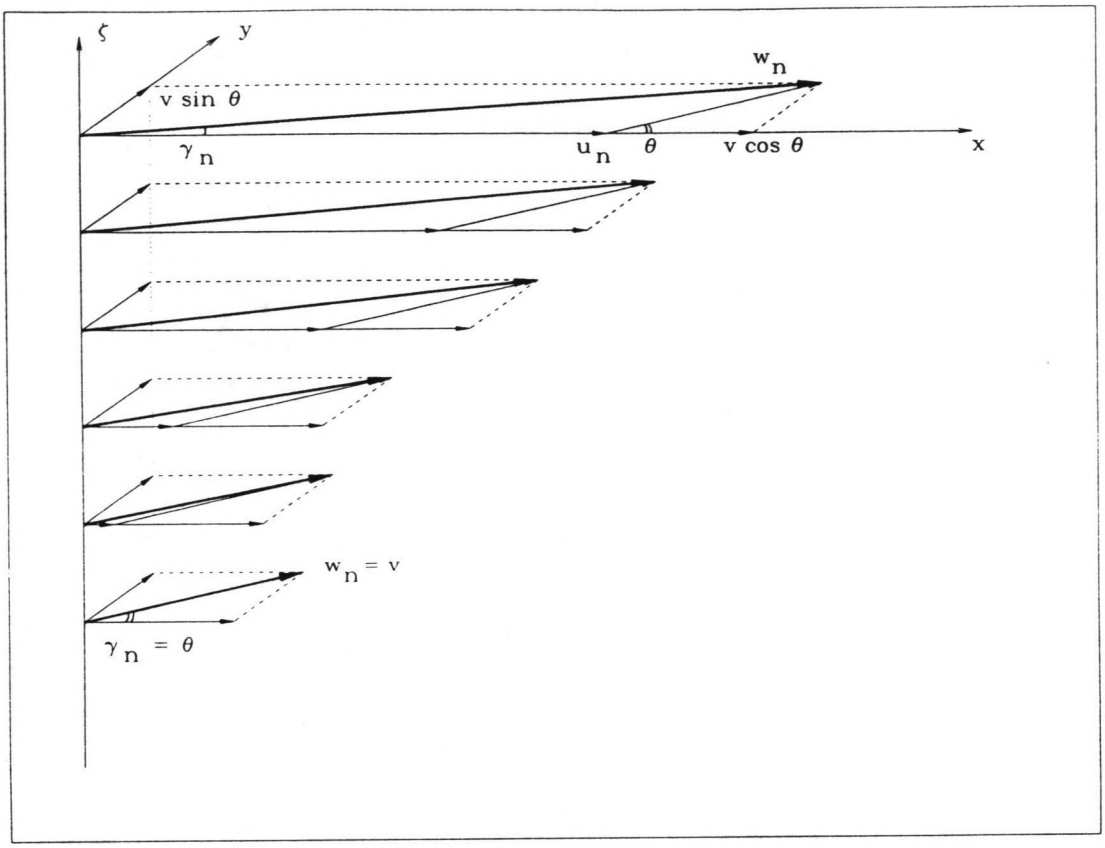

Figure 4.8: The variation with depth of the angle between the inertia and drag force.

For $\theta = 0$ this equation reduces to (4.7) and even for small theta's the assumption that $\gamma_n \simeq 0$ over the whole depth is appropriate. However, this is not the case if θ has a relatively large value. Near the sea surface, where under extreme conditions the wave-induced velocity will be much larger than the current velocity, γ_n will always be relatively small, no matter what value θ has. In deeper water, however, where the wave-induced velocity decreases to zero and the current will predominate, the influence of γ_n becomes more significant. By ignoring the influence of γ_n the resultant drag force is assumed to act "in-line" with the inertia force, i.e. in the direction of wave propagation, over the whole depth. So equation (4.27) will result in an overestimate of the total base shear. This effect is mainly of influence for negative currents, thus when: $90 < \theta < 270$ deg, but generally it will be small because of the wave drag dominance.

Working out equation (4.27) according to the analysis described in the previous paragraph results in an analytical relationship similar to (4.22).

$$F(a,v,T,\theta) = A^* \frac{\pi a}{vT\cos\theta+\pi a} + B^* v^2 + C^* vaT\cos\theta + D^* \frac{va^2\cos\theta}{T} + E^* a^2 + F^* \frac{a^3}{T^2} \qquad (4.28)$$

The main problem with putting the directions into the model is that two more or less conflicting goals have to be achieved: on the one hand the model has to describe the behaviour of the loading as accurately as possible and for as many different cases as possible; on the other hand the expression for force, F_n, on a certain depth cannot be too complex like in equation (4.26), because it has to be integrated over depth and result in an analytical relationship which has to be invertable. However, if certain assumptions would lead to for example a general overestimate of the base shear, this can be partly compensated in the calibration of the constants, since these constants are adjusted to match numerical simulations using representative NESS data as an input.

4.4 Wind forces

To take account of the forces due to wind an extra term is put in equation (4.28). An expression for the wind generated drag force in the direction of the waves is given by:

$$F_W = C_W W^2 \cos\theta_W \tag{4.29}$$

where C_W is defined as:

$$C_W = \frac{1}{2} \rho_a S C_D \tag{4.30}$$

So an extra term is added to equation (4.28), dependent on windspeed, W, wind direction - or to be more specific the angle between wind and wave direction - θ_W, air density, ρ_a, a drag coefficient, C_D, and a representative topside area, S. A representative additional wind force term is with:

$$C_W = 0.1 \quad kg/m \tag{4.31}$$

This would lead to a contribution by the wind of 10 % to the total base shear under a conventional design condition of 12.5 m crest height and 1 m/s in-line current.

4.5 Directional spreading

A two-dimensional surface elevation spectrum is defined as $S_{\eta\eta}(\omega,\Theta)$; that is a function of wave frequency, ω, and wave direction, Θ. In the case of directional spreading this spectrum is related to the frequency spectrum $S_{\eta\eta}(\omega)$ by:

$$S_{\eta\eta}(\omega,\Theta) = G(\Theta)\ S_{\eta\eta}(\omega) \tag{4.33}$$

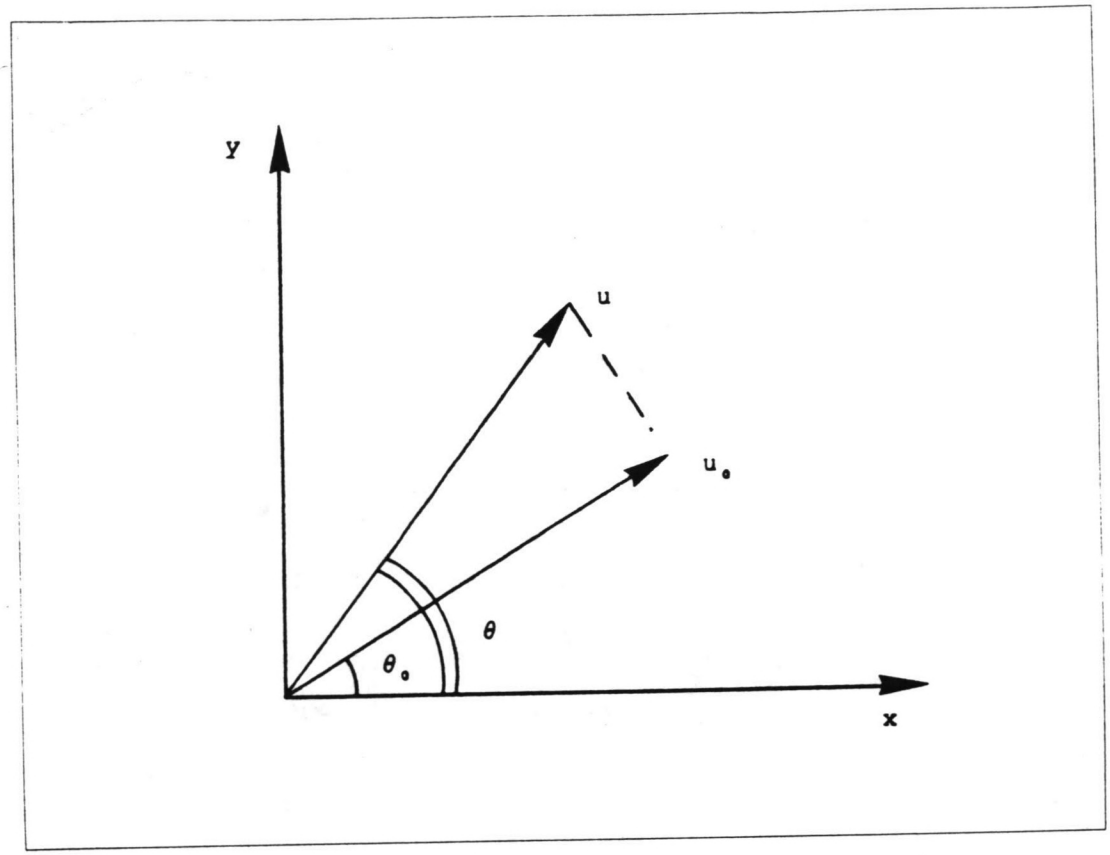

Figure 4.9: Directional spreading.

where $G(\Theta)$ is an angular spreading function. The two-dimensional spectrum of the horizontal fluid particle velocity can then be written as:

$$S_{uu}(\omega,\Theta) = \omega^2 \, S_{\eta\eta}(\omega) \, G(\Theta) \, \cos^2\Theta \tag{4.34}$$

The directional spreading in the wave process leads to a reduction in the variance of the velocity and acceleration in the mean direction of the waves (figure 4.9). This means that less energy is transported in the main wave direction, which causes a reduction of the wave induced water particle velocities and accelerations. The variance of the directional velocity component in the mean direction is:

$$\sigma_u^2 = \int_{-\infty}^{\infty} \int_{-\pi}^{\pi} \omega^2 \, S_{uu}(\omega) \, G(\Theta) \, \cos^2\Theta \, d\omega \, d\Theta \tag{4.35}$$

The variance of the velocity in a uni-directional sea with the same frequency spectrum of surface elevation is given by:

$$\sigma_{u_o}^2 = \int_{-\infty}^{\infty} \int_{-\pi}^{\pi} \omega^2 \, S_{uu}(\omega) \, G(\Theta) \, d\omega \, d\Theta = \int_{-\infty}^{\infty} S_{uu}(\omega) \, d\omega \tag{4.36}$$

In equation (4.28) the wave field is considered to be uni-directional, so that a reduction of the wave induced particle velocities and accelerations due to directional spreading is not taken into account. A correction should be applied to several terms in the equation accounting for this effect. The reduction factor for directional spreading is given by:

$$\Phi^2 = \frac{\sigma_u^2}{\sigma_{u_o}^2} = \int_{-\infty}^{\infty} G(\omega) \, \cos^2\Theta \, d\Theta \tag{4.37}$$

One way to describe the spreading function $G(\Theta)$ is to assume that it follows the shape of a normal density function (figure 4.10), so that:

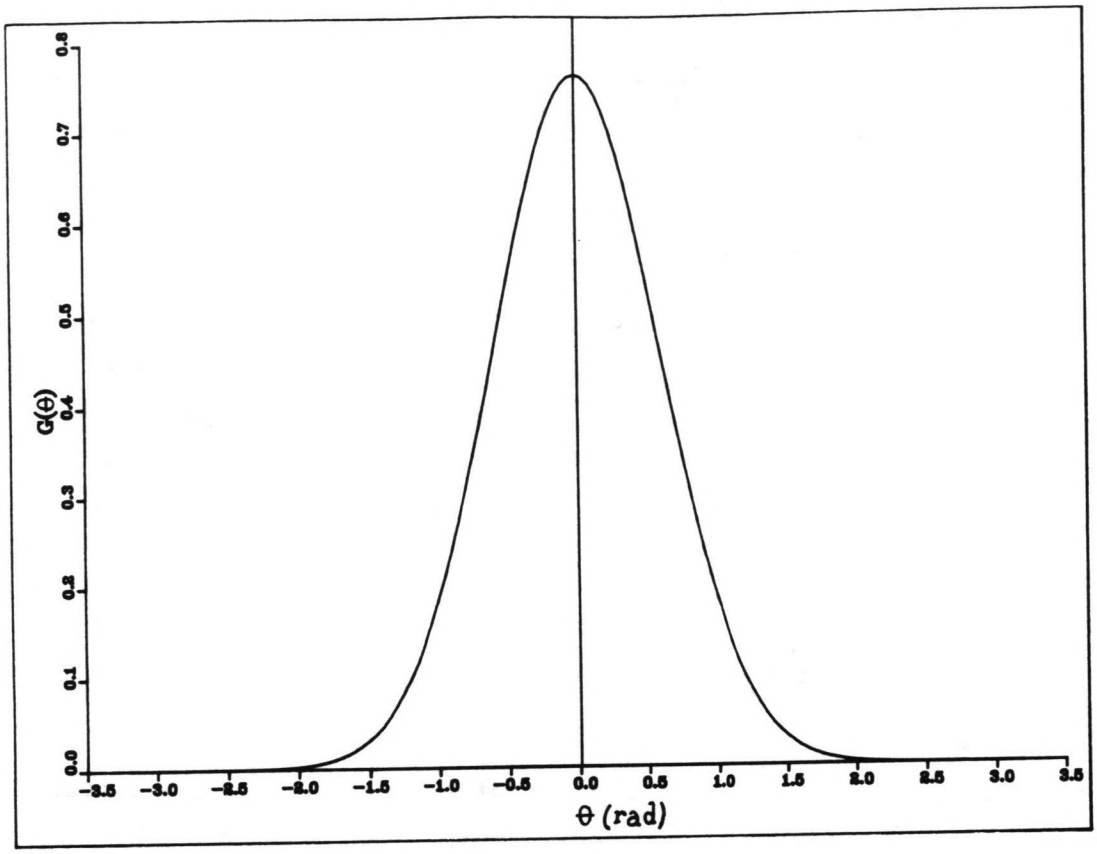

Figure 4.10: Spreading function G(θ) with the shape of a normal density function.

$$G(\Theta) = \frac{1}{\sqrt{(2\pi)}\ \sigma_\theta} \exp\left(\frac{-\Theta^2}{2\sigma_\theta^2}\right) \tag{4.38}$$

where σ_θ is the directional spreading parameter, as given in the NESS data base. Substituting $G(\Theta)$ in equation (4.37) by this function yields:

$$\Phi^2 = \frac{1}{\sqrt{(2\pi)}\ \sigma_\theta} \int_{-\pi}^{\pi} \exp\left(\frac{-\Theta^2}{2\sigma_\theta^2}\right) = \frac{1}{2}\left(1 + \exp(-2\sigma_\theta^2)\right) \tag{4.39}$$

This expression can be further reduced by taking the second order Taylor series, so that:

$$\Phi = (1 - \sigma_\theta^2 + \sigma_\theta^4)^{\frac{1}{2}} \tag{4.40}$$

Taking the reduction due to directional spreading into account and also the wind contribution, the load equation becomes:

$$F = A^* \frac{\pi a}{vT\cos\theta + \pi a} + B^* v^2 \cos^2\theta + C^* \Phi v a T \cos\theta + D^* \Phi \frac{v a^2 \cos\theta}{T} + \ldots$$

$$\ldots E^* \Phi^2 a^2 + F^* \Phi^2 \frac{a^3}{T^2} + C_W W^2 \cos\theta_W \tag{4.42}$$

4.6 Current blockage

Up till now only the single column case has been considered. The analysis may be extended to a real structure, modelled by a group of closely spaced vertical piles, by multiplying all the terms with an adaption factor. In the calculations a steady current measured or estimated for an open sea is used. However, the average current within a structure is lower than that far upstream, due to the divergence of the flow (figure 4.11). This influence would lead to a significant overestimate of the current components in the

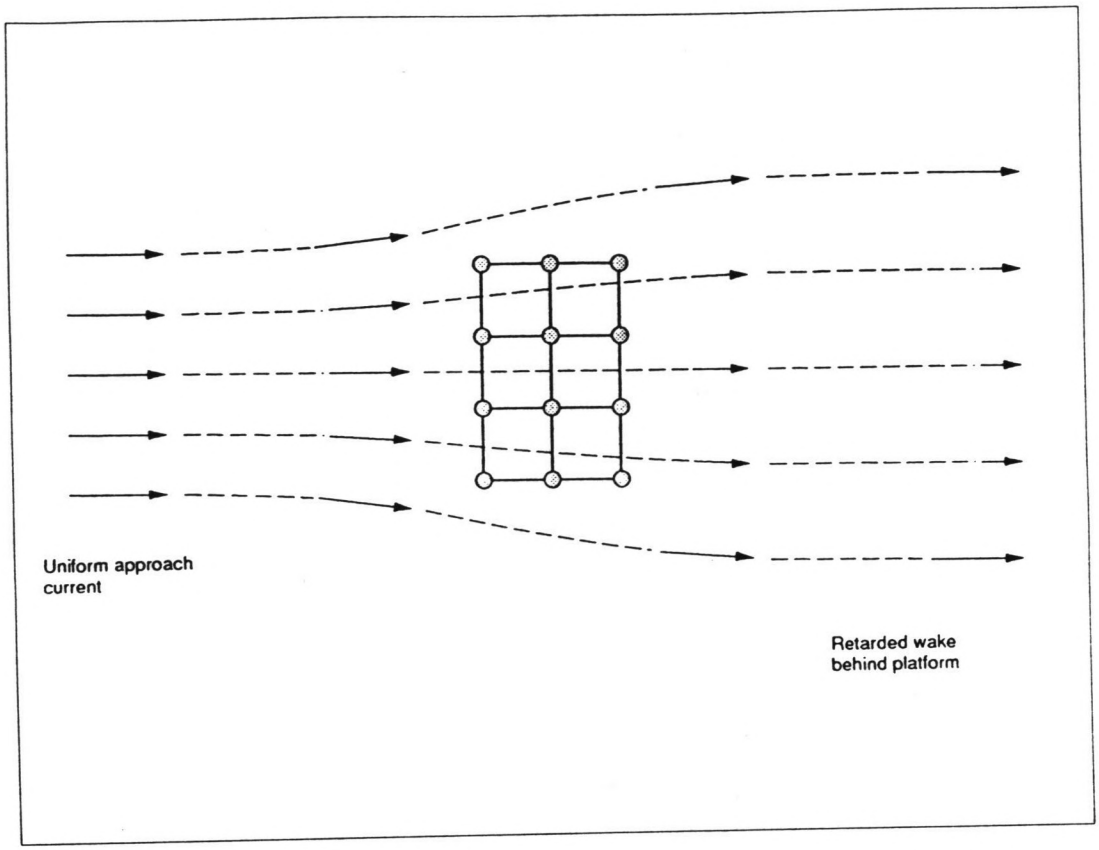

Figure 4.11: Flow field divergence around a steel jacket in a uniform current.

loading equation. Therefore this effect is taken into account by introducing a blockage factor (ref. 14). This factor reduces the current, v, according to:

$$v_s = v \left(\frac{1}{1 + C_D A/4A_c}\right) \qquad (4.43)$$

where A is the projected area of the structural elements, as used in the Morison equation, and A_c is the area normal to the direction of flow enclosed by the cross-section of the structure. The ratio A/A_c typically equals 1, so that with a drag coefficient of value $C_D = 1.2$ the blockage factor reducing the current, v, for this study is estimated to be 0.77.

4.7 Calibration of constants

In the previous paragraphs an analytical relationship has been established for a loading on an offshore structure due to wind, waves and current, including all environmental elements. This equation will be used for load statistics and therefore should be representative for various environmental storm conditions within a range of interest. The constants which appear in the equation can be calibrated against a numerical loading model, for representative data, taken from the NESS data base.

For this purpose a computer program was used, which calculates the fluid load (base shear and overturning moment) on vertical piles separated from each other, by numerical integration over depth. The individual piles are used to simulate lumped circular members, corner posts and gusset plates (when present).

For some representative storm data the loads on a single column with constant diameter submerged in a mean water depth, d, are calculated analytically with the relationship according to equation (4.28) on the one hand, and numerically with the LOAD-program on the other. The results of

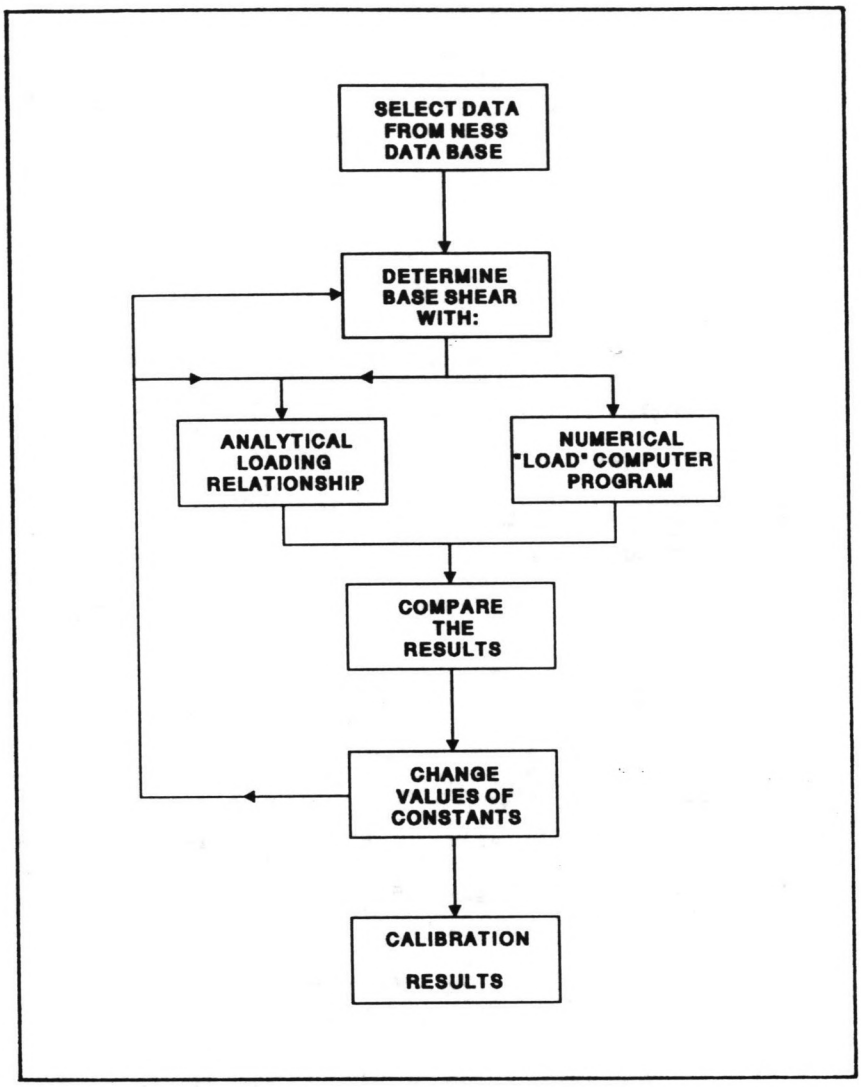

Figure 4.12: Calibration procedure flow diagram.

both calculations are compared and the constants in the equation are adjusted in such a way that for all selected storm data the analytical answers are in as close agreement as possible with the numerical values (figure 4.12). As an illustration figure 4.13 gives the storm history of the significant wave height, H_s, wave period, T_p, current velocity, v, and wind speed, W, for an example storm, S_j.

4.7.1 The base shear model

From the NESS data base twelve representative cases were selected over a range of significant wave height of 5.7 m to 11.2 m. With the LOAD-computer program mentioned above the total base shear for every particular case was calculated and then used as an input for the analytical relationship, looking for the best fit of the constants. First the influence of the current direction was ignored, assuming that current and waves had the same direction (equation 4.22), leading to an overestimate of the base shear, but helpful for the calibration. An obvious method for calibrating the constants seemed to be a linear regression process. However, although this analysis gave the best fitting results, some constants became negative, loosing their physical significance. Therefore another approximation was chosen. All the constants can be written in terms of physical constants and coefficients; according to equation (4.21) this yields:

$$A^* = \frac{A^2 g}{2B} \tag{4.44a}$$

$$B^* = Bd \tag{4.44b}$$

$$C^* = \frac{Bg}{\pi} \tag{4.44c}$$

$$D^* = 4\pi B_s \tag{4.44d}$$

$$E^* = \frac{Bg}{2} \tag{4.44e}$$

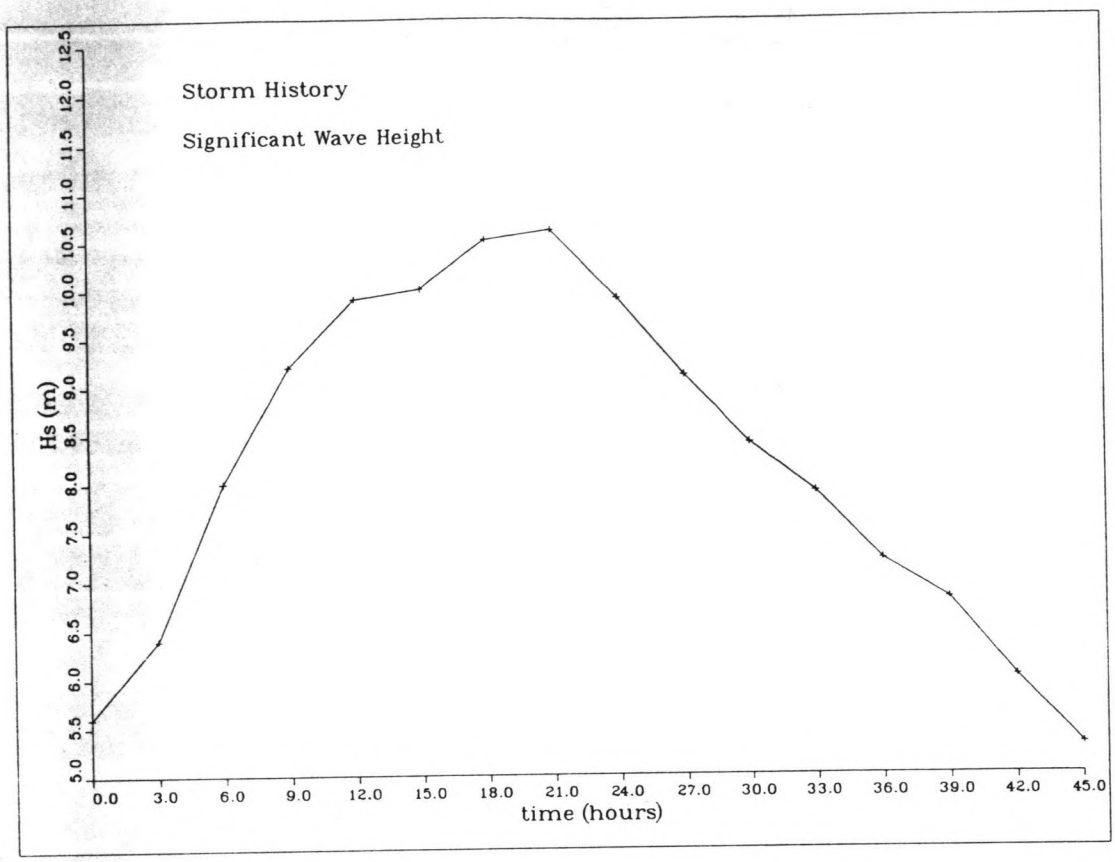

Figure 4.13a: Storm history of significant wave height, H_s, of example storm (27 to 29 november 1969).

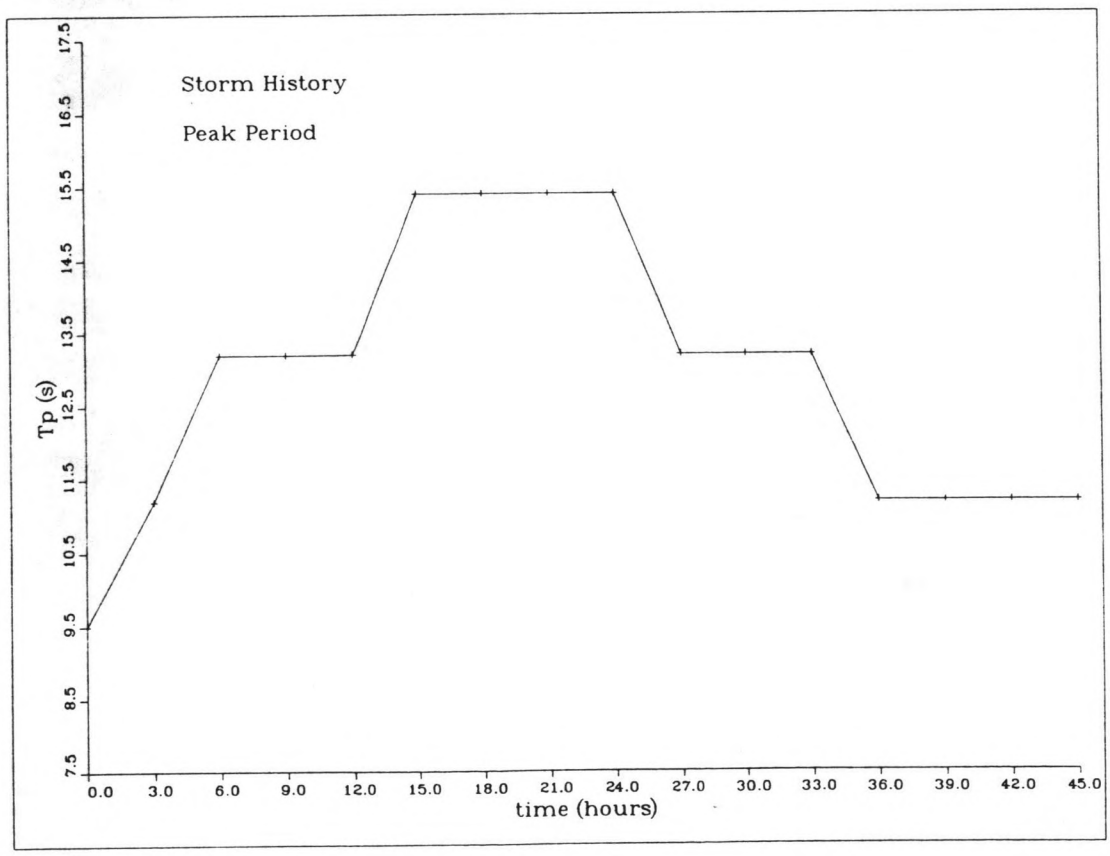

Figure 4.13b: Storm history of peak period, T_p, of example storm.

$$F^* = 4\pi^2 B_s \qquad (4.44f)$$

where d is the depth and A, B, and B_s represent respectively the inertia term, the drag term for rough members and the drag term for smooth members. As a startingpoint the constants (4.44a) to (4.44f) were calculated with the same values for A, B, and B_s as used in the load program. Then they were put in the equation and adjusted by multiplying them simultaneously or independently. Although this approach is not based on any analytical background, but on a trial and error process, the results were quite satisfactory: the numerically generated loads were reproduced with an accuracy of about 5% for base shear. Figures 4.14a and 4.15a illustrate this.

After the calibration the wind term is added and also the reduction factors for directional spreading and current blockage are included, because the load program did not account for these effects. Finally the analytical base shear model is found to be:

$$F = 105*v_s^2 + 2.71*v_s aT\Phi\cos\theta + 4.24*\frac{v_s a^2 \Phi\cos\theta}{T} + 3.69*\Phi^2 a^2 + \ldots$$

$$\ldots + 9.81*\frac{\Phi^2 a^3}{T^2} + 0.1*W^2\cos\theta_W \qquad (4.45)$$

where v_s is a short notation for 0.77*v. The inertia force in this equation is totally neglected. This was a result of the fitting procedure. The contribution of this term in extreme conditions is very small, so neglecting the term is permitted.

4.7.2 The overturning moment model

The generation of an approximate analytical relationship between overturning moment, M, and the environmental parameters is essentially the same as for

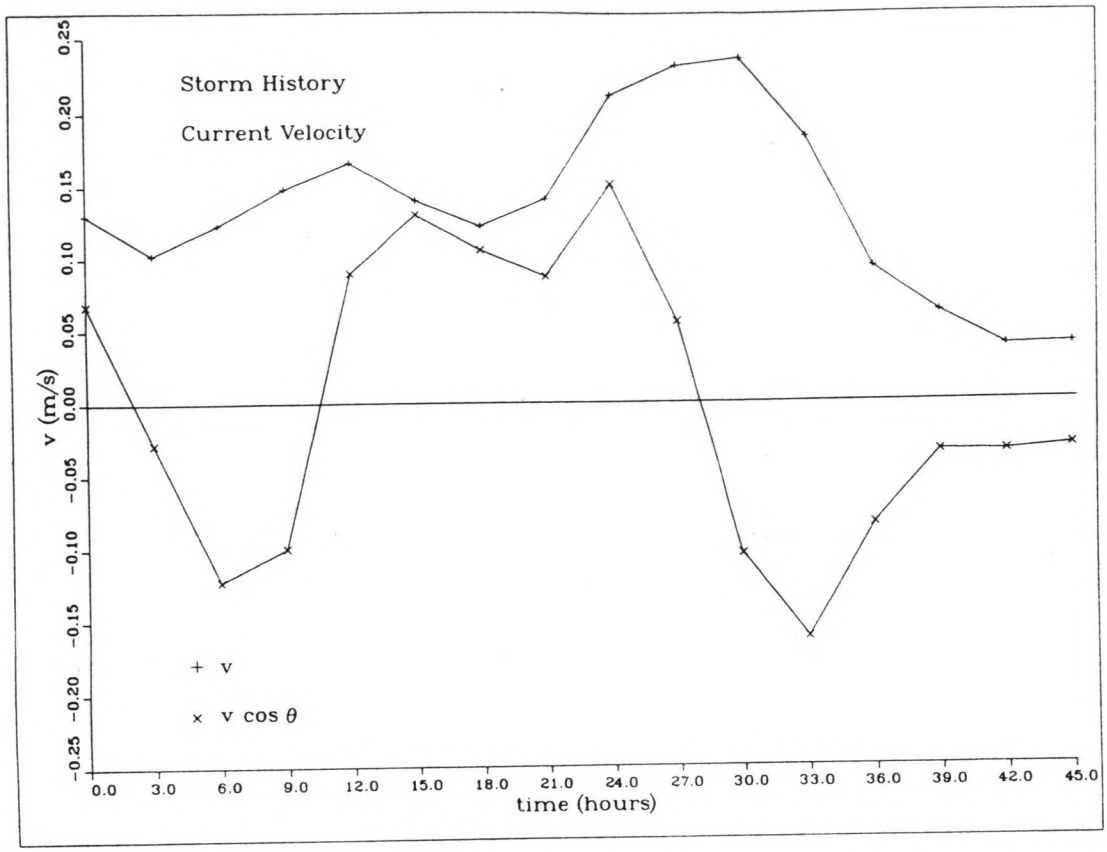

Figure 4.13c: Storm history of current velocity, v, of example storm.

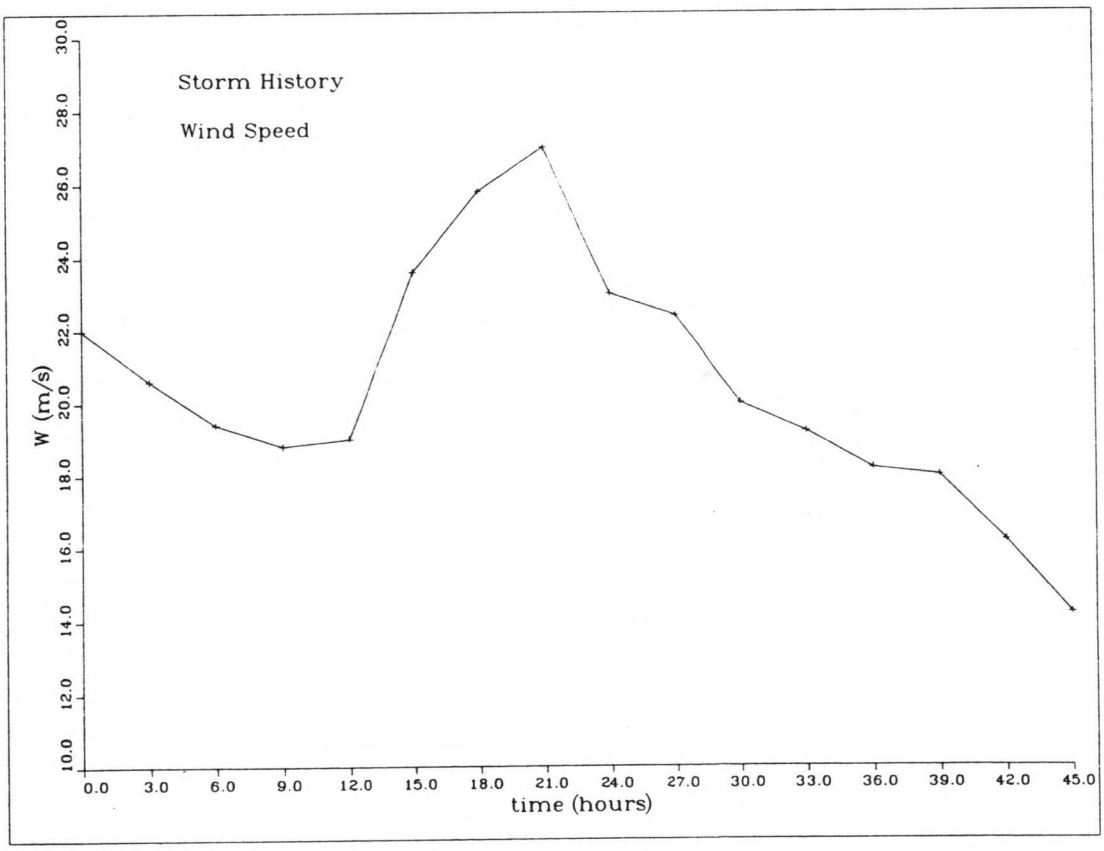

Figure 4.13d: Storm history of wind speed, W, of example storm.

base shear. The Morison equation describing the resultant moment per unit length on a single column with constant diameter, submerged to a mean water depth, d, can be expressed as:

$$M_n = A_n(d + \zeta)\dot{u}_n + B_n(d + \zeta)(v + u_n)^2 \tag{4.46}$$

Similarily as for base shear the total overturning moment is determined by integration of dM over depth.

$$M = \int_{-d}^{\eta} M_n d\zeta \tag{4.47}$$

If the same analysis is applied as for base shear in the final analytical relationship some additional correction terms depending on the wave period, T, are found.

$$M = A^*(1-K^*T^2)\frac{\pi a}{v_s T\cos\theta+\pi a} + B^* v_s^2 + C^*(1-K^*T^2)v_s aT\Phi\cos\theta + D^*\frac{v_s a^2\Phi\cos\theta}{T} + \ldots$$

$$\ldots + E^*(1-K^*T^2)a^2 + F^*\frac{\Phi^2 a^3}{T^2} \tag{4.48}$$

where:

$$A^* = \frac{A^2 gd}{2B} \tag{4.49a}$$

$$B^* = \frac{1}{2}Bd^2 \tag{4.49b}$$

$$C^* = \frac{Bgd}{\pi} \tag{4.49c}$$

$$D^* = 4\pi B_s d \tag{4.49d}$$

$$E^* = \frac{Bgd}{2} \tag{4.49e}$$

$$F^* = 4\pi^2 B_s d \tag{4.49f}$$

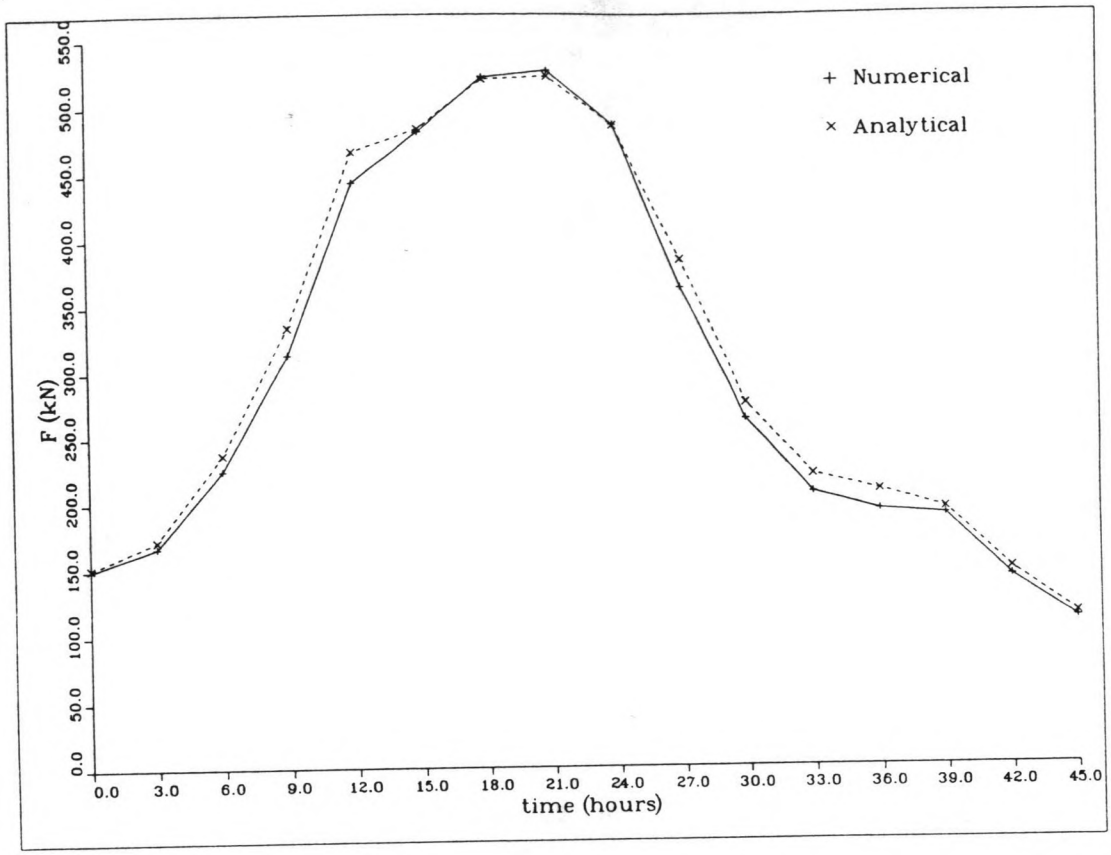

Figure 4.14a: Comparison of the results from the analytical loading equation with numerically computed values of base shear of the example storm from figure 4.13.

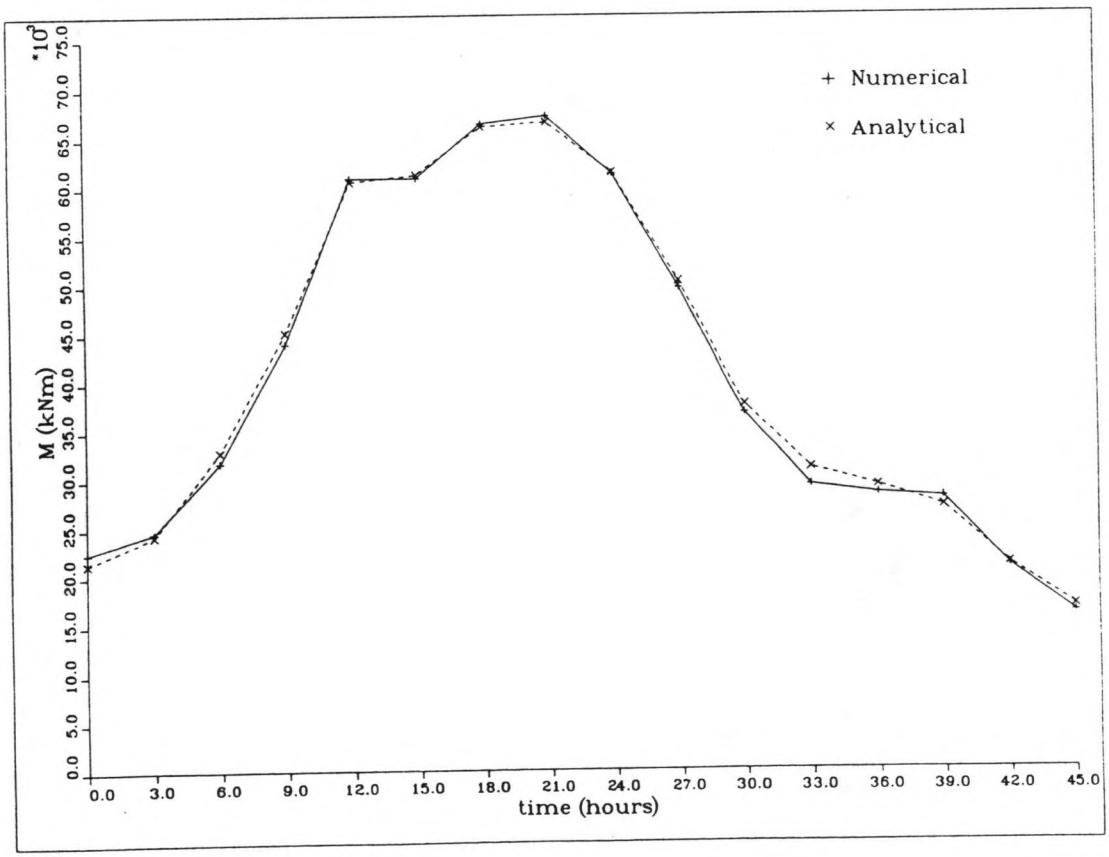

Figure 4.14b: Comparison of the results from the analytical loading equation with numerically computed values of overturning moment of the example storm from figure 4.13.

$$K^* = \frac{g}{4\pi^2 d} \qquad (4.49g)$$

K^* is an extra constant in the equation. However, since period, T, does not vary much, the correction terms are included in the other constants. This is done for convenience, so that the load equation for overturning moment is similar to equation (4.28). Only the constants in the equation will have different numerical values. As a first estimate the constants are calculated according to their physical significance. Subsequently the same calibration procedure is used as for base shear. The accuracy of the calibration was even better than for base shear, namely 3%, as illustrated in figures 4.14b and 4.15b.

The moment due to wind forces is determined by multiplying the base shear wind term by a force arm, r, which is estimated to be 200 meters. In general the moment due to wind can be described as:

$$M_W = F_W * r = G^* W^2 \cos\theta_W \qquad (4.50)$$

The value of G^* then follows from:

$$G^* = C_W * r = 20 \quad kg \qquad (4.51)$$

For the overturning moment the load equation can be expressed as:

$$M = 2480 * \frac{\pi a}{v_s T \cos\theta + \pi a} + 14622 * v_s^2 + 284.6 * v_s a T \Phi \cos\theta + 590.0 * \frac{v_s a^2 \Phi \cos\theta}{T} + \ldots$$

$$\ldots + 446.9 * \Phi^2 a^2 + 1852 * \frac{\Phi^2 a^3}{T^2} + 19.0 * W^2 \cos\theta_W \qquad (4.52)$$

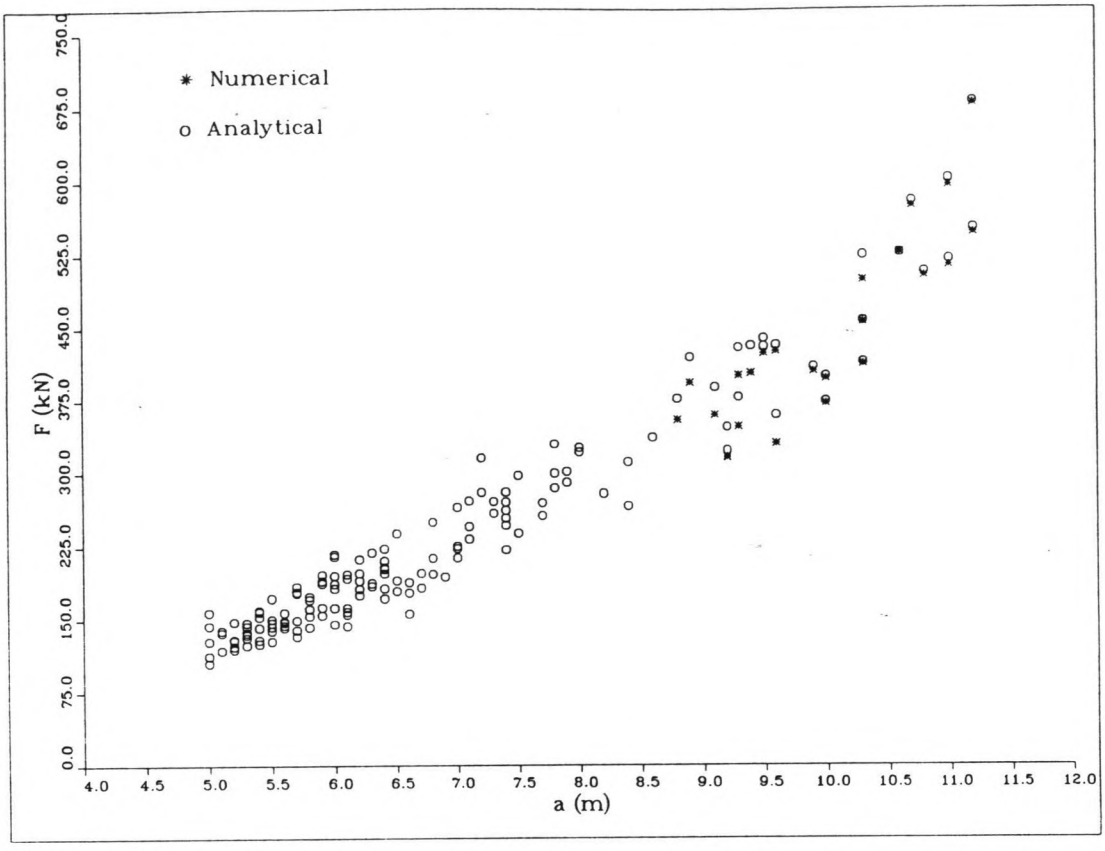

Figure 4.15a: The analytical load relationship for base shear plotted for 3-hour intervals with the highest H_s within every single north-west storm. For the 24 most severe storms the analytical values are compared with numerically computed values for base shear.

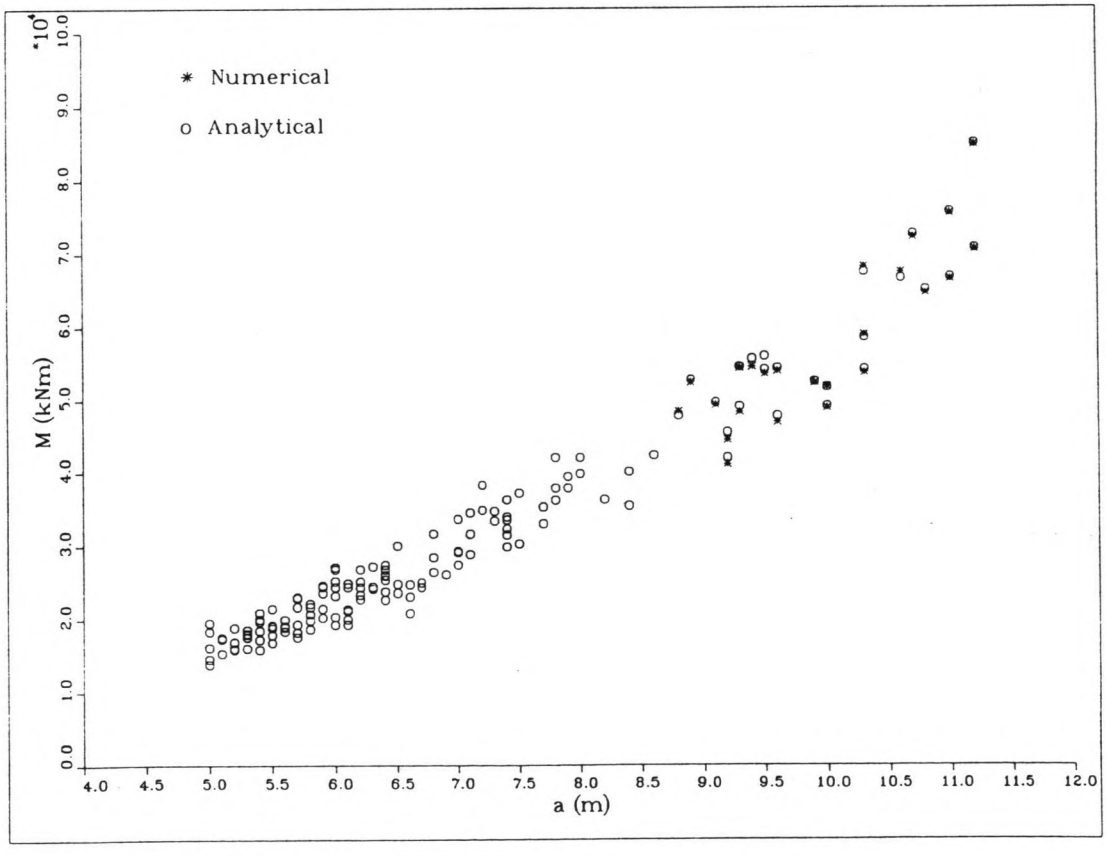

Figure 4.15b: See figure 4.15a, but then for overturning moment.

4.8 Inversion of the analytical load equation

The load equations for base shear and overturning moment can be used to transform the probability distribution functions of wave crest elevation into probability distribution functions of a response, like base shear. This will be explained in paragraph 5.3.2. Hence, equations (4.45) and (4.52) have to be inverted to give an expression for crest height, a, as a function of base shear, F, and overturning moment, M, respectively. For example for F this yields:

$$a(F) = \left(\frac{F-\alpha(a)}{\beta(a)}\right)^{\frac{1}{2}} \tag{4.53}$$

where:

$$\alpha(a) = A^* \frac{\pi a}{v_s T\cos\theta+\pi a} + B^* v_s^2 + C^* v_s a T\Phi\cos\theta + G^* W^2\cos\theta_W \tag{4.54a}$$

and:

$$\beta(a) = D^* \frac{v_s\cos\theta}{T} + E^* + F^* \frac{a}{T^2} \tag{4.54b}$$

As can be seen from these equations both α and β are functions of crest height, a, which means that a(M) can only be solved by iteration:

$$a_i(F) = \left\{ \frac{F-\alpha(a_{i-1})}{\beta(a_{i-1})} \right\}^{\frac{1}{2}} \tag{4.55}$$

Test results show that the iteration process converges rather quickly. The starting value, a_o, used in the iteration process is chosen to be 10 meters.

5. STATISTICAL STORM SIMILARITY MODEL FOR LOADING

5.1 Introduction

Traditional design procedures are based on the extrapolation of wave elevation, current velocity and wind speed to 100 year extremes directly from records of these environmental parameters, taken every 3 hours for a period of 15 or 20 minutes. The variables occurring in 3-hour intervals are treated in such a way that they are assumed to be independent, which they are not. Since individual storms are much more likely to be uncorrelated, it was suggested in KSEPL to consider particularly severe storms and try to find out if there is any similarity between these individual events. Supposing there is, it may be possible to create a model storm, which in one way or another is representative of every random storm. The probability distribution of any environmental parameter for such a storm can be described by its most probable extreme, an event with a probability of not being exceeded of approximately 37 %. For design the distribution for any random storm may be extrapolated to any desirable return period.

According to the line of thoughts sketched briefly above, previous research in KSEPL showed that it is possible to create a model storm for wave heights (ref. 5). From time series of significant wave height, H_s, the probability distribution, P(h), of the extreme wave height of each storm was calculated. Subsequently the corresponding most probable extreme wave heights, H_{mp}, were determined for each storm. Rescaling the various P(h)-distributions, by dividing them by their most probable extreme wave height, resulted in a remarkable resemblance, all functions approximately lying on the same curve. Thus all distribution functions could be well represented by one standard extreme value distribution in which H_{mp} appeared as a parameter. So if H_{mp} for a storm is given, the probability of the largest wave, $Pr(H \leq h | H_{mp})$, is known. This standard curve is called the "model curve" and represents the probability distribution of the largest wave in a storm,

given the most probable extreme wave height. It was concluded from these results that the required similarity can be found in the probability distributions of extreme wave height of individual severe storms.

Simultaneously with the creation of a model distribution curve, representing the short term statistics of all individual storms, a new asymptotic method was developed to estimate the probability distribution of the most probable wave heights, H_{mp}, namely $P(H_{mp})$. Assuming that certain asymptotic properties of extreme values are applicable to storms, it was possible to extrapolate from a short data base to a 100 year level. The combination of $P(H_{mp})$ and $P(h|H_{mp})$ was used to calculate the probability distribution of the largest wave height for any random storm. The probability density of the most probable extreme of the wave heights of storms and the probability distribution of the extreme individual wave height conditioned on that most probable extreme value, are the two ingredients for determining this random storm probability distribution:

$$P(h|\text{random storm}) = \int_{H_o}^{H_\infty} Pr(H<h|H_{mp})*p(H_{mp})*d(H_{mp}) \qquad (5.1)$$

Essentially $Pr(H<h|H_{mp})$ provides short term information, while $p(H_{mp})$ provides the long term information. The density function of the most probable extreme wave height is determined by differentiation of the corresponding probability distribution function, $P(H_{mp})$.

From the NESS data base the average number of storms per year, μ, is given, so that the probability of not exceeding h during a desired return period, y, can be determined by raising the random storm distribution to the power $y*\mu$, thus:

$$P(h|y \text{ years}) = [\ P(h|\text{random storm})\ ]^{y*\mu} \qquad (5.2)$$

The wave height with a 100-year return period is then the most probable extreme wave height of the 100-year distribution function obtained by setting y=100 in equation (5.2).

Applying the storm similarity method to wave heights was rather successful. In a later stage also surge and tide were included in the model (ref. 5). The next step is to apply the same theory to the global loading on an offshore structure, i.e. base shear and base overturning moment, which is the purpose of this project. This may be very interesting, because it may be possible to include all environmental conditions (waves, as well as wind and current) in one model, so that their extremes are no longer treated as independent. The probability distributions for base shear and overturning moment can be deduced from the crest height probabilities by way of the analytical load relationship generated in chapter 4.

5.2 Environmental data and storm selection

The new attempt to describe the joint statistics of wind, waves and current in terms of a structural loading has been made possible by the availability of the NESS data base. This hindcast data base contains almost all relevant data required to describe the behaviour of the North Sea over a period of 25 years (1963 to 1988). The data is simulated with all environmental and meteorological information available, such as wind speed, wind direction, tidal- and surge elevation in coastal areas, etc. The simulation model gives all the environmental variables describing the sea state for three hour intervals continuously from October till March, but in the other months only during storms.

For every three hour interval the NESS data base gives information about 11 environmental parameters, including:

- wind speed, W

- wind direction, θ_W
- significant wave height, H_s
- peak period, T_p
- wave direction, θ_H
- directional spreading, σ_θ
- depth mean residual current, v_{res}
- depth mean total current, v
- residual current direction, $\theta_{v,res}$
- total current direction, θ_v

The total current includes both storm driven and tidal current.

A representative selection of these data was used earlier to calibrate the constants of the analytical load relationship. For the statistical analysis storms are selected according to their H_s-values, since waves provide the dominant contribution to the loading on an offshore structure. Thus a storm may be considered to be severe if its significant wave height is high. Since only extreme events are of interest, it would not make any sense to consider low sea states. That is why a lower limit for H_s of 5 meters is introduced for the selection of the storms. Information for sea states below this limit is not of any significant influence on the results of an extreme event study such as this. Cutting off the continuous random signal at this 5 m-limit, also serves to break the H_s-history into a series of separate storms. This way a storm can be defined as a period of severe sea state in which the significant wave height is continuously higher than 5 meters.

If a continuous time period contains two high peaks it seems to be unreasonable to assume that this is necessarily just one storm with two peaks. If the time period between the two peaks is rather long, it might well be two storms. Therefore an additional definition is made for these special cases. The storm definition used here is the same as was defined by Heijermans (ref. 5), and is described briefly. Let Δt be the duration of the time interval between the two highest values of H_s within a single

continuous time series in which H_s exceeds the threshold value of 5 m, then three cases can be distinguished:

1) If $\Delta t \leq 12$ hours, then the event is described as one storm.

2) If $12 < \Delta t < 24$ hours, then the storm definition depends on the ratio of the lowest H_s between the two highest peaks ($H_{s,trough}$) and the highest value of the lower peak ($H_{s,max2}$).

   2a) If $H_{s,trough} < 0.8*H_{s,max2}$, then the event is described as two storms.

   2b) If $H_{s,trough} > 0.8*H_{s,max2}$, then the event is described as one storm.

3) If $\Delta t \geq 24$ hours, then the event is described as two storms.

The $0.8*H_{s,max2}$-limit in the second case is based on the fact that lower H_s-values of the storm do not contribute to the shape of the probablility distribution function.

If the storms are defined as described above, 451 storms can be selected from the NESS data base for the considered location. Unfortunately there are some gaps in the data base: for the storms during the summer seasons there is no information about current, so that these periods cannot be used directly. Therefore only storms during the winter seasons are considered initially.

The location considered in this study is a NESS grid point in the northern North Sea. It appears that the biggest storms come from two directions: north-west (where: 90 deg $< \theta_{storm} <$ 180 deg from north) and south-east (where: 270 deg $< \theta_{storm} <$ 360 deg). The direction of a storm, θ_{storm}, is defined as the wind direction at the time of the highest H_s-value of a

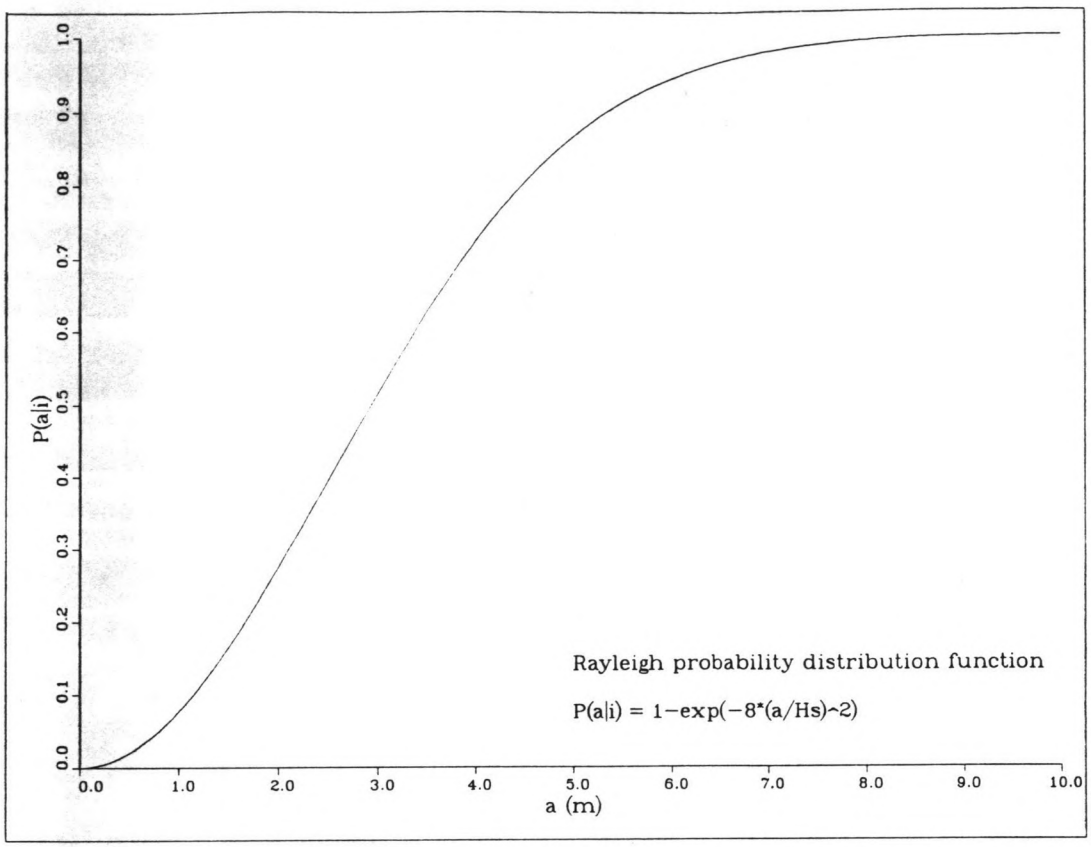

Figure 5.1a: The Rayleigh probability distribution function (with H_s = 10 m).

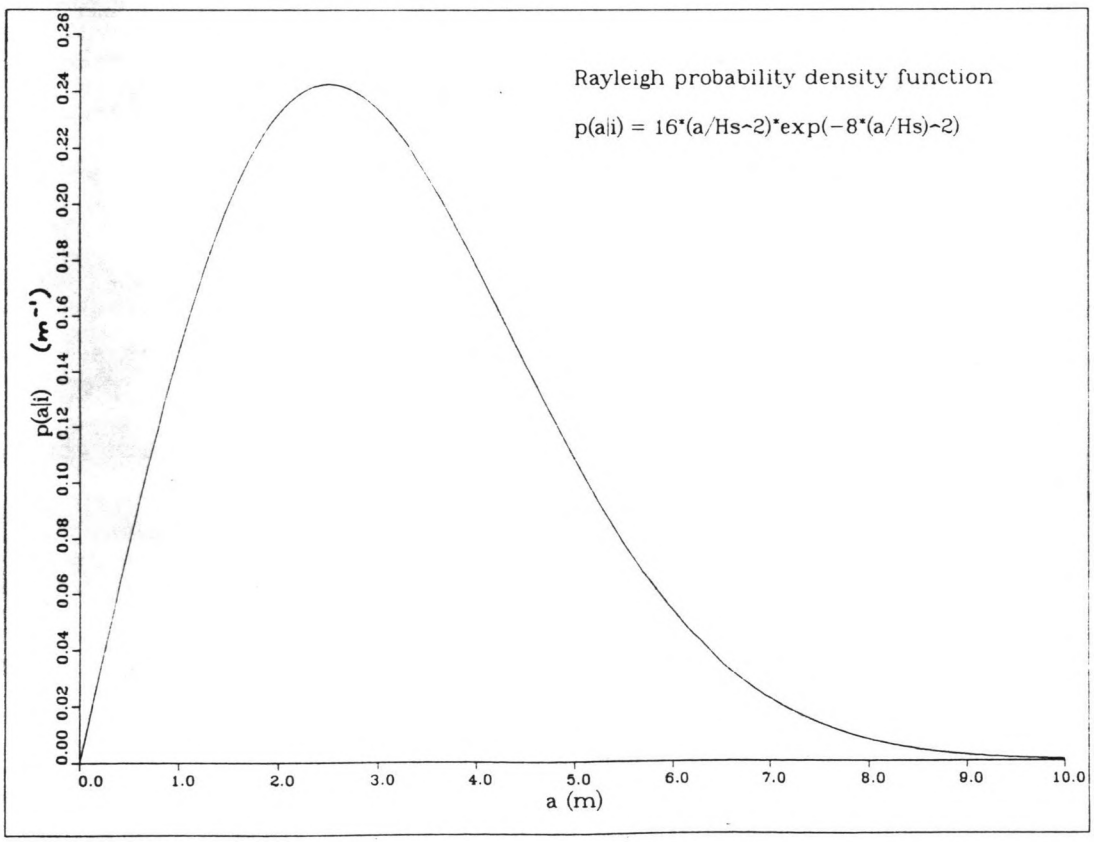

Figure 5.1b: The Rayleigh probability density function (with H_s = 10 m).

storm. Since the north-west storms appear to be more severe than the south-east storms, and storms coming from the two directions are independent, only the north-west storms are considered, which leaves 150 storms to be analysed.

5.3 Loading statistics for a single storm

One of the ultimate objectives is to predict the probability that a certain value of base shear force will not be exceeded in the 25 years of hindcasting. This probability is conditioned on the hindcast storm history and is derived with the help of the approximate analytical load relationship between crest height and response, generated in chapter 4. This relation can be used to transform the probability distribution functions of crest height into probability distribution functions of response.

5.3.1 Crest height statistics within a 3-hour interval

In a Gaussian proces with a narrow banded spectrum the crest elevations are Rayleigh distributed. In the case of a broader spectrum, where theoretically the probability distribution of the crest elevations is more complicated, empirically the Rayleigh distribution appears to be a rather good approximation for the higher crests (ref. 2).

Thus the probability distribution of individual crest elevation, a, in a stationary interval, i (i.e. an interval which is so short, that the statistical parameters, like average and standard deviation, can be treated as if they do not vary with time), with a significant wave height, H_{si}, is given by the Rayleigh distribution (figure 5.1):

$$Pr(a \leq \alpha | i) = R(\alpha | i) = 1 - \exp\{-8(\alpha/H_{si})^2\} \qquad (5.3)$$

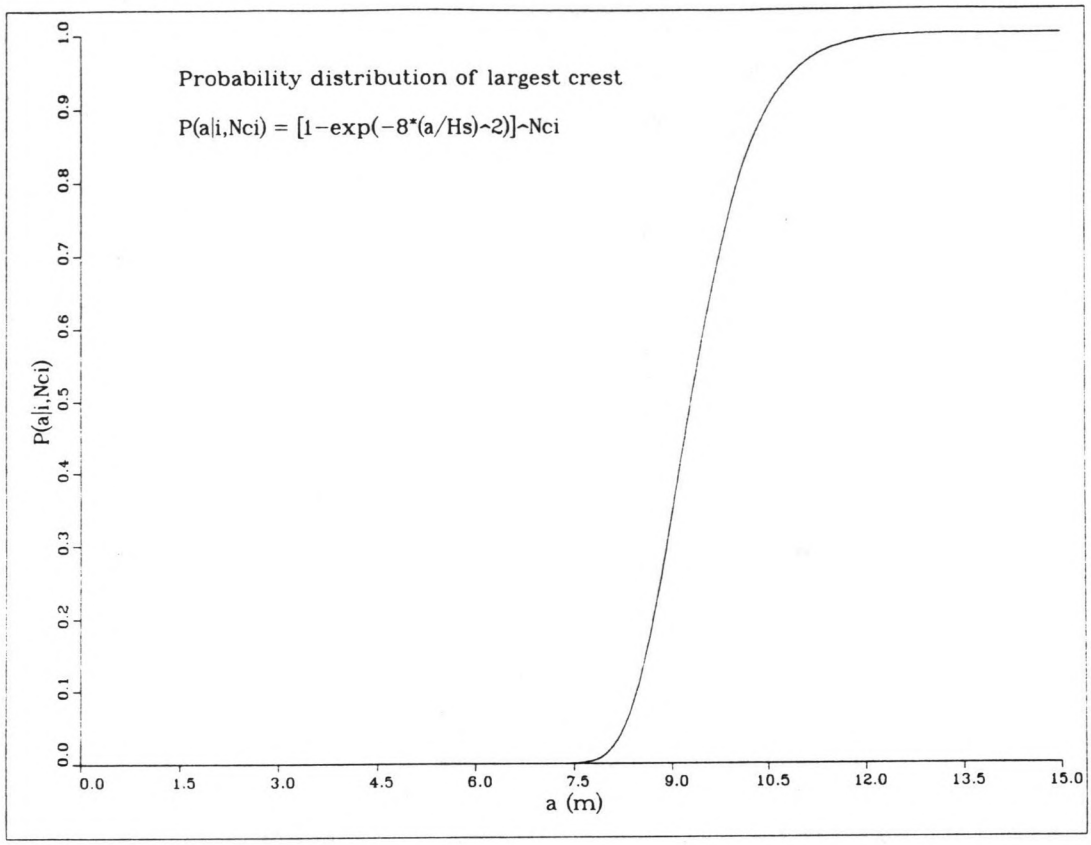

Figure 5.2a: The probability distribution of the largest crest in an interval, i, with N_i crests (with H_s = 10 m and N_i = 900)

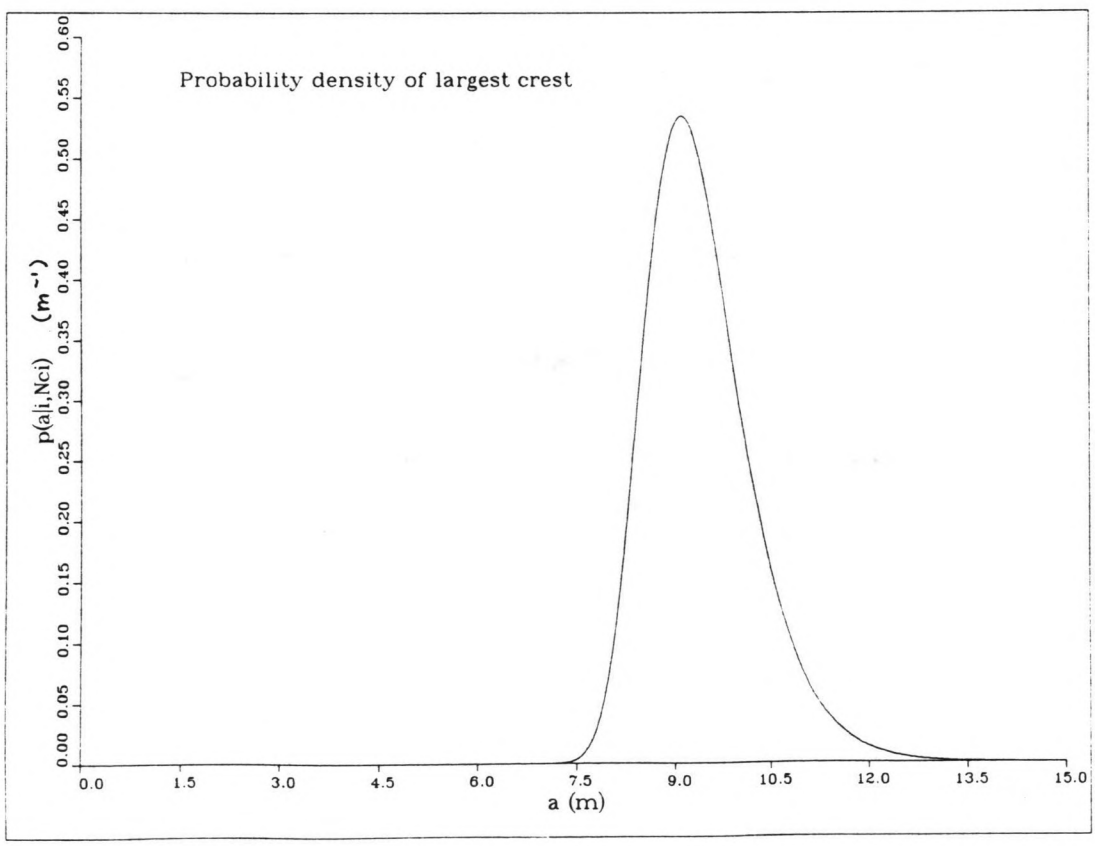

Figure 5.2b: The probability density of the largest crest in an interval, i, with N_i crests (with H_s = 10 m and N_i = 900)

This is a probability conditioned on the interval, i, that is on all the parameters in i. Apart from H_{si}, these include current, v_i, peak period, T_{pi}, wind speed, W_i; and so on. Of course for crest height the controlling paramerer is H_{si}.

The distribution of the largest crest in the interval, i, and hence the probability that in a 3-hour interval a certain level a will not be exceeded, is:

$$Pr(a \leq a | i, N_i) = [R(a|i)]^{N_i} \tag{5.4}$$

where N_i is the number of crests in the interval (figure 5.2). The non-exceedance probability of the individual crest heights is raised to the power of N_i on the assumption that these crest heights are statistically independent. This assumption is made to simplify the calculation of the probability distribution of the largest crest in the interval and is in fact a slightly conservative estimate of this distribution.

The number of crests in the interval depends on the zero crossing period, T_z, of the waves:

$$N_i = \frac{\Delta\tau}{T_z} \tag{5.5}$$

where: $\Delta\tau$ = duration in seconds of a 3-hour interval = 10800 s

However, the NESS data base only gives information of the peak period, T_p, which is linearly related to the zero-up crossing period. This relationship depends on the chosen wave spectrum. The JONSWAP spectrum, usually used for the North Sea, gives the following relation:

$$T_z = 0.778 * T_p \tag{5.6}$$

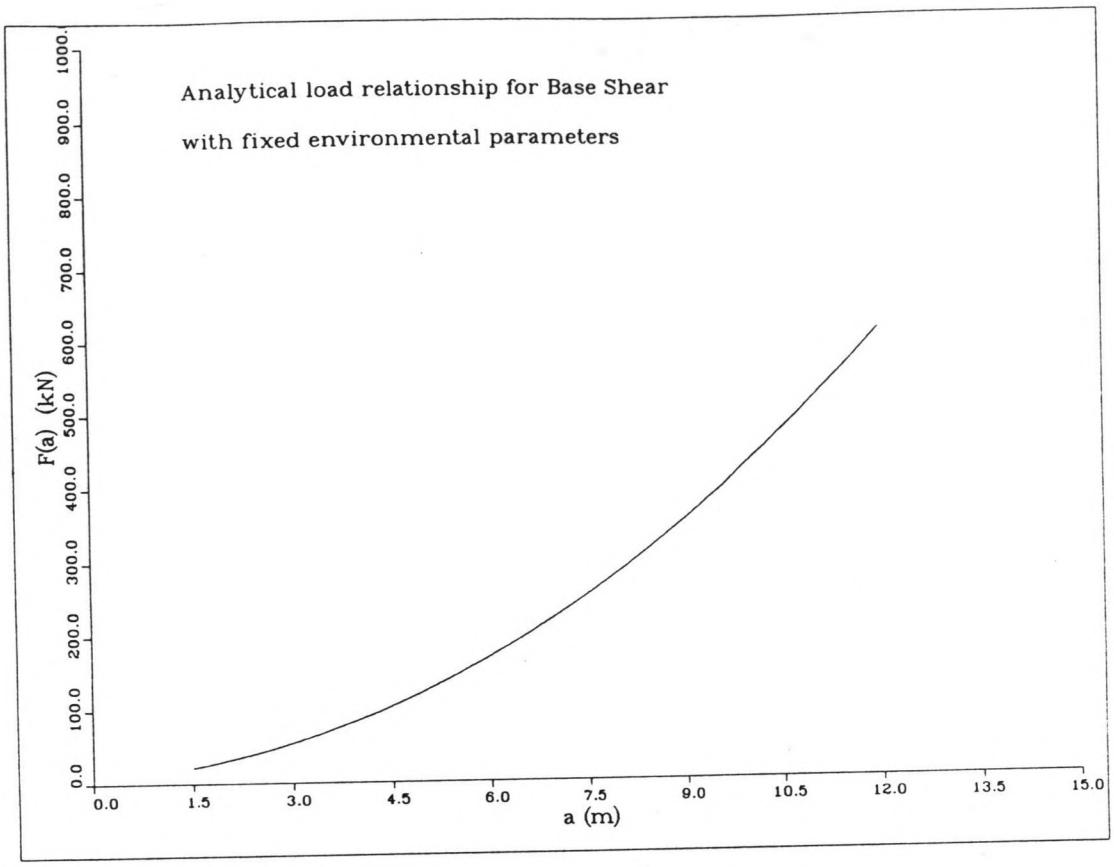

Figure 5.3: Base shear force, F, as a function of crest height, a.

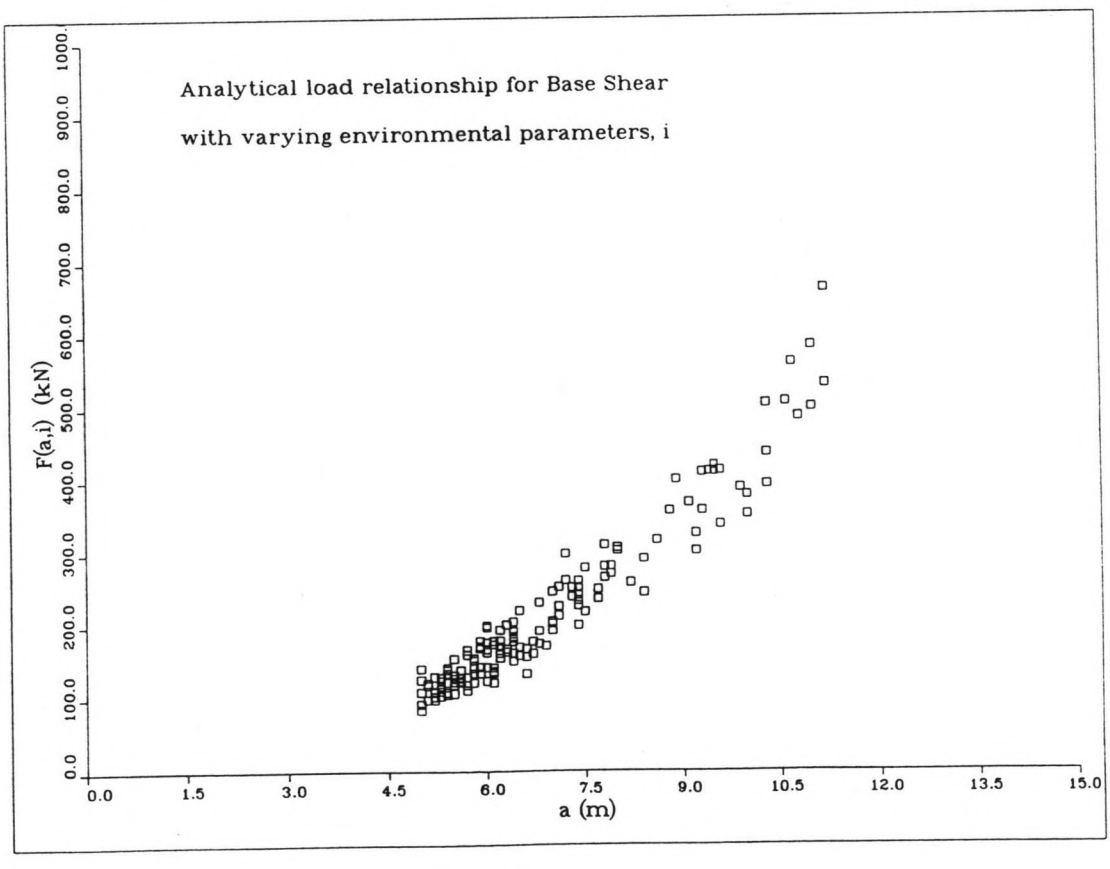

Figure 5.4: Base shear force, F, as a function of crest height, a, and the other environmental parameters, i.

so that:

$$N_i = \frac{\Delta\tau}{0.778*T_p} \tag{5.7}$$

The probability distribution for the extreme value of base shear force F in a 3-hour interval corresponding with (5.4) is:

$$Pr(F \leq f \mid i) = [R(a \mid i)]^{N_i} \tag{5.8}$$

where crest height, a, in this expression is a function of F: a=a(F). This is the inverse of the analytical load relationship, where all environmental parameters are included.

5.3.2 Transformation of probability distribution functions

In the previous chapter an analytical relationship has been generated between base shear force, F, crest height, a, and the other environmental parameters, which vary for different 3-hour intervals (figures 5.3 & 5.4).

$$F = F(a,i) \tag{5.9}$$

These other parameters are:

- wave period, T_i
- current velocity, v_i
- current direction relatively to wave direction, θ_i
- directional spreading parameter, $\sigma_{\theta,i}$
- wind speed, W_i
- wind direction relatively to wave direction, $\theta_{W,i}$

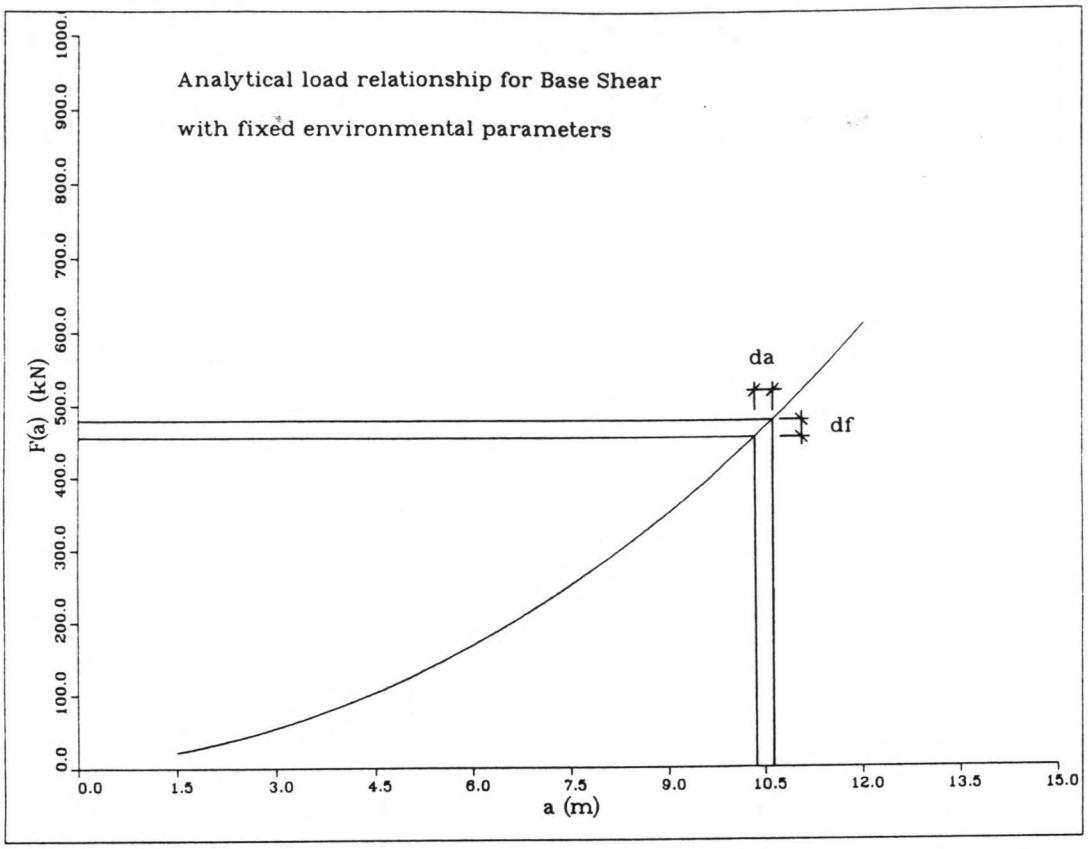

Figure 5.5: Transformation of a probability density function via an invertable function F(a).

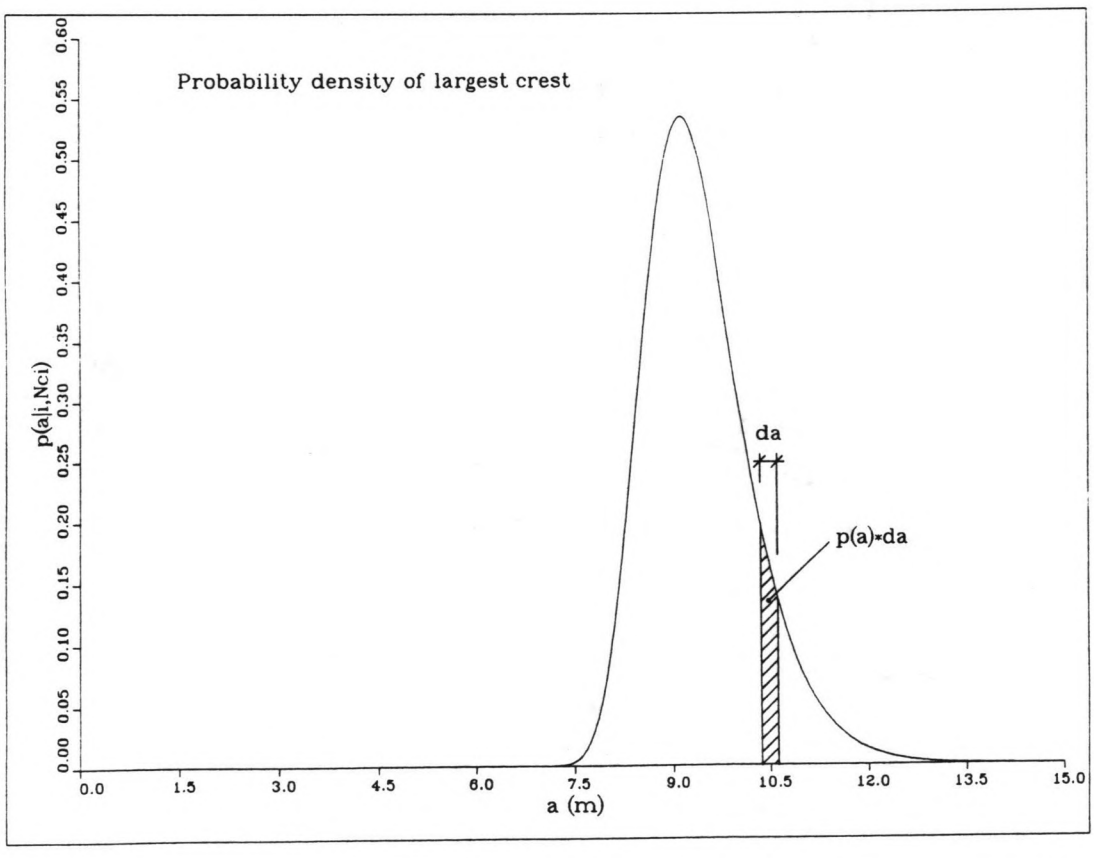

Figure 5.6: Probability density function of the largest crest in an interval, i.

Suppose that the environmental parameters are all constant over the interval, i. Then a monotinic relationship between F and a exists; i.e. F(a) can be inverted to a(F), which means that if a probability density function is known for variable, a, it can be used to determine the the corresponding probability density function for F (figures 5.5 & 5.6).

The probability that crest height, a, lies in a small interval $[a, a+da]$ is:

$$Pr(a<a\leq a+da) = p(a)*da \tag{5.10}$$

It is the same event that base shear, F, lies in the corresponding interval [f,f+df]:

$$Pr(f<F\leq f+df) = p(f)*df \tag{5.11}$$

Hence:

$$p(f)*df = p(a)*da \tag{5.12}$$

By integrating the density function $p(a)$ over the range $[-\infty;a]$ the probability distribution of a is generated, which equals the density function of F integrated over a range $[-\infty;f]$.

$$\int_{-\infty}^{f} p(f)*df = \int_{-\infty}^{a} p(a)*da \tag{5.13}$$

or:

$$Pr(F\leq f) = Pr(a\leq a) \tag{5.14}$$

Since the environmental parameters, i, are different for each 3-hour interval, this transformation of variables between crest elevation and load

is also different for each interval. Thus equations (5.12) and (5.14) are replaced by:

$$p(f|i)*df = p(a|i)*da \tag{5.15}$$

and

$$Pr(F \leq f|i) = Pr(a \leq a|i) \tag{5.16}$$

where the probabilities are conditioned on the environmental variables, i.

5.3.3 Loading statistics for a whole storm

A whole storm contains several 3-hour intervals. The probability distribution of F for the whole storm j is:

$$P(f|S_j) = \prod_{j=1}^{N_j} P(f|i) = \prod_{j=1}^{N_j} [R(a|i)]^{N_i} \tag{5.17}$$

where N_j is the number of intervals of storm j. This is the probability that no maximum base shear force exceeds the level f during the whole storm j.

Note that here the probabilities of F for successive 3-hour intervals are multiplied with each other. This does not imply a traditionally made assumption of statistical independence of slowly varying environmental parameters such as significant wave height, H_s, (see appendix A).

For computational accuracy it is preferable to calculate the probability distribution of F for a whole storm, $P(f|S_j)$, as a sum of the logarithms of the interval distributions, which may be written as:

$$P(f|i) = [1 - Q(f|i)]^{N_i} = \exp\{\ln[1 - Q(f|i)^{N_i}\}$$

$$= \exp\{N_i * \ln[1 - Q(f|i)]\} \tag{5.18}$$

The function $Q(f|i)$ yields the probability of exceeding f and can be expressed as:

$$Q(f|i) = \exp(-8(a(f)/H_{si})^2) \tag{5.19}$$

Equation (5.18) can be further simplified by taking the first order Taylor series approximation of $\ln[1 - Q(f|i)]$:

$$\ln[1 - Q(f|i)] \simeq - Q(f|i) \tag{5.20}$$

so that:

$$P(f|i) \simeq \exp(-N_i * Q(f|i)) \tag{5.21}$$

This approximation is not only valid for relatively large N_i and small $Q(f|i)$, i.e. $Q(f|i) << 1$; but also if $Q(f|i)$ is not so small as long as $N_i * Q(f|i) >> 1$ (ref. 2). In fact equation (5.21) is a special case of the Poisson distribution, as is shown in Appendix B.

The logarithm of the probability distribution of storm j then equals the sum of the logarithms of the distributions of all the intervals of the storm:

$$\ln\{P(f|S_j)\} = \sum_{j=1}^{N_j} -N_i * Q(f|i) \tag{5.22}$$

so that the distribution of storm j can be expressed as:

$$P(f|S_j) = \exp\left(\sum_{j=1}^{N_j} -N_i * Q(f|i) \right) \tag{5.23}$$

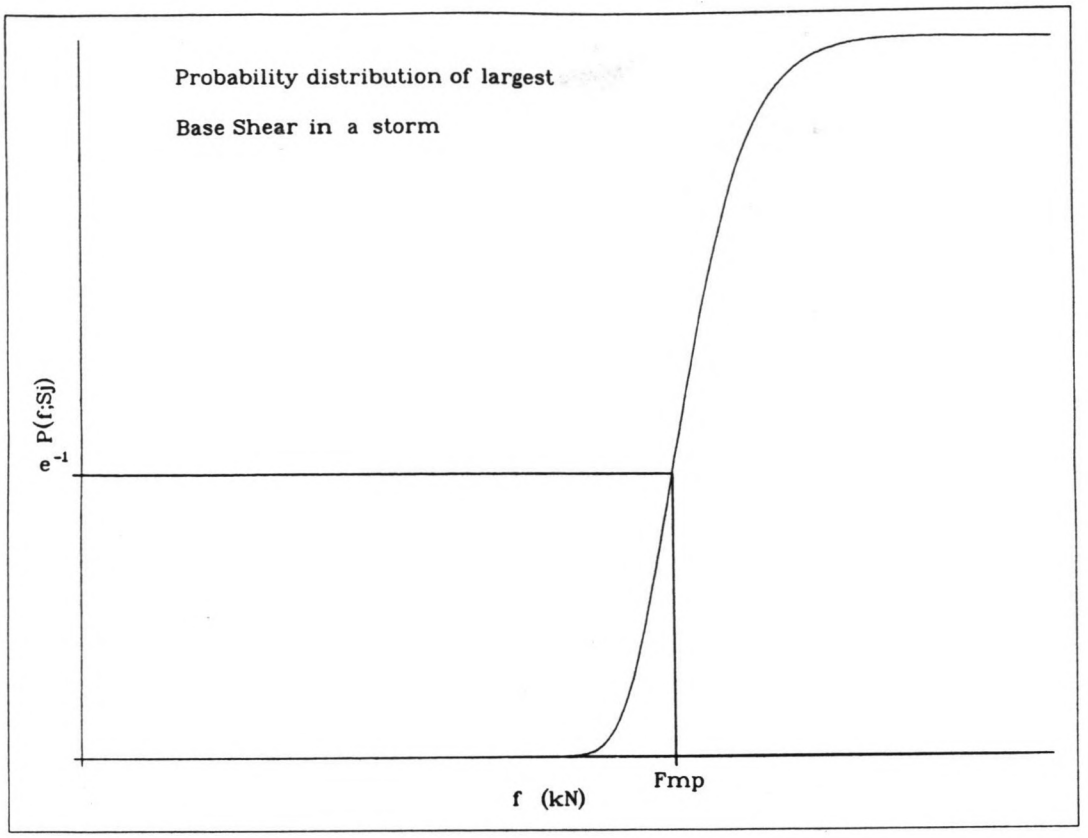

Figure 5.7: The probability distribution and density of extreme base shear for a single storm, with the most probable extreme base shear defined as the base shear where the density fuction reaches its maximum value.

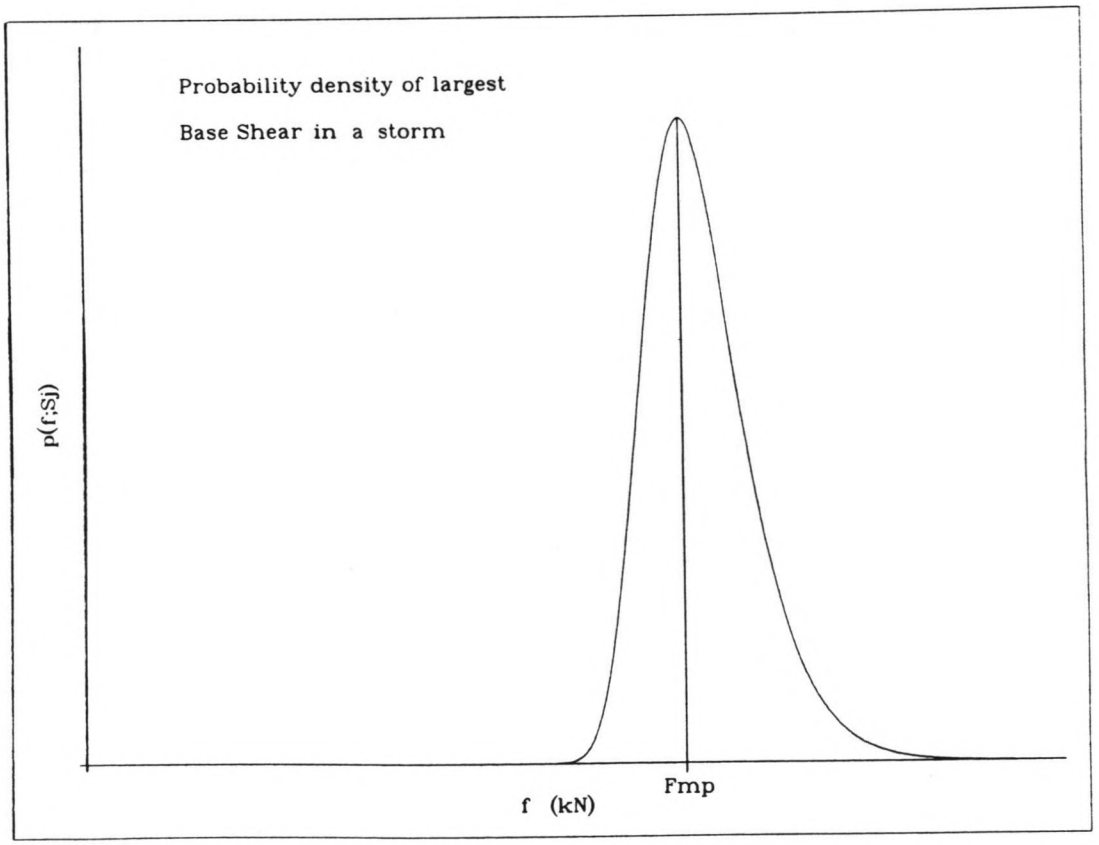

It can be shown that the probability density function corresponding to this distribution function has its maximum value (ref. 2), when:

$$\sum_{j=1}^{N_j} N_i * Q(f|i) = 1 \qquad (5.24)$$

The base shear value at this maximum is called the most probable extreme, $F_{mp,j}$ (figure 5.7). This value will be used to characterize every individual storm j. The probability of not exceeding the value of $F_{mp,j}$ equals e^{-1}, thus:

$$P(F_{mp}|S_j) = e^{-1} \qquad (5.25)$$

The F_{mp} value can be determined by interpolation of the storm distribution curve between the two nearest points adjacent to e^{-1}.

Subsequently it shall be demonstrated that knowledge of the value of F_{mp} of a storm is sufficient information to specify the probability distribution of extreme base shear of that storm.

5.4 The random storm probability distribution of extreme base shear

The probability distribution function of the extreme base shear force, F, for any random storm with an F_{mp}-value exceeding F_o; i.e. the probability that a maximum base shear in a random storm will not exceed a certain level f, can be expressed as:

$$P(F_o \leq F_{mp} \leq F_\infty) = \int_{F_o}^{F_\infty} P(f|F_{mp}) * p(F_{mp}) * dF_{mp} \qquad (5.26)$$

This equation is called the random storm formula. The upper integration limit F_∞ accounts for the possibility of an upper bound on the F_{mp}-values.

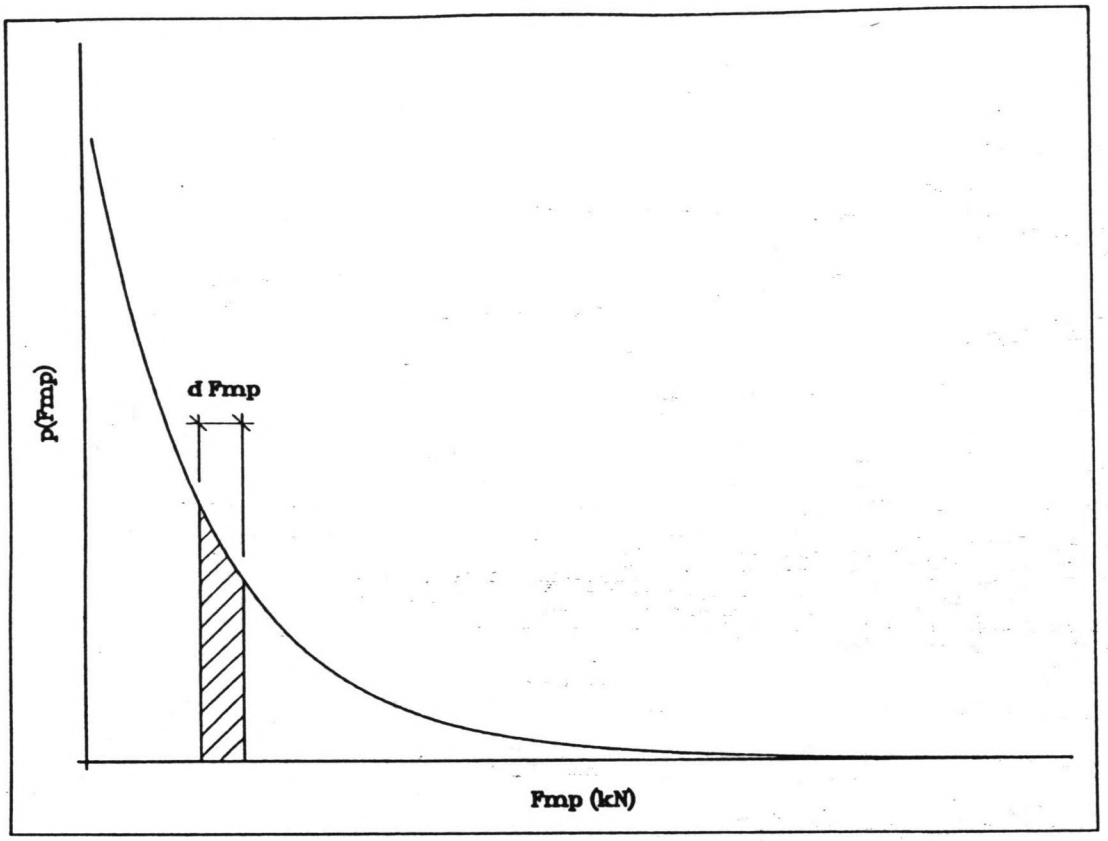

Figure 5.8: The probability density function of most probable extreme base shear forces.

If there is no upperbound then F_∞ becomes infinity. The lower limit F_0 arises because data for small storms have not been used. Thus the probability from equation (5.26) is conditioned on any storm with a most probable extreme base shear, F_{mp}, exceeding the level F_0. Since small storms do not contribute to the probability of occurence of an extreme (say 100-year return) value, this lower limit will not influence the validity of the method.

The random storm formula is composed of two parts:

1) the "model curve" distribution function, $P(f|F_{mp})$, to be generated in the next paragraph and representing the short term base shear variability

2) the probability density function of the F_{mp}-values, $p(F_{mp})$, to be derived in paragraph 5.6 and representing the long term base shear statistics

In the analysis in the next three sections 5.5 to 5.7 the wind is not taken into account. This is done for interpretational reasons. Wind forces are added in paragraph 5.8.

5.5 Short term statistics: the generation of the "model curve"

The "model curve" represents the probability distribution of the extreme base shear, F, for a particular storm, given the most probable extreme base shear value, i.e. $P(f|F_{mp})$. With the statistical analysis described in paragraph 5.3 the probability distributions of F for each of the 150 selected storms, $P(f|S_j)$, are determined. The corresponding most probable extremes are determined by interpolation of these distributions functions round the probability with the value e^{-1}. These characterizing parameters give an indication of the intensity of the storm. The storm with the highest

$H_{s,max}$ does not necessarily have to be the storm with the largest value of F_{mp}, because there is also a significant influence of the storm duration, the distribution of the H_s-values over the storm duration, and of course the contribution of wind and currents.

In principle the "model curve" is generated as follows: first the distribution functions of the storms are rescaled by dividing the F-values by the F_{mp}-value of each particular storm. It appears that the rescaled distribution functions fall approximately on one curve. This reflects the storm similarity, mentioned before. By averaging the rescaled distribution functions the "model curve" is created.

5.5.1 A "model curve" for base shear

In order to check whether the severest storms are more similar than the less severe ones, the selected storms are distributed over 9 bands on the basis of their F_{mp}-values. The first band has a range of F_{mp} from 50 to 100 kN, and the last band has a range of F_{mp} from 550 to 600 kN.

If the rescaled distributions in each band are averaged and if the averaged band curves are plotted, then it is notable that some curves strongly deviate, despite the expectation of all the curves having approximately the same position. Further investigation shows that the deviating curves are from the bands with the lower F_{mp}-values. It is evident that this deviation is caused by the fact that many storms with a small F_{mp}-value are influenced by the 5 m lower limit on significant wave height. For these storms some 3-hour intervals with H_s below 5 m would have a significant influence on the shape of the probability distribution function of extreme load, but are not taken into account.

Uncensored storm distributions are probability distributions of F for storms of which all the contributing 3-hour intervals have an H_s-value larger than

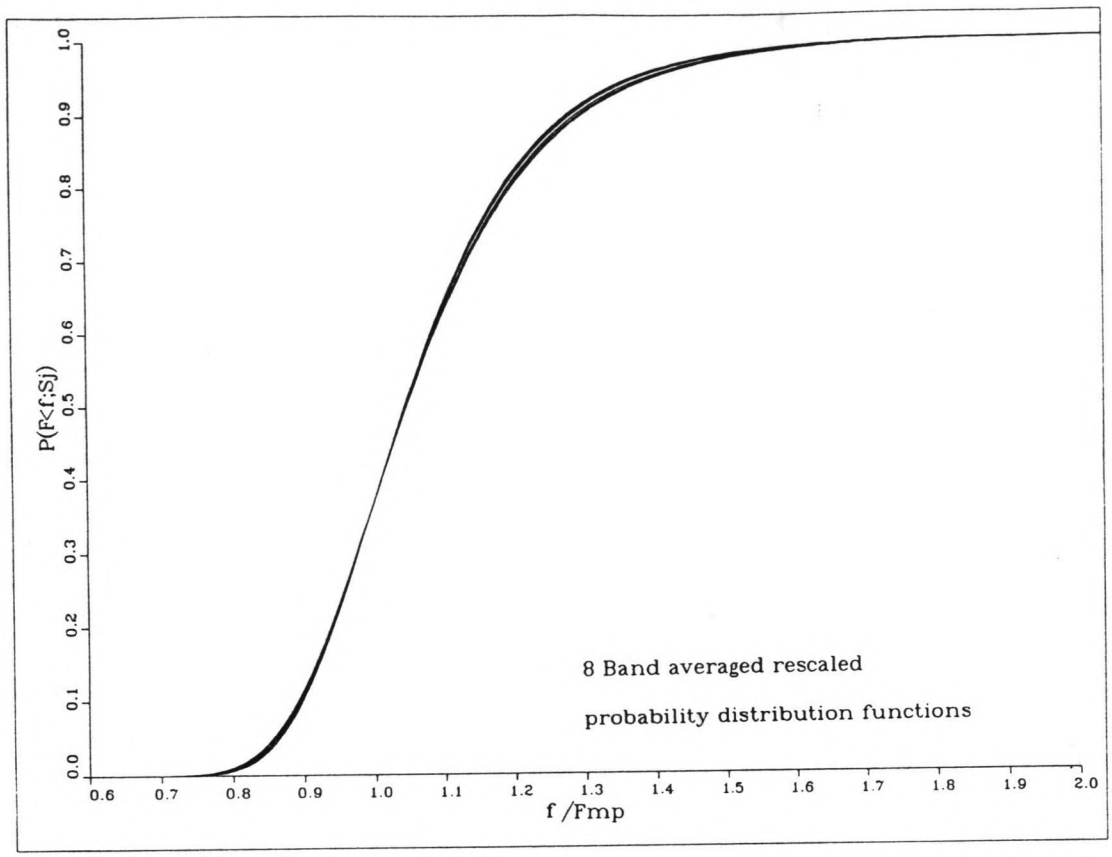

Figure 5.9: 8 Band averaged rescaled probability distribution functions for extreme base shear.

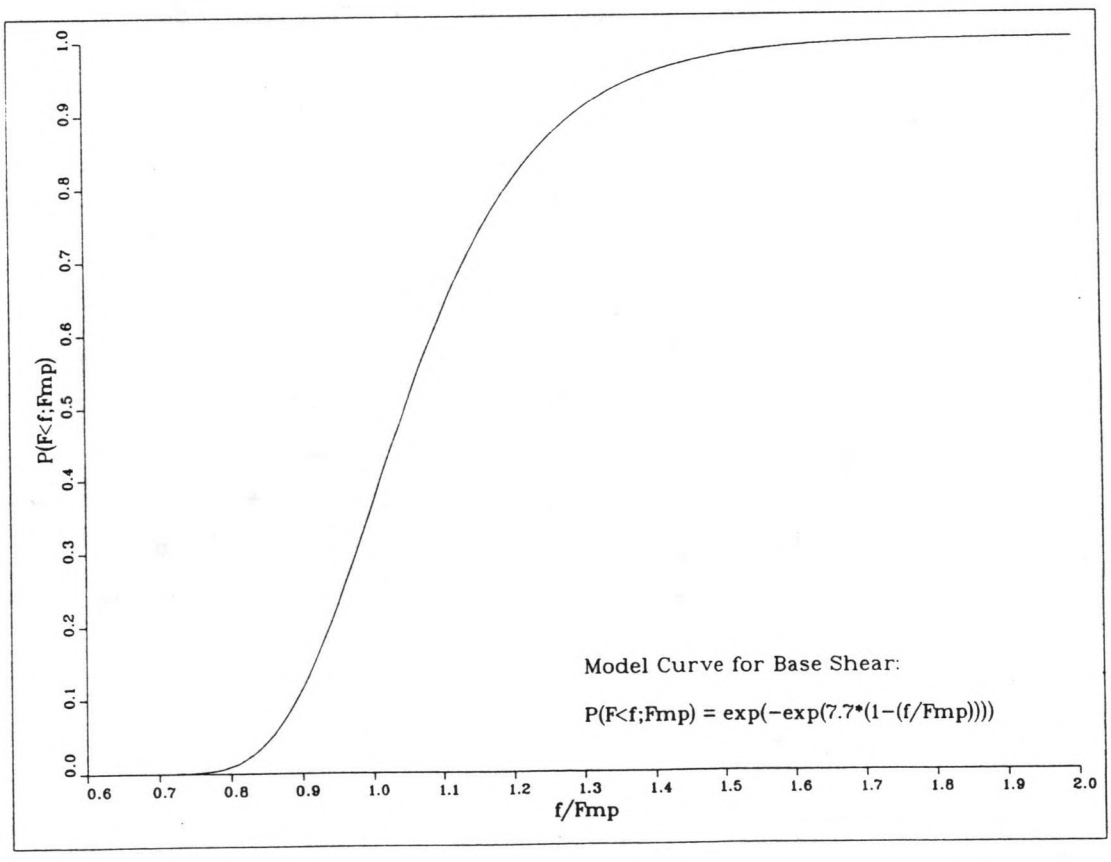

Figure 5.10: A "model curve" for the probability distribution of extreme base shear.

5 m. In the application of the random storm method to the airgap problem an 80%-rule was introduced: only the intervals with a H_s-value larger than 0.8 times the largest H_s-value during a storm, $H_{s,max}$, influence the distribution of extreme wave height, $P(h|S_j)$, of the continuous storm period, if $h \geq 2*H_{s,max}$ (ref. 5). This rule is also useful for the distribution of extreme base shear, because the forces are wave drag dominated and, for the main part, dependent on the significant wave height. Thus a storm distribution is uncensored if 0.8 times the maximum significant wave height in a storm, $H_{s,max}$, is larger than 5 m, or:

$$0.8*H_{s,max} \geq 5.0 \text{ m} \quad \text{----->} \quad H_{s,max} \geq 6.25 \text{ m} \tag{5.27}$$

If only the uncensored storm distributions are considered 79 storms remain, distributed over 8 bands, and the strongly deviating curves disappear (figure 5.9).

Averaging the band distribution functions results in one curve which has approximately the shape of a double exponential function. This is called the "model curve" for base shear. The distribution of extreme values is described by the Fisher Tippett FT-1 distribution function:

$$F(x) = \exp(-\exp(-\frac{x-\alpha}{\beta})) \tag{5.28}$$

Since extreme values are the issue here it may be worthwile trying to describe the "model curve" with a function similar to FT-1:

$$P(f|F_{mp}) = F(f,F_{mp}) = \exp\{-\exp\{-\frac{(f/F_{mp})^{\alpha}-1}{\beta}\}\} \tag{5.29}$$

where α an β are the fitting parameters. For fitting the "model curve" for wave height in earlier research it was found that: $\alpha = 2$ and $\beta^{-1} = 8$ (ref. 5). Since base shear, F, is roughly proportional to H^2 because of drag-dominance, it may be appropriate to take: $\alpha = 1$. After some trial and error

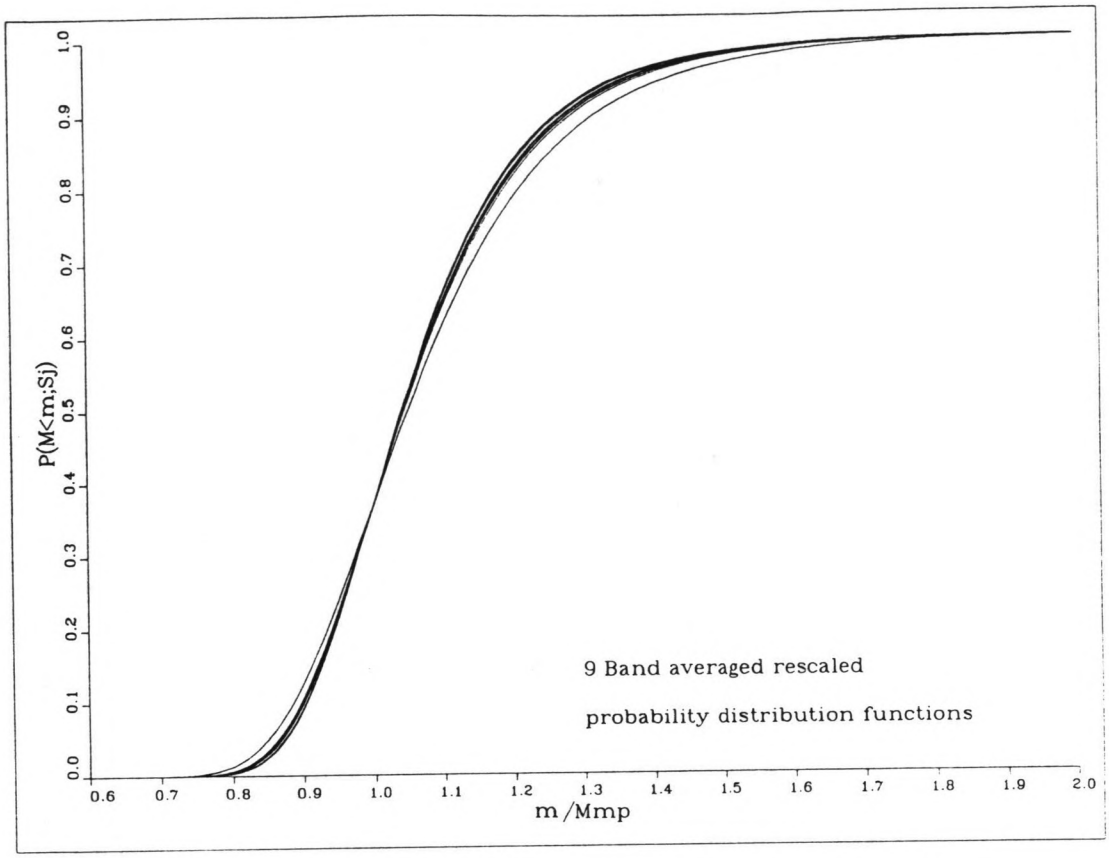

Figure 5.11: 9 Band averaged rescaled probability distribution functions for extreme overturning moment.

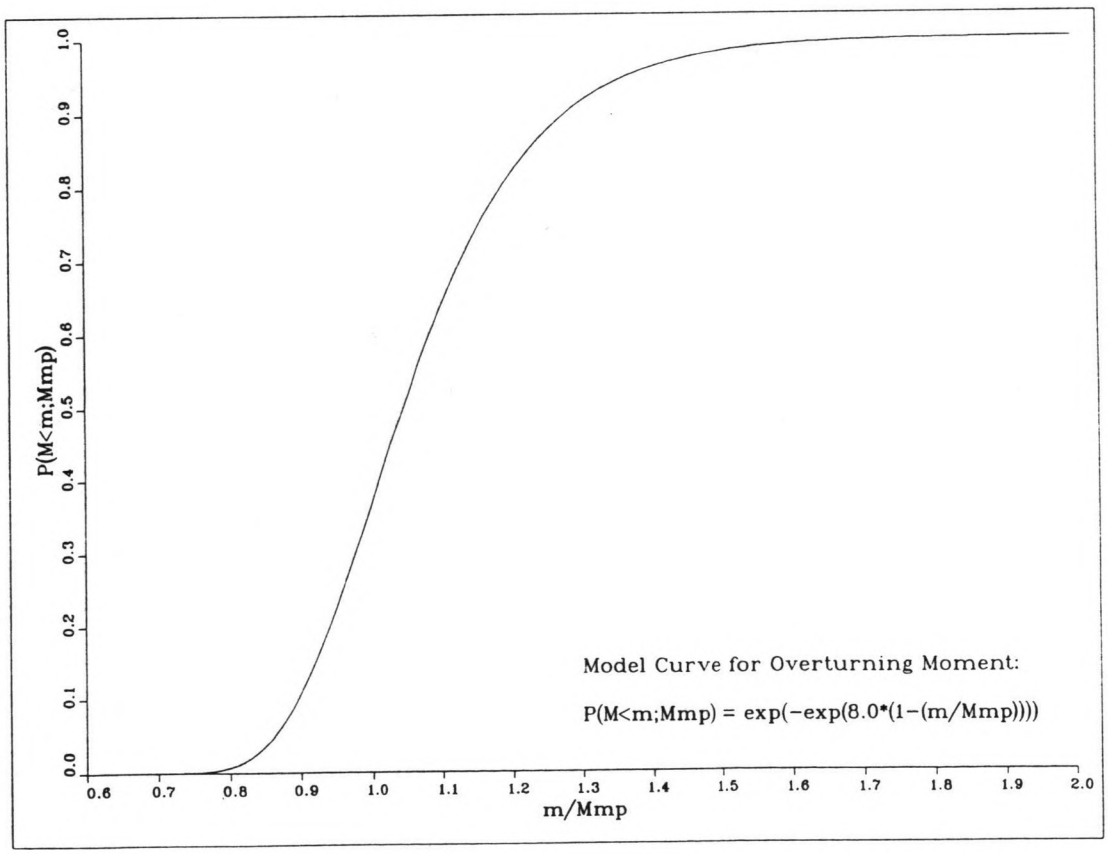

Figure 5.12: A "model curve" for the probability distribution of extreme overturning moment.

for best fitting purposes β^{-1} is found to be 7.7, so that the distribution function of the model curve can be expressed as (see figure 5.10):

$$P(f|F_{mp}) = \exp\{-\exp\{7.7*(1 - (f/F_{mp}))\}\} \qquad (5.30)$$

The fact that the short term statistics of all storms can rather well be expressed by one single "model curve"-function such as equation (5.30) confirms the idea that there exists a statistical similarity between individual severe storms.

5.5.2 A "model curve" for overturning moment

Similar to base shear the "model curve" for overturning moment, M, is generated. The 150 north-west storms are distributed over 11 bands based on their M_{mp}-values. The bands have a range length of 5 MNm, with the first and the last band having a range of M_{mp} respectively from 7.5 to 12.5 MNm and from 57.5 to 62.5. Considering the uncensored distributions only and averaging the remaining 9 band distributions the "model curve" for overturning moment, M, is generated. Figure 5.11 shows that one curve still deviates strongly from the others. This may be caused by the small number of storm samples in this band. Fitting the "model curve" to a FT-1 function results in (see figure 5.12):

$$P(m|M_{mp}) = \exp\{-\exp\{8.0*(1-(m/M_{mp}))\}\} \qquad (5.31)$$

A smaller value for the parameter β indicates that the model curve for overturning moment is a bit steeper than the model curve for base shear.

5.6 The probability density function of most probable extremes

In the random storm formula, generated in paragraph 5.4, the long term force statistics are represented by the density function of the most probable extreme values of base shear, F_{mp}. This $p(F_{mp})$-function is needed for extrapolation purposes to predict extremes with say a 100-year return period. However, the NESS data base only covers 25 years of hindcasting. The available information is limited to the largest value deduced from the data base. For extrapolation beyond this value an additional assumption has to be made on the behaviour of the upper tail of the distribution function of F_{mp}, $P(F_{mp})$, where $P(F_{mp})$ approaches the value 1. Then it may be possible to predict the $P(F_{mp})$-function beyond the finite sample. Two options for such an assumption are: a parametric assumption or a semi-parametric one.

If it is assumed that the distribution function is known, except for some parameters, the required information may be expressed in terms of these parameters. Then some method can be used to find an estimate of this information. Often used for this purpose are the Weibull or Gumbel distribution functions as parametric assumptions of the function of the tail. The number of samples used for the estimate is chosen arbitrarily.

On the contrary, for the semi-parametric assumption only an optimum number, k, of the largest samples is used, determined by minimizing the mean squared error of the estimate of the index of variation, γ (ref.18). The smallest F_{mp}-value of these k samples is denoted as F_0. Assumptions are made on the behaviour of the distribution near the upper end, where: $F_{mp} > F_0$. The function is fixed by the samples. This semi-parametric method has been developed by P.P. de Wolf, a thesis student of the mathematics department of the Technical University of Delft (ref. 18).

With the F_{mp}-values of all the storms considered as an input, the method results in a expression for the distribution function of F_{mp}:

$$P(f_{mp}|F_{mp}>F_o) = Pr(F_{mp} \leq f_{mp}|F_{mp}>F_o) \qquad (5.32)$$

This function is conditioned on the event that F_{mp} is larger than the lower integration limit, F_o. The probability density function of the F_{mp}-values is generated by differentiation of the distribution function:

$$p(f_{mp}) = \frac{dP(f_{mp}|F_{mp}>F_o)}{df_{mp}} \qquad (5.33)$$

5.6.1 The p.d.f. of the most probable extreme base shear force

During the application of the semi-parametric method to the most probable extreme base shear forces, F_{mp}, some problems appeared: on the one hand the extrapolation was disturbed by the influence of the presence of 71 censored storms; on the other hand, however, the number of 79 uncensored storms appeared to be too little for a proper extrapolation. So both including and ignoring the uncensored storms led to silly answers.

One way to solve this problem is to extend the number of data. This can be done by lowering the 5 m-limit, which was introduced for the defining and selecting of storms. An alternative is to fill the gaps in the data base, which arise because currents were not hindcasted for summer storms, as mentioned in paragraph 5.2. This can be achieved by introducing some "bogus" data. In spite of the fact that the extrapolation worked rather well with this additional data, in an absolute sense the results should be interpreted with care.

Figure (5.13) shows the correlation between the most probable extreme wave height, H_{mp}, and the most probable extreme base shear force, F_{mp}. It can be seen from this plot that the F_{mp}-value is roughly proportional to the H_{mp}-value squared. In fact this correlation can be described roughly by the following relation:

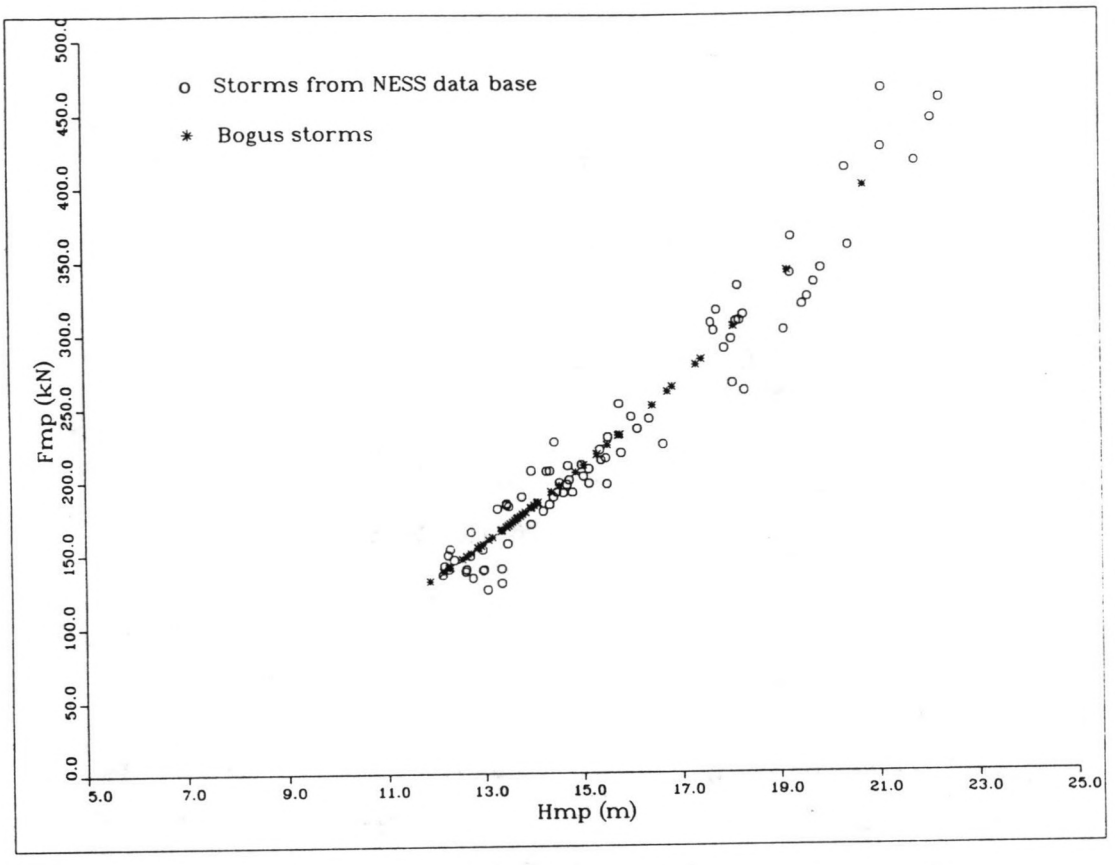

Figure 5.13: The correlation between the most probable extreme wave height, H_{mp}, and the most probable extreme base shear force, F_{mp}, including some "bogus" F_{mp}-values.

$$F_{mp} \simeq C_0 * H_{mp}^2 \tag{5.34}$$

where: $C_0 = 0.93$ kg/ms²

Since the H_{mp}-values for all storms can be obtained from the data base and the lack of information in the data base only concerns currents and current directions, this relationship can be used to invent "bogus" F_{mp}-values of the storms for which the current data is missing. This provides a total number of 128 uncensored storms, of which 49 storms have a "bogus" F_{mp}-value. Figure (5.13) shows that most of the "bogus" storms are relatively not so severe, lying in a range of F_{mp} from 125 to 175 kN. The extrapolation with this number of storms, where there is no influence of censored data, was much more succesfull. The influence of the number of data on the extrapolation will be discussed in the next chapter.

As a result of the semi-parametric method the optimum number of storms, k, is: k = 84, of which 26 were "bogus" storms. The estimate for the distribution function is found to be:

$$P(f_{mp}) \simeq 1 - [1 + \xi * (f_{mp} - F_0)]^{-\frac{1}{\gamma}} \tag{5.35}$$

for: $F_0 \leq f_{mp} \leq \infty$

where: $\xi = 0.774 * 10^{-3}$ kN^{-1}

$\gamma = 0.0544$

$F_0 = 174.3$ kN

Differentiation of this function yields:

$$p(f_{mp}) = \frac{dP(f_{mp})}{df_{mp}} \simeq \frac{\xi}{\gamma} * [1 + \xi * (f_{mp} - F_0)]^{-\frac{1}{\gamma} - 1} \tag{5.36}$$

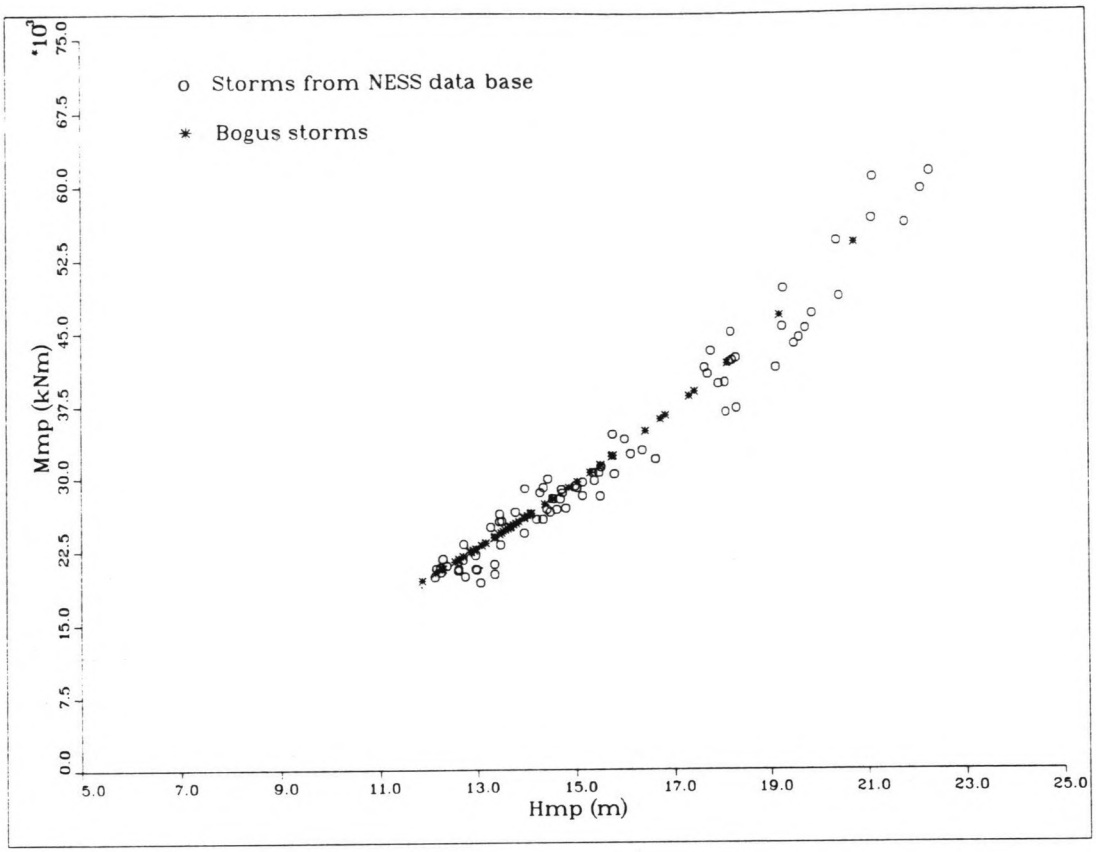

Figure 5.14: The correlation between the most probable extreme wave height, H_{mp}, and the most probable extreme overturning moment, M_{mp}, including some "bogus" M_{mp}-values.

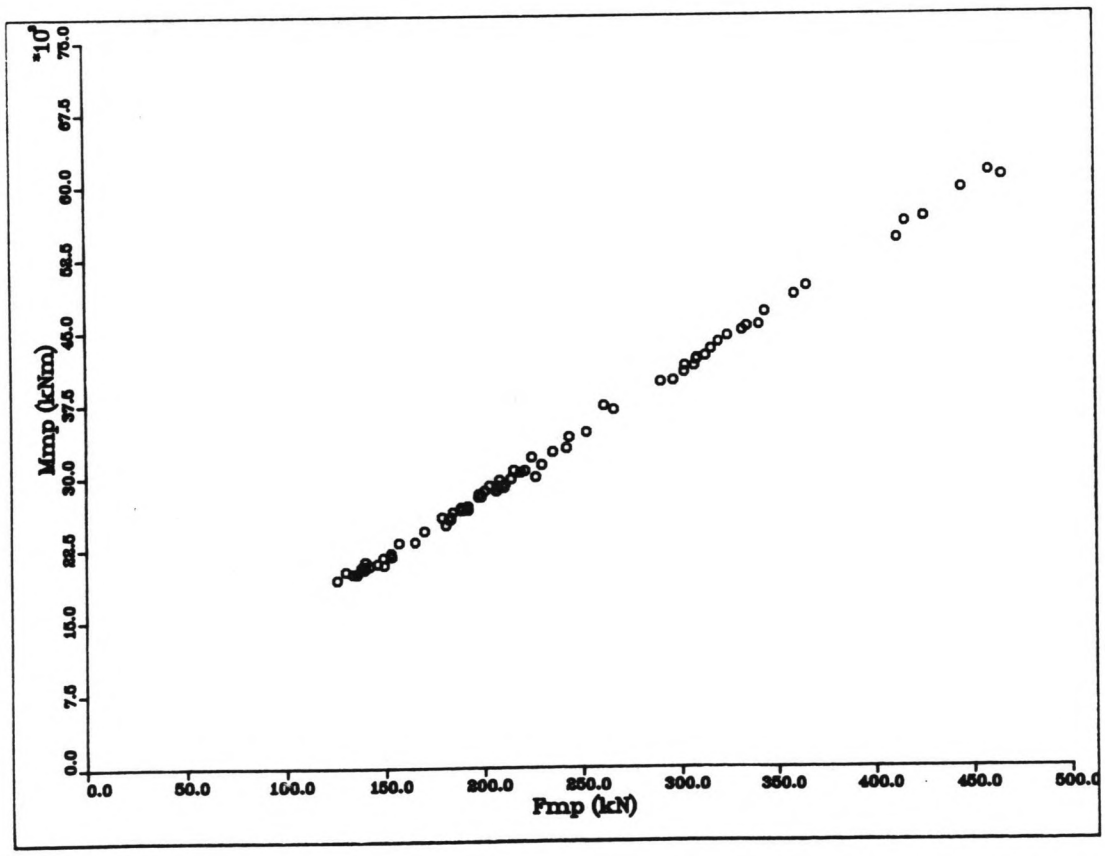

Figure 5.15: The correlation between the most probable extreme base shear force, F_{mp}, and most probable extreme overturning moment, M_{mp}.

where: $\frac{\xi}{\gamma} = 0.0142 \quad kN^{-1}$

5.6.2 The p.d.f. of the most probable extreme overturning moment

The same procedure is followed for the derivation of the probability density function of the most probable extreme overturning moment, M_{mp}. The "bogus" M_{mp}-values again are found from a relation between M_{mp} and H_{mp} squared, based upon the correlation between these two parameters (figure 5.14).

$$M_{mp} \simeq C_1 * H_{mp}^2 + C_2 \tag{5.37}$$

where: $C_1 = 120 \quad kg/s^2$

$C_2 = 2500 \quad kNm$

The constants in relations (5.34) and (5.37) are adapted in such a way that there is a linear relation between the F_{mp}-values and the M_{mp}-values, which follows from the correlation between F_{mp} and M_{mp} (figure 5.15).

Applying the semi-parametric method to overturning moment, the optimum number of samples is found to be: k = 88, of which 28 samples are from "bogus" storms. The distribution function of M_{mp} is in principle the similar to the distribution of F_{mp}, apart from the parameters ξ, γ and M_o:

$$P(m_{mp}) \simeq 1 - [1 + \xi * (m_{mp} - M_o)]^{-\frac{1}{\gamma}} \tag{5.38}$$

for: $M_o \leq m_{mp} \leq \infty$

where: $\xi = 6.914 * 10^{-6} \quad kNm^{-1}$

$\gamma = 0.0612$

$M_o = 24351.0 \quad kNm$

Differentiation of this function results in:

$$p(m_{mp}) = \frac{dP(m_{mp})}{dm_{mp}} \simeq \frac{\xi}{\gamma} * [1 + \xi * (m_{mp} - M_0)]^{-\frac{1}{\gamma} - 1} \qquad (5.39)$$

where: $\frac{\xi}{\gamma} = 0.113 * 10^{-3}$

5.7 Extrapolation to a 100-year design condition

The random storm formula derived in paragraph 5.4 (equation 5.26) represents the probability distribution for extreme base shear, F, during a single, but random, storm; or in other words: it determines the probability that F will not exceed a certain level f during a random storm with $F_{mp} \geq F_0$. The probability of not exceeding f during the whole hindcasting period of 25 years can be determined by raising the random storm formula to the power k, i.e. the number of storms with $F_{mp} \geq F_0$:

$$P(f \mid 25 \text{ years}) = [P(f \mid F_{mp} \geq F_0)]^k \qquad (5.40)$$

The probability distribution of F for a period of y years is then:

$$P(f \mid y \text{ years}) = [P(f \mid F_{mp} \geq F_0)]^{y * \mu} \qquad (5.41)$$

where: $\mu = \frac{k}{25}$ = the expected number of storms per year with $F_{mp} \geq F_0$

A base shear, f_y, with a return period of y years can be defined as the most probable extreme base shear value of this y-year distribution and is determined as the f-value corresponding to a probability of non-exceeding of e^{-1}. This base shear value will be exceeded on the average once in y years.

The distribution from equation (5.41) can be replaced by a Poisson distribution (see also Appendix B). When Q(f) is the probability of

6. DISCUSSION OF THE RESULTS

6.1 Introduction

As a result from the application of the random storm method to base shear and overturning moment, a 100-year base shear and overturning moment have been derived. However these are numbers which are not directly applicable to design. Therefore a back calculation on the basis of the analytical load relationship is performed in order to obtain some interpretation of these results. It may also be interesting to determine the 1,000 and 10,000-year base shear and overturning moment. The validity of the models and methods used is further checked by a carefully considering their inaccuracies and uncertainties, and estimating their probable influence on the final results.

6.2 Interpretation of the results by way of a back calculation

If all environmental parameters, apart from crest height, a, and current velocity, v, are set constant in extreme environmental conditions, for a 100-year design base shear or design overturning moment a relation can be created between current velocity, v, and wave height, H, where the wave height equals two times the crest height. Looking at such a relation is useful, because it gives an idea of what sort of current occurs in combination with a design wave height to produce the design base shear or design overturning moment.

Figure (6.1) shows the wave-current relations for both constant base shear and overturning moment, where wind, waves and currents are fixed to have the same direction. This means that these curves are valid only for "in-line" currents. The wave period T is set to be, T = 15.5 s and the reduction factor due to directional spreading, $\Phi = 0.92$. It shows that the two curves are rather close to each other, which gives some confidence in the method.

exceeding f per storm, then the expected number of exceedings in y years equals: $y*\mu*Q(f)$, so that:

$$P(f|y \text{ years}) = e^{-y*\mu*Q(f)} \tag{5.42}$$

The f_y-value is then determined from:

$$y*\mu*Q(f_y) = y*\mu*[1-P(f_y|F_{mp} \geq F_o)] = 1 \tag{5.43}$$

or:

$$P(f_y|F_{mp} \geq F_o) = 1 - \frac{1}{y*\mu} \tag{5.44}$$

For a 100-year base shear force this expression yields:

$$P(f_{100}|F_{mp} \geq F_o) = 1 - \frac{1}{100*\mu} = 1 - \frac{1}{4*k} \tag{5.45}$$

There is a minimum return period for which this analysis will work. This arises from the condition that $F_{mp} \geq F_o$. When the return period, y, is sufficiently short that the storms with a most probable extreme value smaller than F_o begin to contribute to $P(f_y|y \text{ years})$, the present theory will be less useful. This is shown in Appendix C.

5.7.1 A 100-year design base shear

As stated in the previous paragraph a 100-year design base shear force can be determined from the random storm curve as the f-value corresponding to a probability of $(1 - \frac{1}{4*k})$, where k is the optimum number of samples used for the estimate of the density function of F_{mp}. Since k was found to be: $k = 84$, the probability that a design base shear value, f_{100}, will not be exceeded by an extreme base shear, F, during any random storm equals:

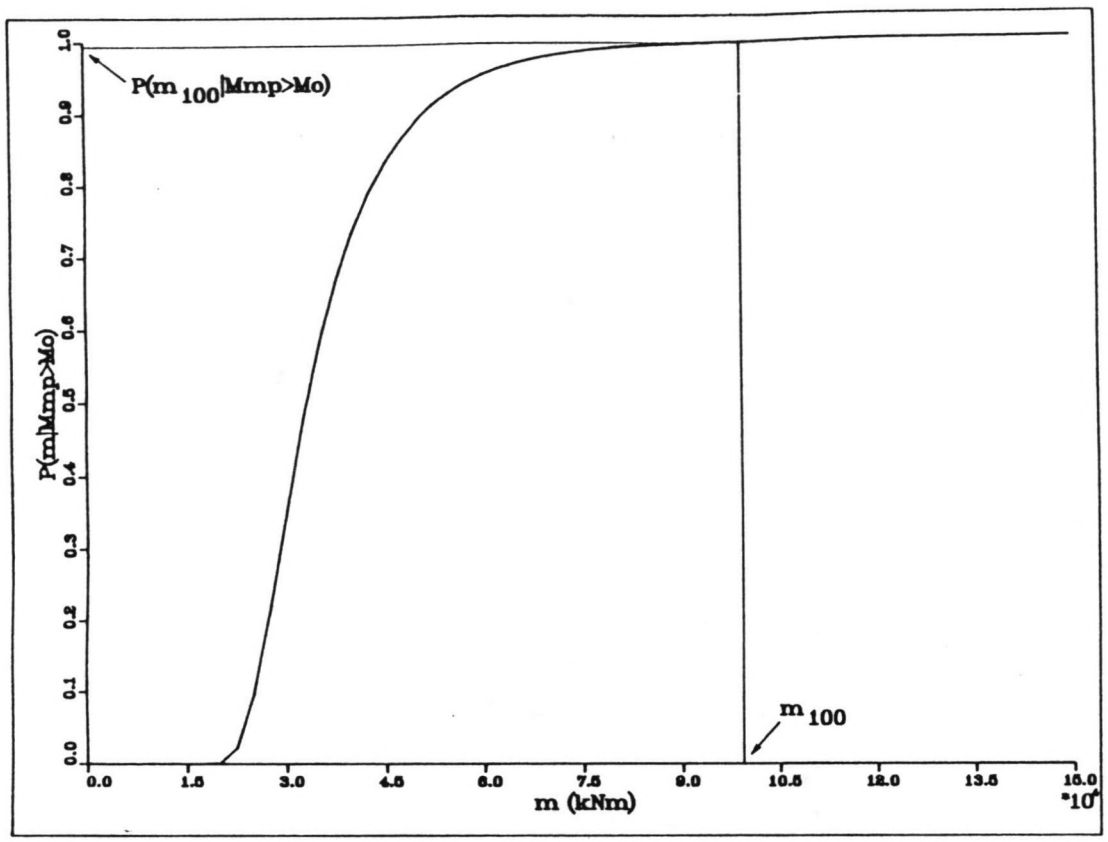

Figure 5.16: Extrapolation to a 100-year overturning moment value by way of interpolation of the random storm distribution.

$$Pr(F \leq f_{100} | F_{mp} \geq F_0) = 1 - \frac{1}{336} = 0.99702 \qquad (5.46)$$

The 100-year design base shear is found by interpolation of the random storm curve for F which results in:

$$f_{100} = 755 \quad kN \qquad (5.47)$$

5.7.2 A 100-year design overturning moment

For overturning moment k was found earlier as: k = 88, so that the probability that a design overturning moment value, m_{100}, will not be exceeded by an extreme moment, M, during any random storm equals:

$$Pr(M \leq m_{100} | F_{mp} \geq F_0) = 1 - \frac{1}{352} = 0.99716 \qquad (5.48)$$

The 100-year design overturning moment is found by interpolation of the random storm curve for M, as shown in figure 5.16, which results in:

$$m_{100} = 99605 \quad kNm \qquad (5.49)$$

5.8 Including wind forces

As stated in paragraph 4.4, wind forces are included by adding an extra term in the loading equation depending on wind speed and wind direction. The additional wind force influences both the "model curve" and the probability density function of the most probable extremes.

The model curves of base shear and overturning moment, i.e. the probability distributions of F and M, conditioned on their most probable extremes, are steeper than those without wind forces (figures 5.17 & 5.18). This is due to the fact that the F_{mp} and M_{mp}-values are higher and since the model curves

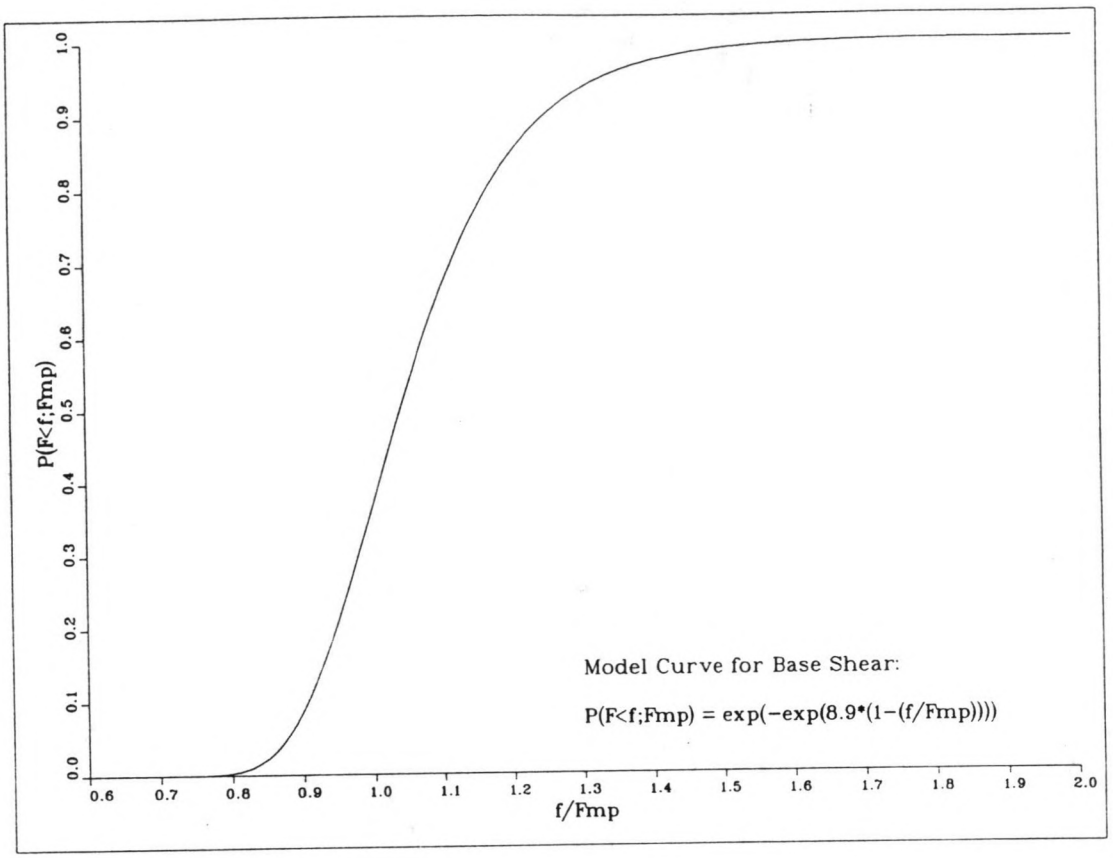

Figure 5.17: A "model curve" for base shear including wind.

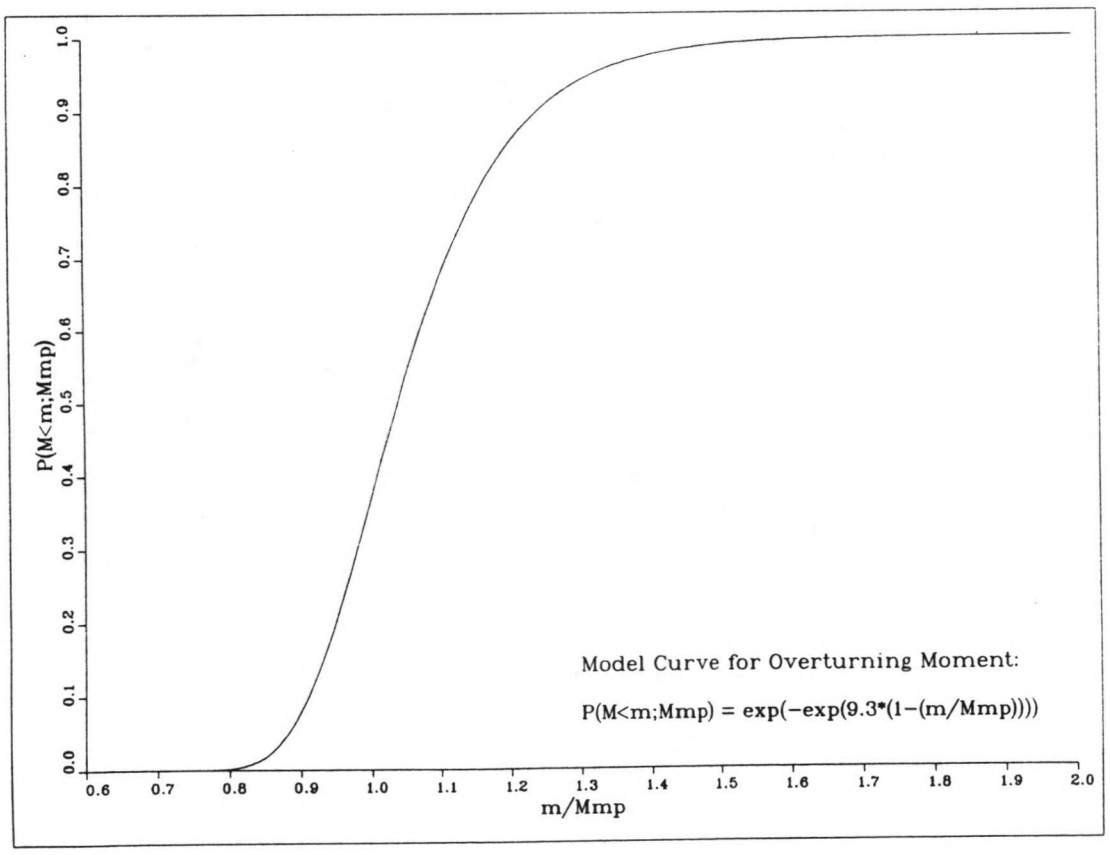

Figure 5.18: A "model curve" for overturning moment including wind.

are rescaled distribution functions, where F and M are divided by their most probable extremes, the values of F and M tend to be compressed a little. The values found for the parameter β from equation (5.29) for base shear and overturning moment respectively is found: $\beta^{-1} = 9.3$ and $\beta^{-1} = 8.9$.

The generation of the probability density function of the most probable extremes is effected in two ways: besides the fact that the F_{mp} and M_{mp}-values have been increased, also the sequence of these values has been changed. This is caused by the relatively large wind force contribution in the less severe storms. While this contribution in severe storms varies around 10 % of the total value for base shear, in a storm of a relatively small intensity it can rise to a percentage of about 25 %. This means that a certain storm, being represented by a lower F_{mp}-value than another storm when wind is neglected, can get a higher F_{mp}-value than the other storm after including the wind forces in the model. Apparently this mixing up of most probable extreme values does not disturb the estimation procedure for the probability density function of these extremes.

After introducing some bogus F_{mp} and M_{mp}-values for the summer storms in the same way as described previously in order to obtain enough data for the extrapolation, the results for a 100 year design base shear and a 100 year design overturning moment including the wind forces are:

$$f_{100} = 781 \quad kN \tag{5.50}$$

$$m_{100} = 112725 \quad kNm \tag{5.51}$$

The design base shear has increased about 3%, while the design overturning moment has grown by 15%. The increase of the m_{100}-value is higher as was expected, because a large moment arm is associated with the wind load, so that the wind contribution is of more importance for overturning moment. However, the growth of the design base shear force seems to be rather low. The possible causes of this will be discussed in the next chapter.

	f (kN)		m (kNm)	
	excl. wind	incl. wind	excl. wind	incl. wind
excl. s.t.v.	655	689	86790	100425
incl. s.t.v.	755	781	99605	112725

Table 5.1: Extrapolation results with 100-year return period with and without the short term variability (s.t.v.) taken into account.

Summarizing, in table 5.1 all the 100-year design loads are listed, i.e. both excluding and including wind forces. Moreover also the 100-year values are given not accounting for the short term variability. These values can be determined directly from equations (5.35) and (5.38). It can be seen from these values that neglecting the short term statistics yield a significant reduction of about 15% of the 100-year design loads.

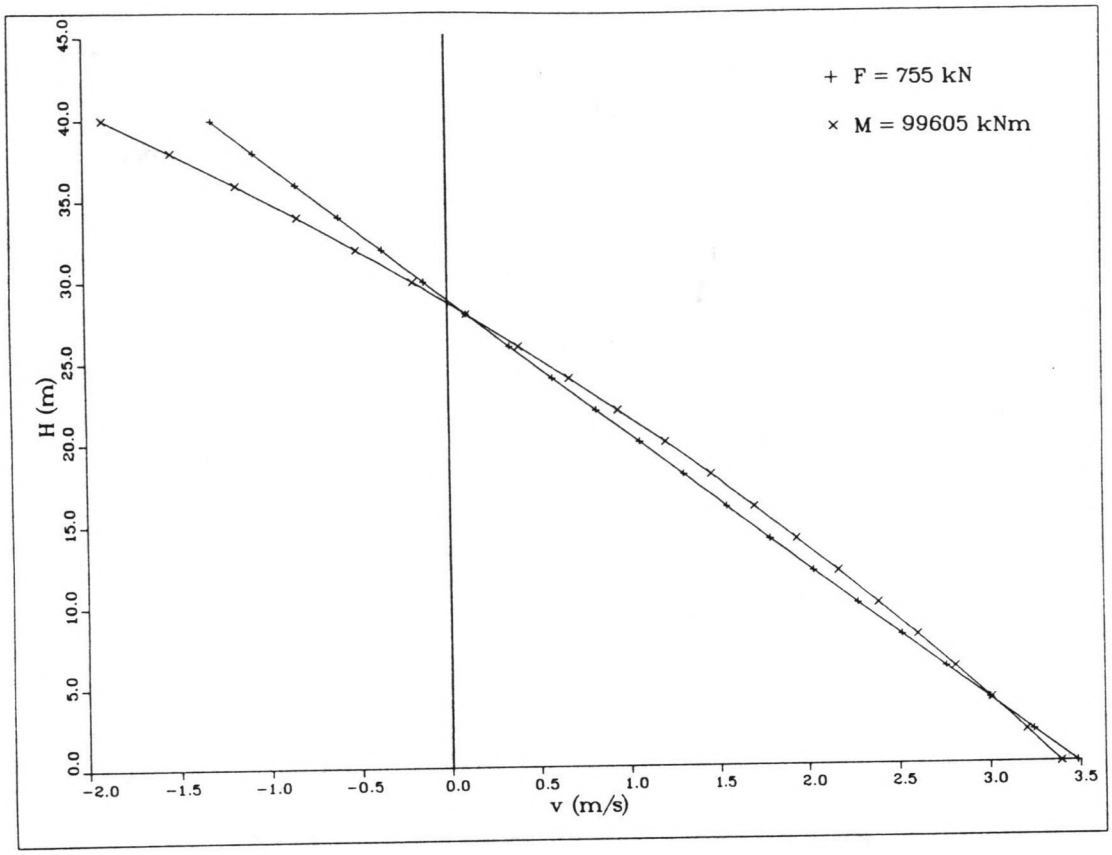

Figure 6.1: The relation between wave height and current following from the loading equation for a fixed 100-year base shear and overturning moment.

However, the wave-current relation based on the design base shear is approximately linear, while the other line is more curved.

In the application of the random storm method to wave heights, a 100-year design wave including short term variability was found to be 26.35 meters (ref. 5). The corresponding current according to the relations of figure 6.1 is:

$$H_{100} = 26.35 \text{ m} \quad \text{-----} > \quad v = 0.28 \text{ m/s} \quad \text{for } F = F_{100} \tag{6.1a}$$

$$v = 0.30 \text{ m/s} \quad \text{for } M = M_{100} \tag{6.1b}$$

These currents are considerably less strong than commonly used 100-year design currents of about 1.0 m/s. However, it is not to say that the currents from (6.1a) and (6.1b) have a 100-year return period; the 100-year current may rather well occur in combination with a lower wave height. This illustrates exactly one of the main differences of this method from the traditional approach, where 100-year waves and 100-year currents are assumed to occur simultaneously.

If wind is included, a similar back calculation can be performed. It appears that the wind speeds occurring in combination with a 100-year design wave height of 26.35 m and a current of 0.30 m/s according to the 100-year base shear and overturning moment are respectively:

$$H_{100} = 26.35 \text{ m}$$
$$v = 0.30 \text{ m/s} \quad \text{-----} > \quad W = 17 \text{ m/s} \quad \text{for } F = F_{100} \tag{6.2a}$$

$$W = 30 \text{ m/s} \quad \text{for } M = M_{100} \tag{6.2b}$$

The difference for the wind speeds is probably due to the extrapolation; this will be explained in paragraph 6.4.3.

	f (kN)		m (kNm)	
RP (years)	excl. wind	incl. wind	excl. wind	incl. wind
100	755	781	99605	112725
1,000	1046	1012	137230	148785
10,000	1391	1252	182425	187395

Table 6.1: Base shear forces and overturning moments extrapolated to various return periods.

a = 5.0 m T = 9.5 s	a = 7.5 m T = 11.2 s	a = 10.0 m T = 13.2 s	a = 12.5 m T = 15.4 s
10.7	9.0	7.2	5.7

Table 6.2: Inertial contribution to total base shear force in % for various combinations of crest height and wave period.

6.3 Extrapolation to a 1,000-year and 10,000-year level

For the interpretation of the results for a 100-year condition it may be relevant to calculate the 1,000 and 10,000-year base shear and overturning moment. This can be done rather easily by changing equation (5.45) into:

$$P(f_{1000} | F \geq F_0) = 1 - \frac{1}{40*k} \tag{6.3}$$

and:

$$P(f_{10000} | F \geq F_0) = 1 - \frac{1}{400*k} \tag{6.4}$$

The results of these calculations are listed in table 6.1. It is striking from these results that the 1,000 and 10,000-year base shear values including wind are lower than the values excluding wind, which can not be right of course. It is confirmed once again that something went wrong with the extrapolation in this case. A probable cause will be given in paragraph 6.4.3.

6.4 Inaccuracies and uncertainties

The total analysis involved in generating the 100-year design conditions is roughly built up of two main parts:

1) the loading model, represented by the approximate analytical load relationship;

2) the storm similarity model, describing the load statistics for any random storm, which can be extrapolated to any desired return period.

	θ (deg)				
v (m/s)	0	45	90	135	180
0.0	7.0	-	-	-	-
0.5	5.4	5.5	6.9	9.1	9.7
1.0	4.3	4.4	6.3	11.0	14.0

Table 6.3: Inertial contribution of total base shear force in % for various combinations of current velocities and directions.

	θ (deg)				
v (m/s)	0	45	90	135	180
0.0	-0.65	-	-	-	-
0.5	-0.37	0.09	-0.99	-2.61	-4.05
1.0	5.49	-1.30	-1.95	-3.51	-11.29

Table 6.4a: Proportional deviations of the analitically determined base shear forces from the numerical values in % for various combinations of current velocities and directions.

Both parts suffer from some significant inaccuracies and uncertainties. They will be discussed here.

6.4.1 Evaluation of the analytical loading equation

The main objective of the loading model is to describe the response of a simplified offshore structure in such a way that it can be expressed in one single equation including all the environmental parameters. This must be done carefully, so that results from the equation approximately coincide with answers from numerical models. Since the calibration of constants has been performed within a accuracy range of about 5 %, it seems to work rather well.

However, the loading model suffers from some major inaccuracies arising from several assumptions. One is the assumption of drag dominance. It may be appropriate to check if the partial or total neglect of the inertia term is reasonable. Table 6.2 shows the percentages of the inertial contributions relatively to the total base shear force for various combinations of crest height and wave period with a fixed "in-line" current of 0.5 m/s. These were obtained by the numerical LOAD-program. It shows that the inertial contribution decreases as the environmental conditions becoming more severe. The relative contribution of the inertia force also depends on the current velocity and the current direction. It can be seen from table 6.3, where current velocities and directions vary with fixed crest height (10 m) and period (15.5 s), that the inertia term is the biggest for negative currents. Thus a neglect of the inertia force affects the forces from the loading model most strongly if the currents are negative. This can also be seen from table 6.4, which gives for the same combinations of current velocities and directions the proportional deviations of the analytically determined base shear forces from the numerical values. A positive percentage means an overestimate of the numerically generated force and a negative value stands

	θ (deg)				
v (m/s)	0	45	90	135	180
0.0	-1.85	-	-	-	-
0.5	-1.30	-0.48	-1.28	-1.72	-2.15
1.0	5.59	-0.32	-0.27	-0.09	-9.03

Table 6.4b: Proportional deviations of the analitically determined overturning moments from the numerical values in % for various combinations of current velocities and directions.

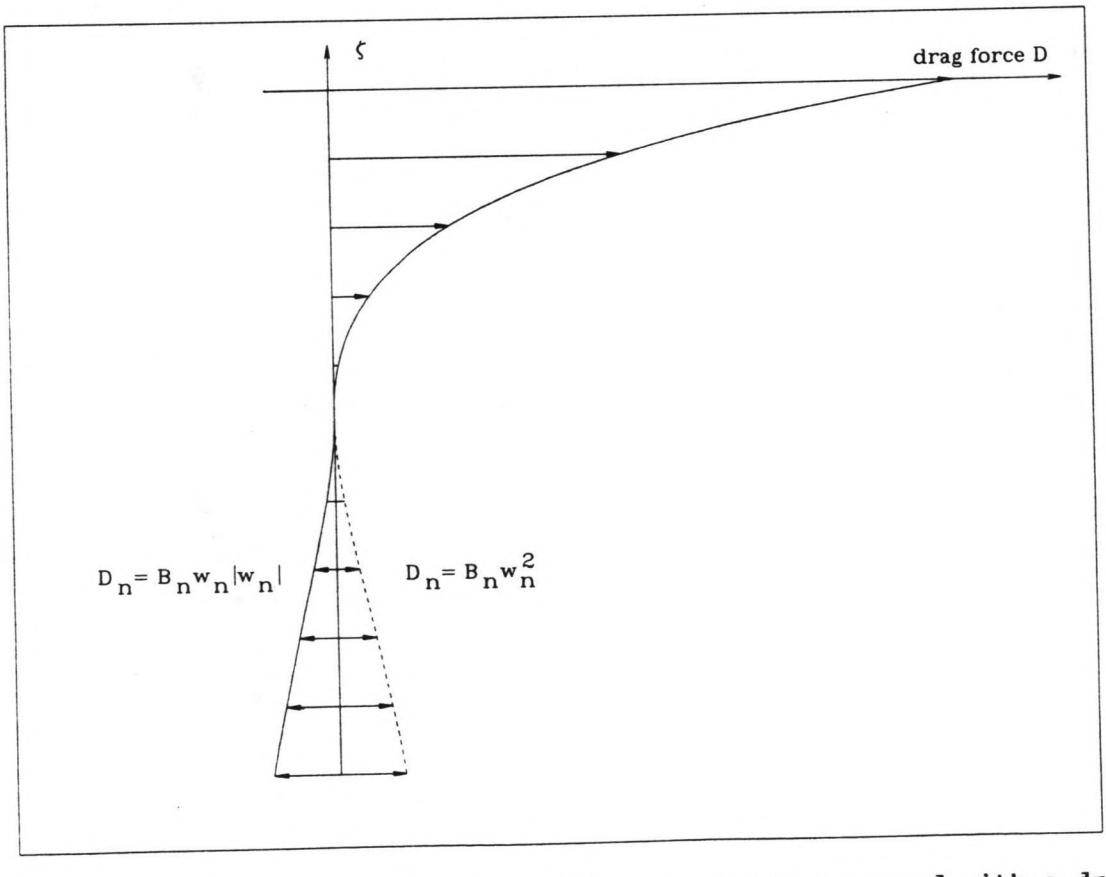

Figure 6.2: Typical drag force profile over depth compared with a drag not accounting for the change of sign for negative currents.

for an underestimate. The underestimate is the biggest for strong and negative currents.

Though for the calibration of constants an accuracy range of 5 % was mentioned earlier, in table 6.4 some percentages exceed this value. However, the calibration was based upon data from the NESS data base, where current velocities as large as 1 m/s do not appear. The loading equations therefore are only valid for a limited range of data.

The effect of underestimating the base shear for negative currents by neglecting the inertia forces is partially compensated by the ignorance of the absolute value of the water particle velocity in the drag term of the Morison equation. The drag force is assumed to increase as the square root of the water speed - compare equation (4.2) with (4.3) -, which results in an overestimate of the drag force especially near the sea bed (figure 6.2). Near the surface this effect is not of interest, since under extreme conditions the wave induced velocity is much larger than the current velocity, but well below the surface, where the wave induced velocity is smaller, there is a significant influence leading to a conservative approach. This effect may be more important for base shear than overturning moment, since the small moment arms make the latter less sensitive to forces near the sea bed.

Other inaccuracies are involved with the NESS data base. The values of the environmental parameters in the NESS data base are determined from a hindcast simulation technique with all environmental and meteorological information available used as an input. This simulation contains significant uncertainties.

β^{-1}	7.4	7.7	8.1
f_{100} (kN)	761	755	749
deviation in %	0.7	0.0	-0.8
β^{-1}	7.6	8.0	8.4
m_{100} (kNm)	100570	99605	98785
deviation in %	0.9	0.0	-0.8

Table 6.5: Influence of the fitting parameter β from the "model curve" on the 100-year base shear and overturning moment values.

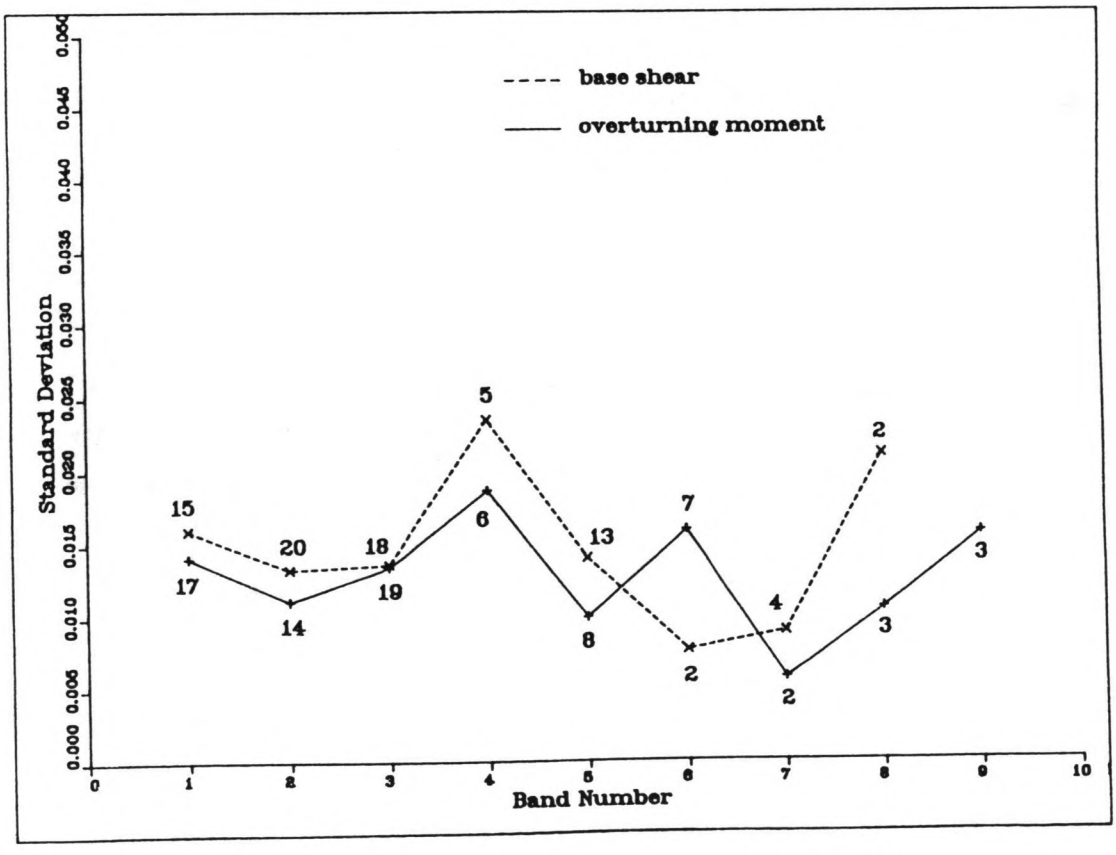

Figure 6.3: Standard deviation of the rescaled probability distributions for base shear (f/F_{mp}=1.2) and overturning moment (m/M_{mp}=1.2) within each band. The numbers indicate the number of storm samples per band.

6.4.2 Evaluation of the "model curve"

The "model curve" represents the short term variability of every storm and is generated by taking the average of the rescaled probability distributions of all the storms selected from the NESS data base. It may be appropriate to check how representative the "model curves" are actually. This can be done by calculating the standard deviation of the curves in each band for a value of f/F_{mp}, where the deviation of the curves from each other seems to be the most significant, that is for $f/F_{mp} = 1.2$ (see figure 5.9). The standard deviation is then defined as:

$$\sigma_{n-1} = \left[\frac{1}{n-1}\left(\Sigma x_j^2 - \frac{1}{n}(\Sigma x_j)^2\right)\right]^{\frac{1}{2}} \qquad (6.5)$$

where x_j is the probability that the ratio $f/F_{mp} = 1.2$ will not be exceeded during storm j and n is the number of storms in a band. Although the number of storms in several bands is rather small, the standard deviations can give an indication of the fit of the "model curve".

Figure 6.3 shows the standard deviations of the storm distribution functions within each band both for base shear and overturning moment. There is no clear indication that the standard deviation decreases for bands with more severe storms, which would have indicated that very severe storms are more similar than less severe ones. The lack of this trend may be due to the small number of storms in the highest bands.

The average values of the standard deviations for base shear and overturning moment are respectively 1.4 % and 1.3 % (figure 6.3). A curve based upon a deviation of say 1.5 % from the "model curve" for $f/F_{mp} = 1.2$ tends to be steeper for a positive and less steep for a negative deviation. This is controlled by the fitting parameter β (equation 5.29). However, it appears that a small change of β, caused by 1.5 % deviation from the "model curve" has a negligible influence on the final results as shown in table 6.5.

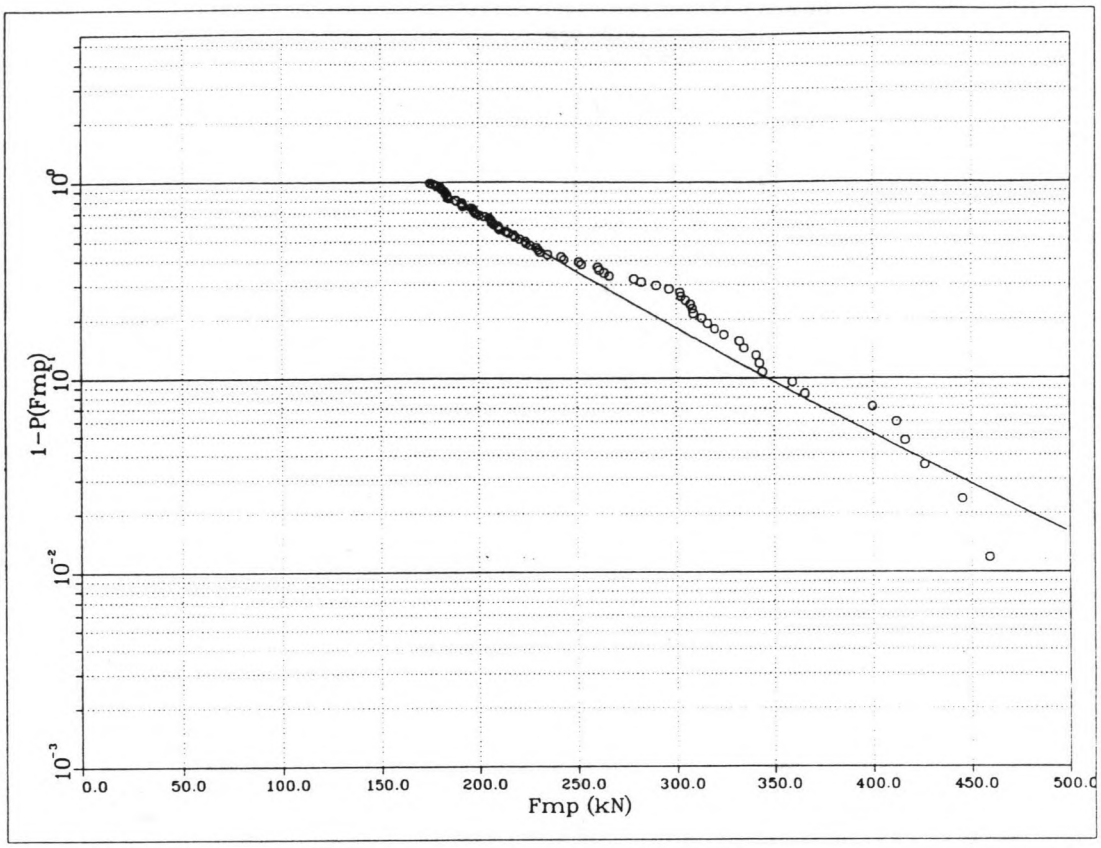

Figure 6.4: Comparison of the probability distribution of F_{mp} with the normalized number of samples used for the estimation of the distribution.

	f (kN)	
RP (years)	excl. wind	incl. wind
100	755	812
1,000	1046	1069
10,000	1391	1353

Table 6.6: Base shear forces extrapolated to various return periods, with γ = +0.0514 for f incl. wind.

6.6 Evaluation of the extrapolation

The validity of the probability density function of the most probable extremes can be checked by comparing one minus the distribution function of these extremes, following from the semi-parametric estimation method, with for every storm one minus the normalized ranking number of the storm sample, which is a rough estimate of the discrete distribution function. The number of each sample from 1 to the optimum number of samples k is then divided by k. Figure 6.4 shows that the the curve representing the values of 1 minus the distribution function fits rather well for the lowest 50 values, compared to the dots representing the values of 1 minus the normalized number of samples. For overturing moment this picture looks similar. The deviation of the highest values may be due to the noise in the data, extracted from a simulation containing some uncertainties.

Generally the curve representing the continuous distribution function seems to be a good fit. However, some comments have to be made upon this. As stated earlier the index of variation, γ, in the probability density function of the most probable extremes (see equations (5.36) and (5.39)) is determined by the minimization of the mean squared error of the estimate (ref. 18). Figure (6.5) shows that the minimum of this mean squared error corresponds with a value of γ which is used for the density fuction. The course of γ round the optimum k is not very stable. Although γ seems to be approximately zero and the variation is only within a range of γ from -0.1 to +0.1, for extrapolation even the slighest change of γ is of significant influence for the results.

For example when wind was included for base shear a minimum of the MSE was found for k = 121, where γ = -0.028. A closer look at figure (6.6) reveals that there is a second minimum of MSE for k = 114. The γ corresponding to this value of k is positive γ = +0.0514. Performing the extrapolation for this γ results in a 100-year design base shear of 812 kN, where the wind contribution is 8 % instead of 3 % as found earlier and listed in table 6.1.

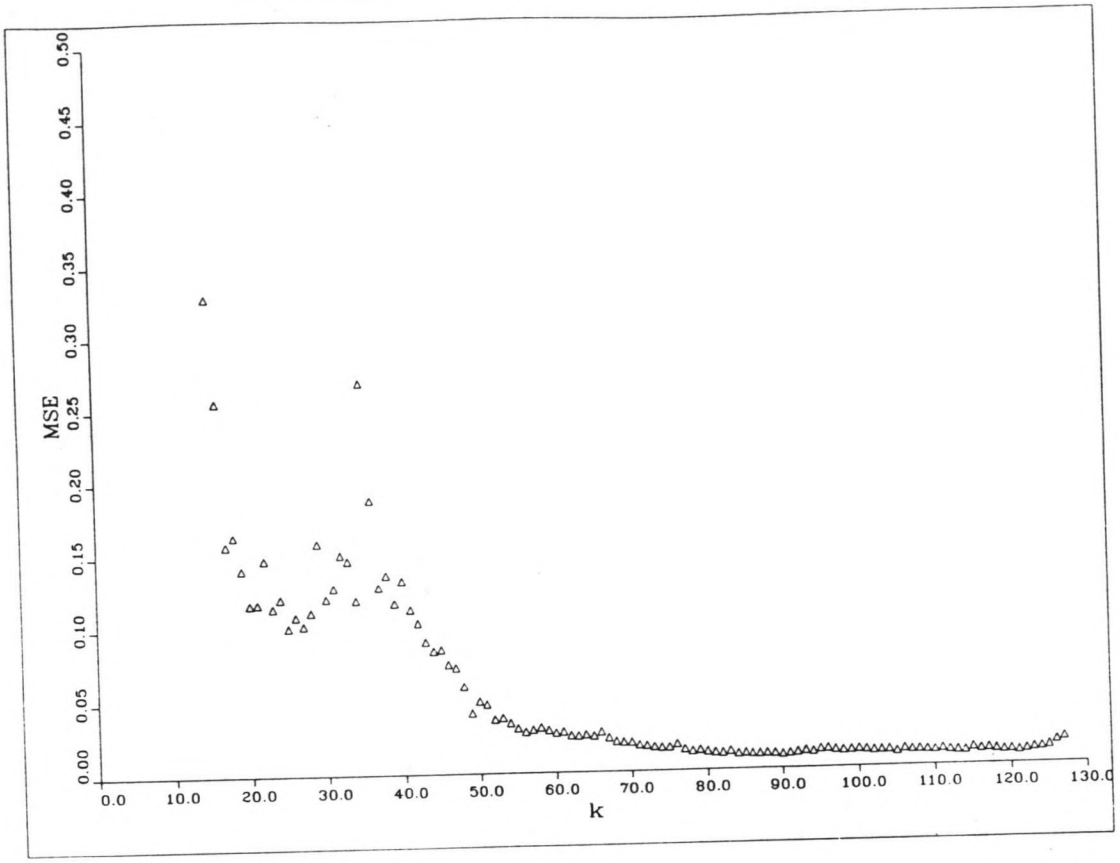

Figure 6.5a: Course of the mean squared error of the estimate of the index of variation, γ, for a varying number of storm samples, k, for base shear force including wind.

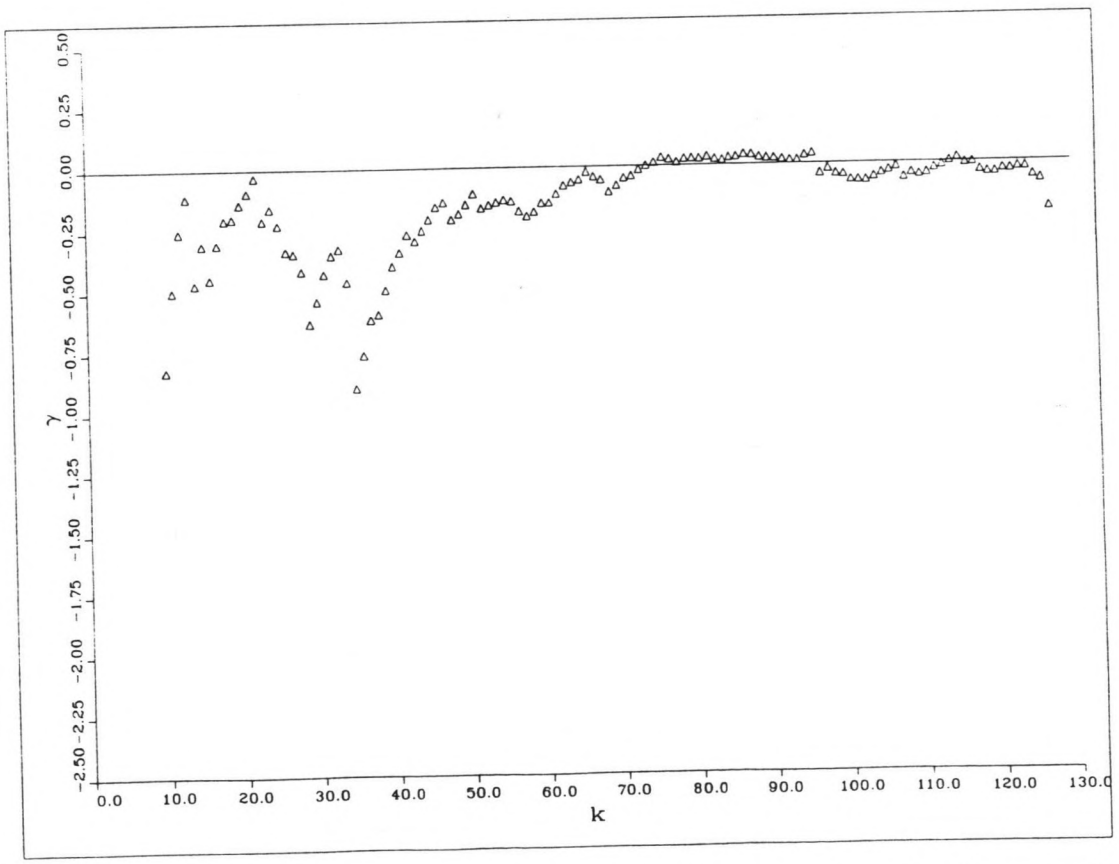

Figure 6.5b: Course of the estimate of the index of variation, γ, for a varying number of storm samples, k, for base shear including wind.

This base shear including wind forces seems to be much more realistic than the value resulting from the negative γ. Moreover the 1,000-year base shear value inluding wind now is higher than the value excluding wind (table 6.6).

This example illustrates that the extrapolation procedure is very sensitive to the estimate of γ. In figure (6.4) a positive γ yields a convex curve, while the curve would be concave if γ were negative. When these curves are extrapolated to a 100-year level they diverge from each other significantly (figure 6.6).

It can also be seen from figure (6.5) that if not enough data is used the MSE-value will not be able to create a real global minimum. For example when the 79 uncensored storms mentioned in paragraph 5.6.1 were used, the corresponding minimum of MSE was found for k = 79. This mimimum, however, is a boundary minumum, rather than a global one. Thus, in order to be sure that the minimum of MSE found is really a global minimum and not a local or a boundary minimum, sufficient data has to be available.

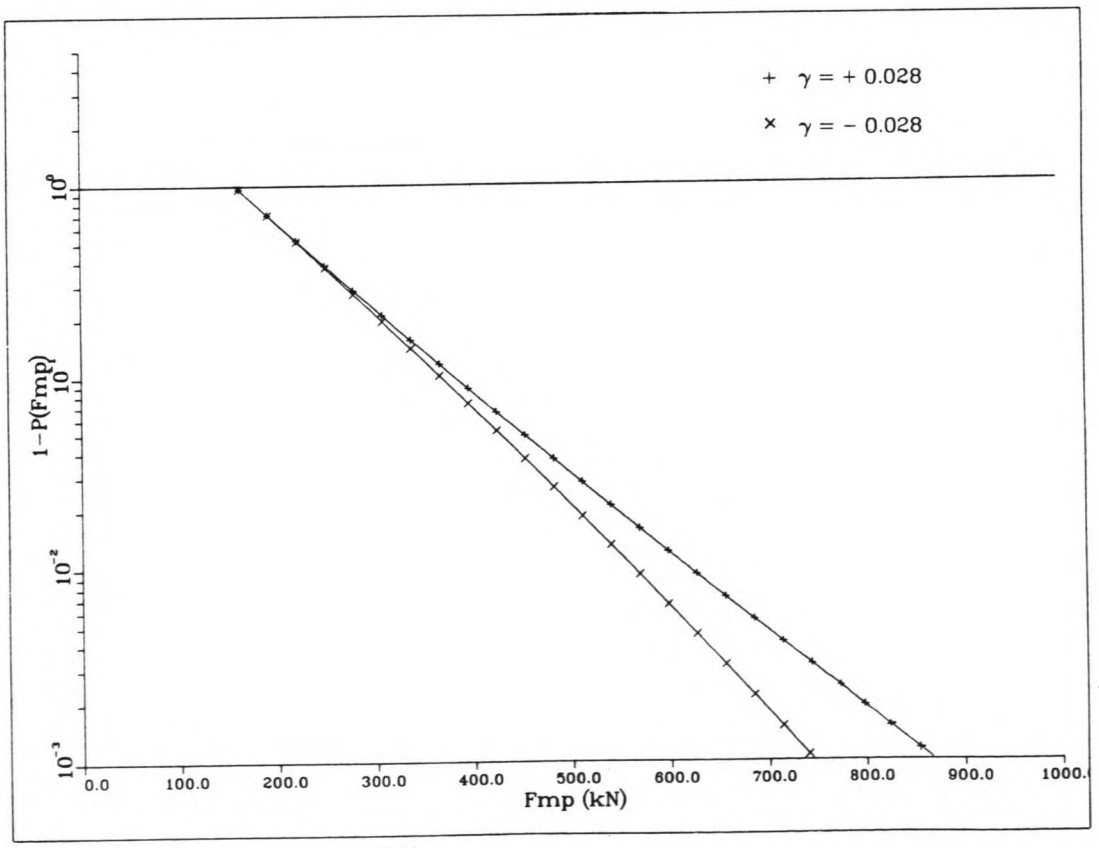

Figure 6.6: Comparison of the probability distributions of F_{mp}, with a positive and a negative value of γ.

7. CONCLUSIONS AND RECOMMENDATIONS

7.1 Introduction

From the results presented in this report it can be concluded that in principle the random storm method is applicable to global structural loading. However, in an absolute sense the numerical values of the 100-year design base shear and overturning moment have to be treated with great care, not only because they are partially based on bogus data, but also because the models contain certain uncertainties asking for further research. On the other hand in a relative sense there is a trend in the answers: the application of the random storm method leads to a significant reduction of the design forces and moments. This implies that further research is certainly worthwile.

7.2 The advantages and disadvantages of the random storm method

During the project it became clear that the random storm method has some major advantages over the traditional design procedures, but like any method it has its disadvantages as well. Both advantages and disadvantages are enumerated here.

Advantages are:

1) The statistical parameters from successive 3-hour intervals are no longer treated as independent. Instead, individual storms are assumed to be independent, which is much more likely to be the case.

2) Extreme winds, waves and currents do not necessarily occur simultaneously and they are not assumed to have the same direction.

3) The random storm method accounts for the short term variability by way of a representative "model curve" in the random storm formula.

4) Since the extrapolation is based on the fitting of the tail of the probability density function, only severe storms are used, so that less data have to be analysed, without loss of information about the tail.

Disadvantages are:

1) There is no straightforward analytical method available yet for the calibration of the constants in the loading equation. This does not only mean that this process is rather laborious, but also that the values of the constants have to be tested for a large number of data.

2) For different structures and locations the constants in the loading equation have to be determined all over again. However, for using the equation for other cases, multiplying the constants with some factor may be sufficient, but that has to be investigated.

3) For a successful extrapolation a large data base is required.

4) In the generation of the parameters of the probability density function of the most probable extremes a huge amount of CPU time is involved.

7.3 Conclusions

1) The random storm method is indeed applicable to global structural loading.

2) The use of the random storm method leads to significant reductions of design forces and moments.

3) The possibility of an application of the random storm method is at present dependent on the amount of data available.

4) Considering base shear and overturning moment a similarity for severe storms is found as for wave heights: the rescaled probability distributions of base shear and overturning moment approximately lie on the same curve. This confirms the idea of the existance of a similarity for severe storms.

5) The random storm method is in principle applicable for any fixed structure in any other location. However, the consequences of a different structure and location for the "model curve" and the loading equations have to be investigated.

7.4 Recommendations

It is shown that an application of the random storm method to global structural loading is possible. The indications that the use of this new method will lead to significant reductions of the design forces and moments make it certainly worthwile to do some further research in order to improve the models and methods. There are of course a lot of uncertainties, that require some extra consideration. On the one hand some attempts have to be undertaken to eliminate these uncertainties, on the other hand the method needs more testing, which means that a repetition of the calculations for different structures and different locations may be advisable. In this sense a few practical recommendations are enumerated here.

1) The constants in the loading equation were calibrated by way of trial and error. It would be worthwile to find a more sophisticated way of doing the calibration.

2) The modelling of the base shear and overturning moment by way of the

analytical loading equation may be improved. Especially the influence of wave and current directions needs more attention.

3) It is advisable to repeat the calculations for adjacent grid points of the considered location in order to check the validity of the method and the results.

4) It has been indicated in this report that extension of the loading model to a real structure may be done easily by multiplying the constants in the loading equation by a certain factor. This has to investigated.

5) Although the extrapolation procedure seems to work rather well, it is still very sensitive to the influence of the rather unstable course of the estimate parameter, γ. Further study is required.

6) The application in design of joint wave, current and wind conditions as derived here would have consequences for platform reliability. These should be investigated carefully.

REFERENCES

1. Battjes, J.A.
   "Korte golven, b76"
   Faculty of Civil Engineering, University of Technology, Delft
   January 1988

2. Battjes, J.A.
   "Windgolven, Handleiding college b78"
   Faculty of Civil Engineering, University of Technology, Delft
   September 1982

3. Carter, D.J.T. & Challenor, P.J.
   "Estimating return values of wave height"
   Report 116
   Institute of Oceanographic Sciences, Wormley, 1981

4. Graaf, J.W. van de & Tromans, P.S.
   "Statistical verification of predicted loading and ultimate strength against observed storm damage for an offshore structure"
   Offshore Technology Conference
   Paper OTC 6573, May 1991

5. Heijermans, B.H.
   "Application of the random storm method to the airgap problem"
   Student Report STUDREP.91.070
   KSEPL, Rijswijk, May 1991

6. McClelland, B. & Reifel, M.D.
   "Planning and design of fixed offshore platforms"
   Van Nostrand Reinhold Company, New York, 1986

7. Nielsen, J.B.; Grant, C.K.; Webb, R.M. & Brink-Kjaer, O.
"An investigation of the importance of joint probability and directionality of environmental data for platform design"
Offshore Technology Conference
Paper OTC 5140, May 1986

8. Patel, M.H.
"Dynamics of offshore structures"
Butterworth & Co., London, 1989

9. Petruaskas, C. & Aagaard, P.M.
"Extrapolation of Historical Storm Data for Estimating Design Wave Heights"
Offshore Technology Conference
Paper OTC 1190, April 1970

10. Pugh, D.T.
"Tides, Surges and Mean Sea-Level"
John Wiley & Sons, Chichester, 1987

11. Rodenbusch, G. & Forristal, G.Z.
"An empirical model for random directional wave kinematics near the free surface"
Proc. 18th Annual Offshore Techmology Conference, Houston, May 1986

12. Sarpkaya, T. & Isaacson, M.
"Mechanics of Wave Forces on Offshore Structures"
Van Nostrand Reinhold Company, New York, 1981

13. Soest, J. van
"Elementaire Statistiek"
Delftsche Uitgevers Maatschappij, 1985

14. Taylor, P.H.
"Current blockage: reduced forces on offshore space-frame structures"
Offshore Technology Conference
Paper OTC 6519, May 1991

15. Tromans, P.S.
"Large ocean waves"
Group Research Report
KSEPL, Rijswijk, June 1990

16. Tromans, P.S. & Hagemeijer, P.M.
"The statistics of the extreme response of offshore structures"
Publication 858
KSEPL, Rijswijk, August 1990

17. Tucker, M.J.
"An improved 'Battjes' method for predicting the probability of extreme waves"
Applied Ocean Research, 1989, Vol. 11, No. 4

18. Wolf, P.P. de
"On the estimation of the index of variation"
Student Report STUDREP.91.116
KSEPL, Rijswijk, August 1991

LIST OF SYMBOLS

ROMAN:

a	crest height	[m]
d	depth	[m]
f,F	base shear force	[kN]
g	gravity	[m/s²]
h,H	wave height	[m]
i	environmental parameters apart from wave height	[-]
k	wave number (chapter 4)	[rad/m]
k	optimum number of storm samples (chapters 5 & 6)	[-]
m,M	overturning moment	[kNm]
n	number of successive 3-hour intervals (appendix B)	[-]
n	number of successes in Poisson distribution (appendix C)	[-]
r	radius of a circular cylinder	[m]
u	horizontal wave induced fluid velocity	[m/s]
$\dot{u}$	horizontal wave induced fluid acceleration	[m/s²]
$\hat{u}$	slowly varying amplitude that defines peaks in u_o	[m/s]
v	depth mean total current velocity	[m/s]
v_{res}	depth mean residual current velocity	[m/s]
v_s	depth mean current velocity including current blockage	[m/s]
w	resultant horizontal fluid velocity	[m/s]
y	number of years of a return period	[-]
A	inertia factor for rough cylinder ($\zeta \leq 0$)	[kgm*10³]
A_s	inertia factor for smooth cylinder ($\zeta > 0$)	[kgm*10³]
B	drag factor for rough cylinder ($\zeta \leq 0$)	[kg*10³/m]
B_s	drag factor for smooth cylinder ($\zeta > 0$)	[kg*10³/m]
C_D	drag coefficient	[-]
C_M	inertia coefficient	[-]
C_W	wind drag coefficient	[-]
D	diameter of cylinder	[m]

D_n	instantaneous drag force normal to pipe axis	[kN/m]
D_s	stretching depth	[m]
F_W	total wind force	[kN]
H_s	significant wave height	[m]
$H_{s,max}$	maximum significant wave height in a storm	[m]
$H_{s,max2}$	secondary maximum significant wave height in a storm	[m]
$H_{s,trough}$	lowest significant wave height in between two maxima	[m]
I	total horizontal inertia force normal to pipe axis	[kN/m]
N_i	number of crests in a 3-hour interval	[-]
N_j	number of 3-hour intervals during a storm	[-]
N_s	total number of storms that occcur in 25 year hindcasting	[-]
R	return period	[years]
S	frontal area	[m^2]
S_j	storm history of storm j	[-]
T_p	peak period	[s]
T_z	zero-up crossing period of ocean surface elevation	[s]
T_L	design life time of a structure	[years]
V	volume of cylinder element	[m^3]
W	wind speed	[m/s]
W_{10}	wind speed at 10 meters above mean sea level	[m/s]

GREEK:

α, β	fitting parameters for "model curve"	[-]
γ	estimate of the index of variation used for the estimation of the p.d.f. of most probable extremes	[-]
γ_n	depth depending angle between inertia and drag forces	[deg]
η	instantaneous ocean surface elevation	[m]
$\hat{\eta}$	peak value of surface elevation during passage of a wave	[m]
λ	wave length	[m]
μ	average number of storms per year with $F_{mp} \geq F_o$	[-]
ν	average number of storms per year	[-]
θ	angle between wave propagation and depth mean current	[deg]

θ_H	direction of wave propagation taken form north	[deg]
θ_{storm}	direction of a storm taken from north	[deg]
θ_v	direction of total depth mean current taken from north	[deg]
$\theta_{v,res}$	direction of residual depth mean current taken from north	[deg]
θ_W	angle between wave and wind direction	[deg]
ρ	fluid density	[kg/m³]
ρ_a	air density	[kg/m³]
σ_θ	directional spreading parameter	[deg]
Δt	duration of time interval between two maxima of H_s	[hrs]
$\Delta\tau$	duration of a 3-hour time interval in seconds	[s]
ω_z	zero-up crossing frequency of ocean surface elevation	[rad/s]
ξ	parameter in p.d.f. of F_{mp}	[1/kN]
ψ	smoothly varying phase for defining peak forces	[rad]
ζ	vertical coordinate defined with its origin at m.s.l.	[m]
ζ_s	substitute coordinate from delta stretching	[m]
Θ	individual wave direction relatively to general direction	[rad]
∇	delta stretching parameter	[-]
Φ	reduction factor from directional spreading	[-]

SUBSCRIPTS:

X_{100}	value of parameter X with a 100-year return period
X_y	value of parameter X with a y-year return period
X_i	parameter from interval, i
X_n	instantaneous value of X at a certain depth
X_0	lower integration limit in the random storm formula
X_∞	upper integration limit in the random storm formula
X_{mp}	most probable extreme value of X
X^*	constant from the analytical loading equation

APPENDIX A

INFLUENCE OF THE DEPENDENCE OF SUCCESSIVE 3-HOUR INTERVALS

Suppose a storm with storm history, S_j (i.e. the history of the environmental parameters in all the 3-hour intervals of storm j), contains n 3-hour intervals and the probability distribution of F in the i-th interval is expressed as:

$$P(f|\text{i-th interval}) = P(A_i) \tag{A.1}$$

Then the probability distribution of F in n intervals should be:

$$P(f|\text{n intervals}) = P(A_1)*P(A_2|A_1)*\ldots*P(A_i|A_1\ldots A_{i-1})*\ldots$$

$$\ldots*P(A_n|A_1\ldots A_{n-1}) \tag{A.2}$$

If the statistical parameters in successive 3-hour intervals are assumed to be independent, this distribution becomes:

$$P(f|\text{n intervals}) = P(A_1)*P(A_2)*\ldots*P(A_i)*\ldots*P(A_n) = \prod_{i=1}^{n} P(A_i) \tag{A.3}$$

The probability distribution of equation (5.18) is conditioned on the storm history, S_j, of the considered storm j. Including this condition in equation (A.2) yields:

$$P(f|\text{n intervals},S_j) = P(A_1|S_j)*P(A_2|A_1,S_j)*\ldots*P(A_i|A_1\ldots A_{i-1},S_j)*\ldots$$

$$\ldots*P(A_n|A_1\ldots A_{n-1},S_j) \tag{A.4}$$

By conditioning the probability distributions on the storm history S_j the other events in the condition, namely that in the preceding intervals F will not exceed the value f, have become redundant and can be left out. The event that storm history S_j will occur, completely conditions the problem. Thus, the probability distribution in equation (A.4) changes into an expression similar to (A.3):

$$P(f|S_j) = \prod_{i=1}^{n} P(A_i|S_j) \qquad (A.5)$$

APPENDIX B

THE POISSON DISTRIBUTION APPROXIMATION FOR A PROBABILITY DISTRIBUTION OF EXTREME BASE SHEAR DURING A WHOLE STORM

Suppose exceeding a certain level f during a 3-hour interval with N_i crests is called a success and consequently not exceeding that level during the interval is called a failure, then the probability of n successes can be expressed by a binomial distribution:

$$Pr(\underline{n}=n) = \binom{N_i}{n} * (Q(f))^{n} * (1-Q(f))^{N_i - n} \qquad (B.1)$$

If $Q(f) \to 0$ and $N_i \to \infty$, in such a way that $(N_i * Q(f))$ remains constant, then this probability can be approximated by the Poisson distribution (ref. 13):

$$Pr(\underline{n}=n) = \frac{\mu^n}{n!} \exp(-\mu) \qquad (B.2)$$

where μ is the expected number of successes:

$$\mu = E\{\underline{n}\} = N_i * Q(f) \qquad (B.3)$$

Consequently the probability of no successes in one interval is then:

$$Pr(\underline{n}=0) = \frac{\mu^0}{0!} \exp(-N_i * Q(f)) = \exp(-N_i * Q(f)) \qquad (B.4)$$

This result is the same as equation (5.21).

APPENDIX C

INFLUENCE OF THE LOWER INTEGRATION LIMIT, F_o, ON THE EXTRAPOLATION TO ANY RETURN PERIOD

The semi-parametric approach of predicting the distribution of the most probable extreme base shear forces, $P(F_{mp})$, is based on the estimation of the behaviour of the distribution near the upper end (see paragraph 5.6). Therefore only an optimum number of the k largest samples is used for the extrapolation. That is why a lower integration limit, F_o, is introduced, where F_o equals the lowest F_{mp}-value from the total of k samples. The probability of not exceeding f during a random storm is then conditioned on $F_{mp} \geq F_o$.

If the total number of storms that passed during the hindcasting period of 25 years, N_s, is used for the extrapolation, rather than only an optimum number of k storms, then equation (5.40) changes into:

$$P(f|25 \text{ years}) = [P(f|\text{any storm})]^{N_s} \qquad (C.1)$$

where the probability distribution of F for any random storm, P(f|any storm), is not conditioned on a lower integration limit, but only on the storm histories. According to the subsequent analysis expressed in equations (5.41) to (5.45) the probability that an extreme base shear force f_y, with a return period of y years will not be exceeded during that period is (compare equations 5.41 and 5.44):

$$P(f_y|y \text{ years}) = [P(f_y|\text{any storm})]^{y*\nu} \qquad (C.2)$$

where: ν = the expected number of storms per year

and thus:

$$P(f_y|\text{any storm}) = (1 - \frac{1}{y*\nu}) \qquad (C.3)$$

After introducing the threshold, F_o, the total number of storms, N_s, can be divided into two ranges, one including all storms with $F_{mp}<F_o$, and the other including the storms with $F_{mp}\geq F_o$. Theoretically the probability distribution from equation (C.3) can then be written as:

$$P(f_y|\text{any storm}) = P(f_y|F<F_o)*Pr(F<F_o) + P(f_y|F\geq F_o)*Pr(F\geq F_o) \qquad (C.4)$$

If the return period, y, is sufficiently large then $P(f_y|F<F_o)$ will approach the value of 1, because a large return period implies that f_y will be much larger than the lower limit, F_o. Hence, if F is smaller than F_o, it will always be much smaller than f_y as well.

The probabilities that F is larger than the lower limit, F_o, respectively smaller can be estimated from the fractions of F_{mp}-values:

$$Pr(F\geq F_o) \simeq \frac{k}{N_s} \qquad (C.5)$$

and thus:

$$Pr(F<F_o) \simeq 1 - \frac{k}{N_s} \qquad (C.6)$$

where k is the optimum number of storms used in the estimation procedure for generating the density function for F_{mp} and N_s the number of storms which occured during the hindcasting period of 25 years.

Equation (C.4) can thus be rewritten as:

$$P(f_y|\text{any storm}) = 1 - \frac{k}{N_s} + P(f_y|F\geq F_o)*\frac{k}{N_s} \qquad (C.7)$$

Working out this expression combined with the random storm formula, equation (C.3) results in:

$$P(f_y | F \geq F_o) = 1 - \frac{25}{y*k} = 1 - \frac{1}{y*\mu} \qquad (C.8)$$

This expression is the same as equation (5.29), which proves that as long as the return period, y, is chosen sufficiently large no relevant information is lost, in spite of the use of a number of k storm samples only, rather than a number of N_s.